

# Lecture Notes: Introduction to Machine Learning for the Sciences

Titus Neupert,<sup>1</sup> Mark H Fischer,<sup>1</sup> Eliska Greplova,<sup>2,3</sup> Kenny Choo,<sup>1</sup>  
and Michael Denner<sup>1</sup>

<sup>1</sup>Department of Physics, University of Zurich, 8057 Zurich, Switzerland

<sup>2</sup>Kavli Institute of Nanoscience, Delft University of Technology, 2600 GA Delft, The  
Netherlands

<sup>3</sup>Institute for Theoretical Physics, ETH Zurich, CH-8093, Switzerland

February 28, 2025

# Contents

<b>1</b>	<b>Introduction</b>	<b>3</b>
1.1	Why machine learning for the sciences? . . . . .	3
1.2	Overview and learning goals . . . . .	5
1.3	Resources . . . . .	7
1.4	Prerequisites . . . . .	8
1.5	References . . . . .	8
<b>2</b>	<b>Structuring Data without Neural Networks</b>	<b>9</b>
2.1	Principle component analysis . . . . .	9
2.2	Kernel PCA . . . . .	11
2.3	t-SNE as a nonlinear visualization technique . . . . .	13
2.4	Clustering algorithms: the example of $k$ -means . . . . .	15
<b>3</b>	<b>Supervised Learning without Neural Networks</b>	<b>17</b>
3.1	Linear regression . . . . .	17
3.1.1	Statistical analysis . . . . .	19
3.1.2	Regularization and the bias-variance tradeoff . . . . .	21
3.1.3	Example . . . . .	22
3.2	Linear classifiers and their extensions . . . . .	24
3.2.1	Binary classification and support vector machines . . . . .	24
3.2.2	More than two classes: logistic regression . . . . .	27
<b>4</b>	<b>Supervised Learning with Neural Networks</b>	<b>28</b>
4.1	Computational neurons . . . . .	29
4.2	A simple network structure . . . . .	30
4.3	Training . . . . .	31
4.4	Simple example: MNIST . . . . .	35
4.5	Regularization . . . . .	37
4.6	Convolutional neural networks . . . . .	39
4.6.1	Convolutional layers . . . . .	39
4.6.2	Pooling . . . . .	40
4.6.3	Example: DNA sequencing . . . . .	41
4.6.4	Example: advanced MNIST . . . . .	43
4.7	Recurrent neural networks . . . . .	43
4.7.1	Long short-term memory . . . . .	46
<b>5</b>	<b>Unsupervised Learning</b>	<b>48</b>
5.1	Restricted Boltzmann machine . . . . .	48
5.1.1	Training an RBM . . . . .	50
5.1.2	Example: signal or image reconstruction/denoising . . . . .	52
5.2	Training an RNN without supervision . . . . .	52
5.2.1	Example: generating molecules with an RNN . . . . .	53
5.3	Autoencoders . . . . .	54
5.3.1	Variational autoencoders . . . . .	55
5.4	Generative adversarial networks . . . . .	57
5.4.1	Types of generative models . . . . .	57

5.4.2	The working principle of GANs . . . . .	60
5.4.3	The cost functions . . . . .	61
5.4.4	Remarks . . . . .	61
<b>6</b>	<b>Interpretability of Neural Networks</b>	<b>64</b>
6.1	Dreaming and the problem of extrapolation . . . . .	64
6.2	Adversarial attacks . . . . .	65
6.2.1	Example . . . . .	66
6.3	Interpreting autoencoders . . . . .	68
<b>7</b>	<b>Reinforcement Learning</b>	<b>70</b>
7.1	Exploration versus exploitation . . . . .	71
7.2	Finite Markov decision process . . . . .	71
7.3	Policies and value functions . . . . .	73
7.4	Temporal-difference learning . . . . .	75
7.5	Function approximation . . . . .	77
<b>8</b>	<b>Concluding remarks</b>	<b>78</b>

# 1 Introduction

## 1.1 Why machine learning for the sciences?

Machine learning and artificial neural networks are everywhere and change our daily life more profoundly than we might be aware of. However, these concepts are not a particularly recent invention. Their foundational principles emerged already in the 1940s. The *perceptron*, the predecessor of the artificial neuron, the basic unit of many neural networks to date, was invented by Frank Rosenblatt in 1958, and even cast into a hardware realization by IBM.

It then took half a century for these ideas to become technologically relevant. Now, artificial intelligence based on neural-network algorithms has become an integral part of data processing with widespread applications. The reason for its tremendous success is twofold. First, the availability of big and structured data caters to machine learning applications. Second, the realization that deep (feed-forward) networks (made from many “layers” of artificial neurons) with many variational parameters are tremendously more powerful than few-layer ones was a big leap, the “deep learning revolution”.

Machine learning refers to algorithms that infer information from data in an implicit way. If the algorithms are inspired by the functionality of neural activity in the brain, the term *cognitive* or *neural* computing is used. *Artificial neural networks* refer to a specific, albeit most broadly used, ansatz for machine learning. Another field that concerns itself with inferring information from data is statistics. In that sense, both machine learning and statistics have the same goal. However, the way this goal is achieved is markedly different: while statistics uses insights from mathematics to extract information, machine learning aims at optimizing a variational function using available data through learning.

The mathematical foundations of machine learning with neural networks are poorly understood: we do not know why deep learning works. Nevertheless, there are some exact results for special cases. For instance, certain classes of neural networks are a complete basis of smooth functions, that is, when equipped with enough variational parameters, they can approximate any smooth high-dimensional function with arbitrarily precision. Other variational functions with this property we commonly use are Taylor or Fourier series (with the coefficients as “variational” parameters). We can think of neural networks as a class of variational functions, for which the parameters can be efficiently optimized with respect to a desired objective.

As an example, this objective can be the classification of handwritten digits from ‘0’ to ‘9’. The input to the neural network would be an image of the number, encoded in a vector of grayscale values. The output is a probability distribution saying how likely it is that the image shows a ‘0’, ‘1’, ‘2’, and so on. The variational parameters of the network are adjusted until it accomplishes that task well. This is a classical example of *supervised learning*. To perform the network optimization, we need data consisting of input data (the pixel images) and labels (the integer number shown on the respective image).

Our hope is that the optimized network also recognizes handwritten digits it has not seen during the learning. This property of a network is called *generalization*. It stands in opposition to a tendency called *overfitting*, which means that the network has learned specificities of the data set it was presented with, rather than the ab-



Figure 1: **The MNIST dataset.** Examples of the digits from the handwritten MNIST dataset.

stract features necessary to identify the respective digit. An illustrative example of overfitting is fitting a polynomial of degree 9 to 10 data points, which will always be a perfect fit. Does this mean that this polynomial best characterizes the behavior of the measured system? Of course not! Fighting overfitting and creating algorithms that generalize well are key challenges in machine learning. We will study several approaches to achieve this goal.

Handwritten digit recognition has become one of the standard benchmark problems in the field. Why so? The reason is simple: there exists a very good and freely available data set for it, the MNIST database <sup>1</sup>, see Fig. 1. This curious fact highlights an important aspect of machine learning: it is all about data. The most efficient way to improve machine learning results is to provide more and better data. Thus, one should keep in mind that despite the widespread applications, machine learning is not the hammer for every nail. It is most beneficial if large and **balanced** data sets, meaning roughly that the algorithm can learn all aspects of the problem equally, in a machine-readable way are available.

This lecture is an introduction specifically targeting the use of machine learning in different domains of science. In scientific research, we see a vastly increasing number of applications of machine learning, mirroring the developments in industrial technology. With that, machine learning presents itself as a universal new tool for the exact sciences, standing side-by-side with methods such as calculus, traditional statistics, and numerical simulations. This poses the question, where in the scientific workflow, summerized in Fig. 2, these novel methods are best employed.

Once a specific task has been identified, applying machine learning to the sciences does, furthermore, hold its very specific challenges: (i) scientific data has often very particular structure, such as the nearly perfect periodicity in an image of a crystal; (ii) typically, we have specific knowledge about correlations in the data which should be reflected in a machine learning analysis; (iii) we want to understand why a particular algorithm works, seeking a fundamental insight into mechanisms and laws of nature; (iv) in the sciences we are used to algorithms and laws that provide deterministic answers while machine learning is intrinsically probabilistic - there is no absolute certainty. Nevertheless, quantitative precision is paramount in many areas of science and thus a critical benchmark for machine learning methods.

### A note on the concept of a model

In both machine learning and the sciences, models play a crucial role. However, it is important to recognize the difference in meaning: In the natural sciences, a model is a conceptual representation of a phenomenon. A scientific model does not try to represent the whole world, but only a small part of it. A model is thus

<sup>1</sup><http://yann.lecun.com/exdb/mnist>

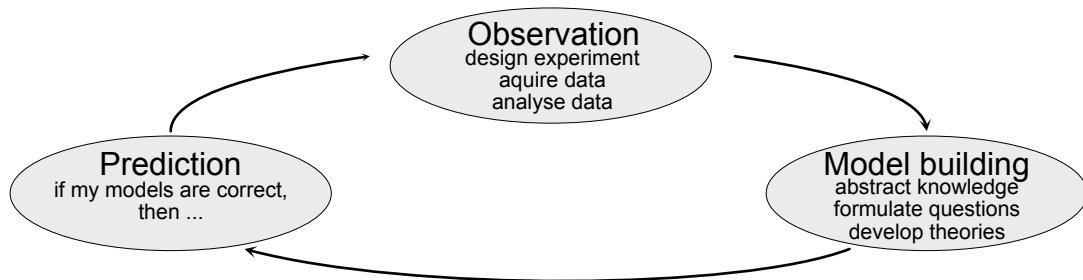


Figure 2: **Simplified scientific workflow.** From observations, via abstraction to building and testing hypothesis or laws, to finally making predictions

a simplification of the phenomenon and can be both a theoretical construct, for example the ideal gas model or the Bohr model of the atom, or an experimental simplification, such as a small version of an airplane in a wind channel.

In machine learning, on the other hand, we most often use a complicated variational function, for example a neural network, to try to approximate a statistical model. But what is a model in statistics? Colloquially speaking, a statistical model comprises a set of statistical assumptions which allow us to calculate the probability  $P(x)$  of *any* event  $x$ . The statistical model does not correspond to the true distribution of all possible events, it simply approximates the distribution. Scientific and statistical models thus share an important property: neither claims to be a representation of reality.

## 1.2 Overview and learning goals

This lecture is an introduction to basic machine learning algorithms for scientists and students of the sciences. We will cover

- the most fundamental machine learning algorithms,
- the terminology of the field, succinctly explained,
- the principles of supervised and unsupervised learning and why it is so successful,
- various architectures of artificial neural networks and the problems they are suitable for,
- how we find out what the machine learning algorithm uses to solve a problem.

The field of machine learning is full of lingo which to the uninitiated obscures what is at the core of the methods. Being a field in constant transformation, new terminology is being introduced at a fast pace. Our aim is to cut through slang with mathematically precise and concise formulations in order to demystify machine learning concepts for someone with an understanding of calculus and linear algebra.

As mentioned above, data is at the core of most machine learning approaches discussed in this lecture. With raw data in many cases very complex and extremely high dimensional, it is often crucial to first understand the data better and reduce their dimensionality. Simple algorithms that can be used before turning to the often heavy machinery of neural networks will be discussed in the next section, Sec. 2.

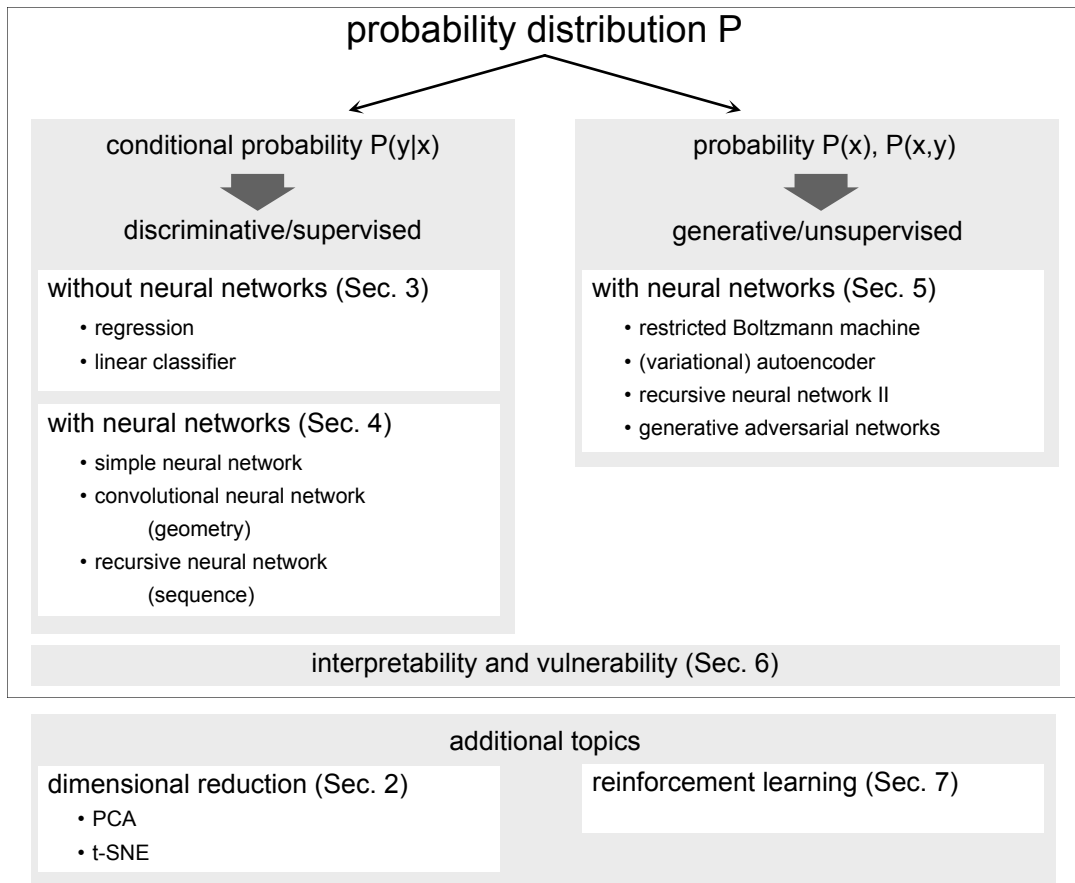


Figure 3: Overview over the plan of the lecture from the perspective of learning probability distributions.

The machine learning algorithms we will focus on most can generally be divided into two classes of algorithms, namely *discriminative* and *generative* algorithms as illustrated in Fig. 3. Examples of discriminative tasks include classification problems, such as the aforementioned digit classification or the classification into solid, liquid and gas phases given some experimental observables. Similarly, regression, in other words estimating relationships between variables, is a discriminative problem. More specifically, we try to approximate the conditional probability distribution  $P(y|x)$  of some variable  $y$  (the label) given some input data  $x$ . As data is provided in the form of input and target data for most of these tasks, these algorithms usually employ supervised learning. Discriminative algorithms are most straight-forwardly applicable in the sciences and we will discuss them in Secs. 3 and 4.

Generative algorithms, on the other hand, model a probability distribution  $P(x)$ . These approaches are—once trained—in principle more powerful, since we can also learn the joint probability distribution  $P(x,y)$  of both the data  $x$  and the labels  $y$  and infer the conditional probability of  $y$ . Still, the more targeted approach of discriminative learning is better suited for many problems. However, generative algorithms are useful in the natural sciences, as we can sample from a known probability distribution, for example for image denoising, or when trying to find new compounds/molecules resembling known ones with given properties. These algo-

rithms are discussed in Sec. 5.

The promise of artificial *intelligence* may trigger unreasonable expectations in the sciences. After all, scientific knowledge generation is one of the most complex intellectual processes. Computer algorithms are certainly far from achieving anything on that level of complexity and will in the near future not formulate new laws of nature independently. Nevertheless, researchers study how machine learning can help with individual segments of the scientific workflow (Fig. 2). While the type of abstraction needed to formulate Newton's laws of classical mechanics seems incredibly complex, neural networks are very good at *implicit knowledge representation*. To understand precisely how they achieve certain tasks, however, is not an easy undertaking. We will discuss this question of *interpretability* in Sec. 6.

A third class of algorithms, which does not neatly fit the framework of approximating a statistical model and thus the distinction into discriminative and generative algorithms is known as reinforcement learning. Instead of approximating a statistical model, reinforcement learning tries to optimize strategies (actions) for achieving a given task. Reinforcement learning has gained a lot of attention with Google's AlphaGo Zero, a computer program that beat the best Go players in the world. As an example for an application in the sciences, reinforcement learning can be used to decide on what experimental configuration to perform next. While the whole topic is beyond the scope of this lecture, we will give an introduction to the basic concepts of reinforcement learning in Sec. 7.

A final note on the practice of learning. While the machine learning machinery is extremely powerful, using an appropriate architecture and the right training details, captured in what are called *hyperparameters*, is crucial for its successful application. Though there are attempts to learn a suitable model and all hyperparameters as part of the overall learning process, this is not a simple task and requires immense computational resources. A large part of the machine learning success is thus connected to the experience of the scientist using the appropriate algorithms. We thus strongly encourage solving the accompanying exercises carefully and taking advantage of the exercise classes.

## 1.3 Resources

While it may seem that implementing ML tasks is computationally challenging, actually almost any ML task one might be interested in can be done with relatively few lines of code simply by relying on external libraries or mathematical computing systems such as Mathematica or Matlab. At the moment, most of the external libraries are written for the Python programming language. Here are some useful Python libraries:

1. **TensorFlow.** Developed by Google, Tensorflow is one of the most popular and flexible library for machine learning with complex models, with full GPU support.
2. **PyTorch.** Developed by Facebook, Pytorch is the biggest rival library to Tensorflow, with pretty much the same functionalities.
3. **Scikit-Learn.** Whereas TensorFlow and PyTorch are catered for deep learning practitioners, Scikit-Learn provides much of the traditional machine learn-

ing tools, including linear regression and PCA.

4. **Pandas.** Modern machine learning is largely reliant on big datasets. This library provides many helpful tools to handle these large datasets.

## 1.4 Prerequisites

This course is aimed at students of the (natural) sciences with a basic mathematics education and some experience in programming. In particular, we assume the following prerequisites:

- Basic knowledge of calculus and linear algebra.
- Rudimentary knowledge of statistics and probability theory (advantageous).
- Basic knowledge of a programming language. For the teaching assignments, you are free to choose your preferable one. The solutions will typically be distributed in Python in the form of Jupyter notebooks.

Please, don't hesitate to ask questions if any notions are unclear.

## 1.5 References

For further reading, we recommend the following books:

- **ML without neural networks:** *The Elements of Statistical Learning*, T. Hastie, R. Tibshirani, and J. Friedman (Springer)
- **ML with neural networks:** *Neural Networks and Deep Learning*, M. Nielson (<http://neuralnetworksanddeeplearning.com>)
- **Deep Learning Theory:** *Deep Learning*, I. Goodfellow, Y. Bengio and A. Courville (<http://www.deeplearningbook.org>)
- **Reinforcement Learning:** *Reinforcement Learning*, R. S. Sutton and A. G. Barto (MIT Press)

## 2 Structuring Data without Neural Networks

Deep learning with neural networks is very much at the forefront of the recent renaissance in machine learning. However, machine learning is not synonymous with neural networks. There is a wealth of machine learning approaches without neural networks, and the boundary between them and conventional statistical analysis is not always sharp.

It is a common misconception that neural network techniques would always outperform these approaches. In fact, in some cases, a simple linear method could achieve faster and better results. Even when we might eventually want to use a deep network, simpler approaches may help to understand the problem we are facing and the specificity of the data so as to better formulate our machine learning strategy. In this chapter, we shall explore machine learning approaches without the use of neural networks. This will further allow us to introduce basic concepts and the general form of a machine learning workflow.

### 2.1 Principle component analysis

At the heart of any machine learning task is data. In order to choose the most appropriate machine learning strategy, it is essential that we understand the data we are working with. However, very often, we are presented with a dataset containing many types of information, called *features* of the data. Such a dataset is also described as being high-dimensional. Techniques that extract information from such a dataset are broadly summarised as *high-dimensional inference*. For instance, we could be interested in predicting the progress of diabetes in patients given features such as age, sex, body mass index, or average blood pressure. Extremely high-dimensional data can occur in biology, where we might want to compare gene expression pattern in cells. Given a multitude of features, it is neither easy to visualise the data nor pick out the most relevant information. This is where *principle component analysis* (PCA) can be helpful.

Very briefly, PCA is a systematic way to find out which feature or combination of features varies the most across the data samples. We can think of PCA as approximating the data with a high-dimensional ellipsoid, where the principal axes of this ellipsoid correspond to the principal components. A feature, which is almost constant across the samples, in other words has a very short principal axis, might not be very useful. PCA then has two main applications: (1) It helps to visualise the data in a low dimensional space and (2) it can reduce the dimensionality of the input data to an amount that a more complex algorithm can handle.

#### PCA algorithm

Given a dataset of  $m$  samples with  $n$  data features, we can arrange our data in the form of a  $m$  by  $n$  matrix  $X$  where the element  $x_{ij}$  corresponds to the value of the  $j$ th data feature of the  $i$ th sample. We will also use the *feature vector*  $\mathbf{x}_i$  for all the  $n$  features of one sample  $i = 1, \dots, m$ . The vector  $\mathbf{x}_i$  can take values in the *feature space*, for example  $\mathbf{x}_i \in \mathbb{R}^n$ . Going back to our diabetes example, we might have 10 data features. Furthermore if we are given information regarding 100 patients, our

data matrix  $X$  would have 100 rows and 10 columns.

The procedure to perform PCA can then be described as follows:

### Algorithm 1: Principle Component Analysis

1. Center the data by subtracting from each column the mean of that column,

$$\mathbf{x}_i \mapsto \mathbf{x}_i - \frac{1}{m} \sum_{i=1}^m \mathbf{x}_i. \quad (2.1)$$

This ensures that the mean of each data feature is zero.

2. Form the  $n$  by  $n$  (unnormalised) covariance matrix

$$C = X^T X = \sum_{i=1}^m \mathbf{x}_i \mathbf{x}_i^T. \quad (2.2)$$

3. Diagonalize the matrix to the form  $C = X^T X = W \Lambda W^T$ , where the columns of  $W$  are the normalised eigenvectors, or principal components, and  $\Lambda$  is a diagonal matrix containing the eigenvalues. It will be helpful to arrange the eigenvalues from largest to smallest.
4. Pick the  $l$  largest eigenvalues  $\lambda_1, \dots, \lambda_l$ ,  $l \leq n$  and their corresponding eigenvectors  $\mathbf{v}_1 \dots \mathbf{v}_l$ . Construct the  $n$  by  $l$  matrix  $\tilde{W} = [\mathbf{v}_1 \dots \mathbf{v}_l]$ .
5. Dimensional reduction: Transform the data matrix as

$$\tilde{X} = X \tilde{W}. \quad (2.3)$$

The transformed data matrix  $\tilde{X}$  now has dimensions  $m$  by  $l$ .

We have thus reduced the dimensionality of the data from  $n$  to  $l$ . Notice that there are actually two things happening: First, of course, we now only have  $l$  data features. But second, the  $l$  data features are new features and not simply a selection of the original data. Rather, they are a linear combination of them. Using our diabetes example again, one of the “new” data features could be the sum of the average blood pressure and the body mass index. These new features are automatically extracted by the algorithm.

But why did we have to go through such an elaborate procedure to do this instead of simply removing a couple of features? The reason is that we want to maximize the *variance* in our data. We will give a precise definition of the variance later in the chapter, but briefly the variance just means the spread of the data. Using PCA, we have essentially obtained  $l$  “new” features which maximise the spread of the data when plotted as a function of this feature. We illustrate this with an example.

### Example

Let us consider a very simple dataset with just 2 data features. We have data, from the Iris dataset <sup>2</sup>, a well known dataset on 3 different species of flowers. We are given information about the petal length and petal width. Since there are just 2 features,

<sup>2</sup><https://archive.ics.uci.edu/ml/datasets/iris>

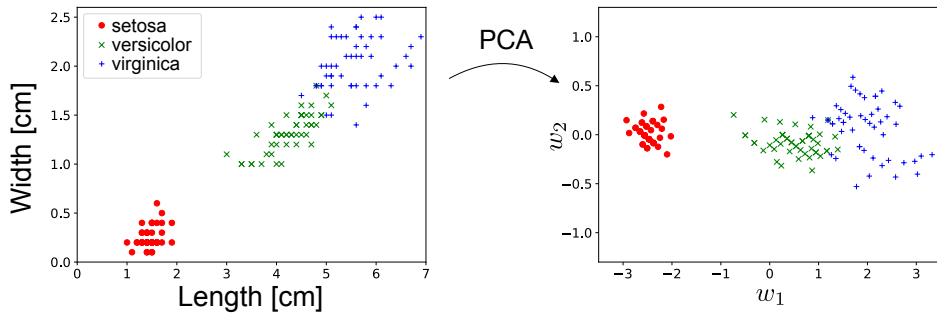


Figure 4: PCA on Iris Dataset.

it is easy to visualise the data. In Fig. 4, we show how the data is transformed under the PCA algorithm.

Notice that there is no dimensional reduction here since  $l = n$ . In this case, the PCA algorithm amounts simply to a rotation of the original data. However, it still produces 2 new features which are orthogonal linear combinations of the original features: petal length and petal width, i.e.

$$\begin{aligned} w_1 &= 0.922 \times \text{Petal Length} + 0.388 \times \text{Petal Width}, \\ w_2 &= -0.388 \times \text{Petal Length} + 0.922 \times \text{Petal Width}. \end{aligned} \quad (2.4)$$

We see very clearly that the first new feature  $w_1$  has a much larger variance than the second feature  $w_2$ . In fact, if we are interested in distinguishing the three different species of flowers, as in a classification task, it's almost sufficient to use only the data feature with the largest variance,  $w_1$ . This is the essence of (PCA) dimensional reduction.

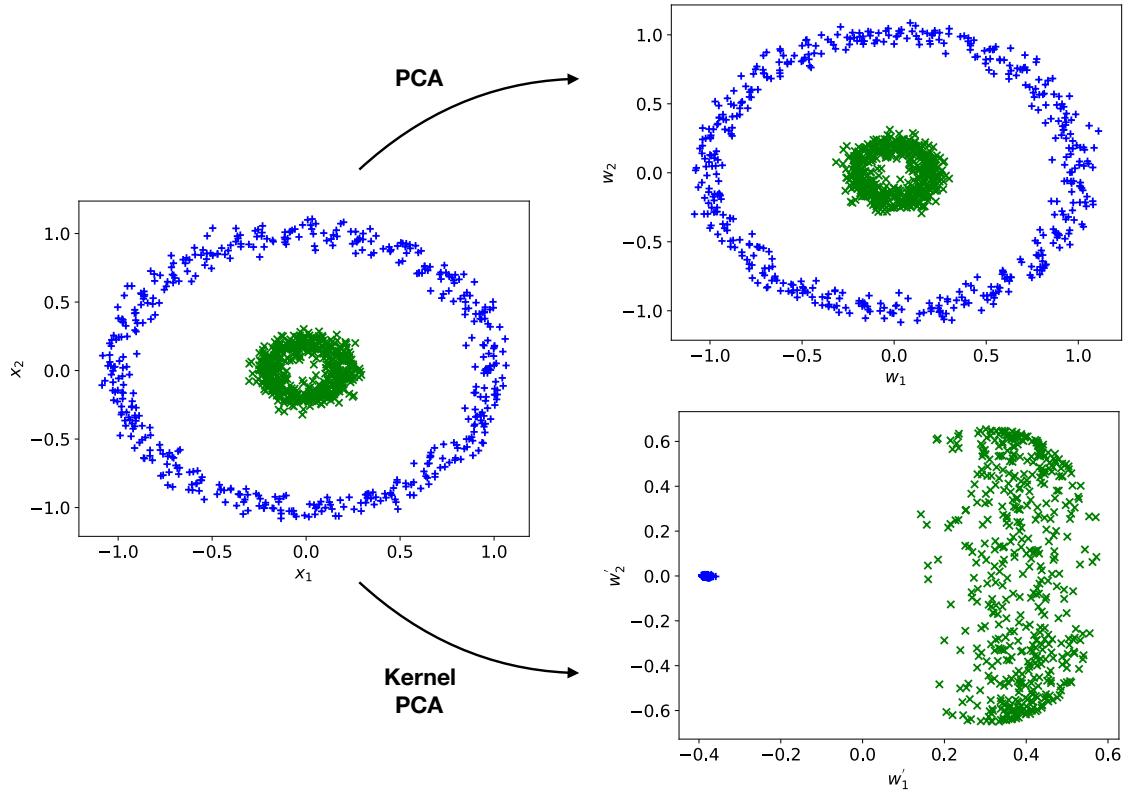
Finally, it is important to note that it is not always true that the feature with the largest variance is the most relevant for the task and it is possible to construct counter examples where the feature with the least variance contains all the useful information. However, PCA is often a good guiding principle and can yield interesting insights in the data. Most importantly, it is also *interpretable*, i.e., not only does it separate the data, but we also learn *which* linear combination of features can achieve this. We will see that for many neural network algorithms, in contrast, a lack of interpretability is a big issue.

## 2.2 Kernel PCA

PCA performs a linear transformation on the data. However, there are cases where such a transformation is unable to produce any meaningful result. Consider for instance the fictitious dataset with 2 classes and 2 data features as shown on the left of Fig. (5). We see by naked eye that it should be possible to separate this data well, for instance by the distance of the datapoint from the origin, but it is also clear that a linear function cannot be used to compute it. In this case, it can be helpful to consider a non-linear extension of PCA, known as *kernel PCA*.

The basic idea of this method is to apply to the data  $\mathbf{x} \in \mathbb{R}^n$  a chosen non-linear vector-valued transformation function  $\Phi(\mathbf{x})$  with

$$\Phi : \mathbb{R}^n \rightarrow \mathbb{R}^N, \quad (2.5)$$

Figure 5: **Kernel PCA versus PCA.**

which is a map from the original  $n$ -dimensional space (corresponding to the  $n$  original data features) to a  $N$ -dimensional feature space. Kernel PCA then simply involves performing the standard PCA on the transformed data  $\Phi(\mathbf{x})$ . Here, we will assume that the transformed data is centered, i.e.,

$$\sum_i \Phi(\mathbf{x}_i) = 0 \quad (2.6)$$

to have simpler formulas.

In practice, when  $N$  is large, it is not efficient or even possible to explicitly perform the transformation  $\Phi$ . Instead we can make use of a method known as the kernel trick. Recall that in standard PCA, the primary aim is to find the eigenvectors and eigenvalues of the covariance matrix  $C$ . In the case of kernel PCA, this matrix becomes

$$C = \sum_{i=1}^m \Phi(\mathbf{x}_i) \Phi(\mathbf{x}_i)^T, \quad (2.7)$$

with the eigenvalue equation

$$\sum_{i=1}^m \Phi(\mathbf{x}_i) \Phi(\mathbf{x}_i)^T \mathbf{v}_j = \lambda_j \mathbf{v}_j. \quad (2.8)$$

By writing the eigenvectors  $\mathbf{v}_j$  as a linear combination of the transformed data features

$$\mathbf{v}_j = \sum_{i=1}^m a_{ji} \Phi(\mathbf{x}_i), \quad (2.9)$$

we see that finding the eigenvectors is equivalent to finding the coefficients  $a_{ji}$ . On substituting this form back into Eq. (2.8), we find

$$\sum_{i=1}^m \Phi(\mathbf{x}_i) \Phi(\mathbf{x}_i)^T \left[ \sum_{i=1}^m a_{ji} \Phi(\mathbf{x}_j) \right] = \lambda_j \left[ \sum_{i=1}^m a_{ji} \Phi(\mathbf{x}_i) \right]. \quad (2.10)$$

By multiplying both sides of the equation by  $\Phi(\mathbf{x}_k)^T$  we arrive at

$$\begin{aligned} \sum_{i=1}^m \Phi(\mathbf{x}_k)^T \Phi(\mathbf{x}_i) \Phi(\mathbf{x}_i)^T \left[ \sum_{l=1}^m a_{jl} \Phi(\mathbf{x}_l) \right] &= \lambda_j \Phi(\mathbf{x}_k)^T \left[ \sum_{l=1}^m a_{jl} \Phi(\mathbf{x}_l) \right] \\ \sum_{i=1}^m [\Phi(\mathbf{x}_k)^T \Phi(\mathbf{x}_i)] \sum_{l=1}^m a_{jl} [\Phi(\mathbf{x}_i)^T \Phi(\mathbf{x}_l)] &= \lambda_j \sum_{l=1}^m a_{jl} [\Phi(\mathbf{x}_k)^T \Phi(\mathbf{x}_l)] \\ \sum_{i=1}^m K(\mathbf{x}_k, \mathbf{x}_i) \sum_{l=1}^m a_{jl} K(\mathbf{x}_i, \mathbf{x}_l) &= \lambda_j \sum_{l=1}^m a_{jl} K(\mathbf{x}_k, \mathbf{x}_l), \end{aligned} \quad (2.11)$$

where  $K(\mathbf{x}, \mathbf{y}) = \Phi(\mathbf{x})^T \Phi(\mathbf{y})$  is known as the *kernel*. Thus we see that if we directly specify the kernels we can avoid explicit performing the transformation  $\Phi$ . In matrix form, we find the eigenvalue equation  $K^2 \mathbf{a}_j = \lambda_j K \mathbf{a}_j$ , which simplifies to

$$K \mathbf{a}_j = \lambda_j \mathbf{a}_j. \quad (2.12)$$

Note that this simplification requires  $\lambda_j \neq 0$ , which will be the case for relevant principle components. (If  $\lambda_j = 0$ , then the corresponding eigenvectors would be irrelevant components to be discarded.) After solving the above equation and obtaining the coefficients  $a_{jl}$ , the kernel PCA transformation is then simply given by the overlap with the eigenvectors  $\mathbf{v}_j$ , i.e.,

$$\mathbf{x} \rightarrow \Phi(\mathbf{x}) \rightarrow y_j = \mathbf{v}_j^T \Phi(\mathbf{x}) = \sum_{i=1}^m a_{ji} \Phi(\mathbf{x}_i)^T \Phi(\mathbf{x}) = \sum_{i=1}^m a_{ji} K(\mathbf{x}_i, \mathbf{x}), \quad (2.13)$$

where once again the explicit  $\Phi$  transformation is avoided.

A common choice for the kernel is known as the radial basis function kernel (RBF) defined by

$$K_{\text{RBF}}(\mathbf{x}, \mathbf{y}) = \exp(-\gamma \|\mathbf{x} - \mathbf{y}\|^2), \quad (2.14)$$

where  $\gamma$  is a tunable parameter. Using the RBF kernel, we compare the result of kernel PCA with that of standard PCA, as shown on the right of Fig. (5). It is clear that kernel PCA leads to a meaningful separation of the data while standard PCA completely fails.

## 2.3 t-SNE as a nonlinear visualization technique

We studied (kernel) PCA as an example for a method that reduces the dimensionality of a dataset and makes features apparent by which data points can be efficiently distinguished. Often, it is desirable to more clearly cluster similar data points and visualize this clustering in a low (two- or three-) dimensional space. We focus our attention on a relatively recent algorithm (from 2008) that has proven very performant. It goes by the name t-distributed stochastic neighborhood embedding (t-SNE).

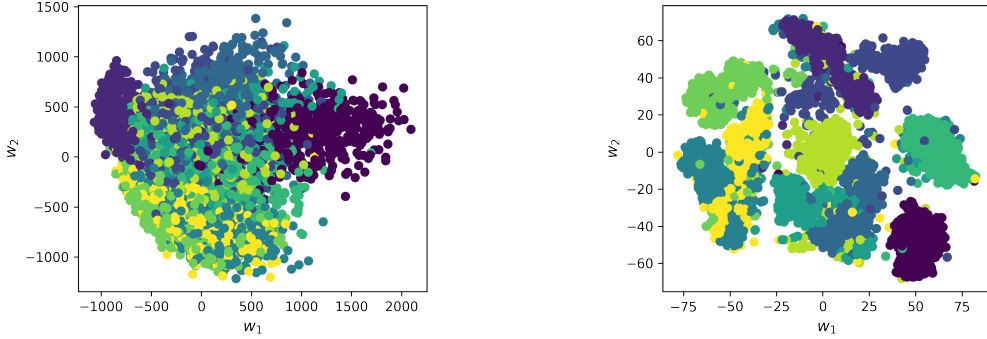


Figure 6: **PCA vs. t-SNE** Application of both methods on 5000 samples from the MNIST handwritten digit dataset. We see that perfect clustering cannot be achieved with either method, but t-SNE delivers the much better result.

The basic idea is to think of the data (images, for instance) as objects  $\mathbf{x}_i$  in a very high-dimensional space and characterize their relation by the Euclidean distance  $\|\mathbf{x}_i - \mathbf{x}_j\|$  between them. These pairwise distances are mapped to a probability distribution  $p_{ij}$ . The same is done for the distances  $\|\mathbf{y}_i - \mathbf{y}_j\|$  of the images of the data points  $\mathbf{y}_i$  in the target low-dimensional space. Their probability distribution is denoted  $q_{ij}$ . The mapping is optimized by changing the locations  $\mathbf{y}_i$  so as to minimize the distance between the two probability distributions. Let us substantiate these words with formulas.

The probability distribution in the space of data points is given as the symmetrized version (joint probability distribution)

$$p_{ij} = \frac{p_{i|j} + p_{j|i}}{2} \quad (2.15)$$

of the conditional probabilities

$$p_{j|i} = \frac{\exp(-\|\mathbf{x}_i - \mathbf{x}_j\|^2/2\sigma_i^2)}{\sum_{k \neq i} \exp(-\|\mathbf{x}_i - \mathbf{x}_k\|^2/2\sigma_i^2)}, \quad (2.16)$$

where the choice of variances  $\sigma_i$  will be explained momentarily. Distances are thus turned into a Gaussian distribution. Note that  $p_{j|i} \neq p_{i|j}$  while  $p_{ji} = p_{ij}$ .

The probability distribution in the target space is chosen to be a Student t-distribution

$$q_{ij} = \frac{(1 + \|\mathbf{y}_i - \mathbf{y}_j\|^2)^{-1}}{\sum_{k \neq l} (1 + \|\mathbf{y}_k - \mathbf{y}_l\|^2)^{-1}}. \quad (2.17)$$

This choice has several advantages: (i) it is symmetric upon interchanging  $i$  and  $j$ , (ii) it is numerically more efficiently evaluated because there are no exponentials, (iii) it has 'fatter' tails which helps to produce more meaningful maps in the lower dimensional space.

Let us now discuss the choice of  $\sigma_i$ . Intuitively, in dense regions of the dataset, a smaller value of  $\sigma_i$  is usually more appropriate than in sparser regions, in order to resolve the distances better. Any particular value of  $\sigma_i$  induces a probability distribution  $P_i$  over all the other data points. This distribution has an *entropy* (here we use the Shannon entropy, in general it is a measure for the "uncertainty"

represented by the distribution)

$$H(P_i) = - \sum_j p_{j|i} \log_2 p_{j|i}. \quad (2.18)$$

The value of  $H(P_i)$  increases as  $\sigma_i$  increases, i.e., the more uncertainty is added to the distances. The algorithm searches for the  $\sigma_i$  that result in a  $P_i$  with fixed perplexity

$$\text{Perp}(P_i) = 2^{H(P_i)}. \quad (2.19)$$

The target value of the perplexity is chosen a priori and is the main parameter that controls the outcome of the t-SNE algorithm. It can be interpreted as a smooth measure for the effective number of neighbors. Typical values for the perplexity are between 5 and 50.

Finally, we have to introduce a measure for the similarity between the two probability distributions  $p_{ij}$  and  $q_{ij}$ . This defines a so-called *loss function*. Here, we choose the *Kullback-Leibler* divergence

$$L(\{\mathbf{y}_i\}) = \sum_i \sum_j p_{ij} \log \frac{p_{ij}}{q_{ij}}, \quad (2.20)$$

which we will frequently encounter during this lecture. The symmetrized  $p_{ij}$  ensures that  $\sum_j p_{ij} > 1/(2n)$ , so that each data point makes a significant contribution to the cost function. The minimization of  $L(\{\mathbf{y}_i\})$  with respect to the positions  $\mathbf{y}_i$  can be achieved with a variety of methods. In the simplest case it can be gradient descent, which we will discuss in more detail in a later chapter. As the name suggests, it follows the direction of largest gradient of the cost function to find the minimum. To this end it is useful that these gradients can be calculated in a simple form

$$\frac{\partial L}{\partial \mathbf{y}_i} = 4 \sum_j (p_{ij} - q_{ij}) (\mathbf{y}_i - \mathbf{y}_j) (1 + \|\mathbf{y}_i - \mathbf{y}_j\|^2)^{-1}. \quad (2.21)$$

By now, t-SNE is implemented as standard in many packages. They involve some extra tweaks that force points  $\mathbf{y}_i$  to stay close together at the initial steps of the optimization and create a lot of empty space. This facilitates the moving of larger clusters in early stages of the optimization until a globally good arrangement is found. If the dataset is very high-dimensional it is advisable to perform an initial dimensionality reduction (to somewhere between 10 and 100 dimensions, for instance) with PCA before running t-SNE.

While t-SNE is a very powerful clustering technique, it has its limitations. (i) The target dimension should be 2 or 3, for much larger dimensions ansatz for  $q_{ij}$  is not suitable. (ii) If the dataset is intrinsically high-dimensional (so that also the PCA pre-processing fails), t-SNE may not be a suitable technique. (iii) Due to the stochastic nature of the optimization, results are not reproducible. The result may end up looking very different when the algorithm is initialized with some slightly different initial values for  $\mathbf{y}_i$ .

## 2.4 Clustering algorithms: the example of $k$ -means

All of PCA, kernel-PCA and t-SNE may or may not deliver a visualization of the dataset, where clusters emerge. They all leave it to the observer to identify these

possible clusters. In this section, we want to introduce an algorithm that actually clusters data, i.e., it will sort any data point into one of  $k$  clusters. Here the desired number of clusters  $k$  is fixed a priori by us. This is a weakness but may be compensated by running the algorithm with different values of  $k$  and asses where the performance is best.

We will exemplify a simple clustering algorithm that goes by the name  $k$ -means. The algorithm is iterative. The key idea is that data points are assigned to clusters such that the squared distances between the data points belonging to one cluster and the centroid of the cluster is minimized. The centroid is defined as the arithmetic mean of all data points in a cluster.

This description already suggests, that we will again minimize a loss function (or maximize an expectation function, which just differs in the overall sign from the loss function). Suppose we are given an assignment of datapoints  $\mathbf{x}_i$  to clusters  $j = 1, \dots, k$  that is represented by

$$w_{ij} = \begin{cases} 1, & \mathbf{x}_i \text{ in cluster } j, \\ 0, & \mathbf{x}_i \text{ not in cluster } j. \end{cases} \quad (2.22)$$

Then the loss function is given by

$$L(\{\mathbf{x}_i\}, \{w_{ij}\}) = \sum_{i=1}^m \sum_{j=1}^k w_{ij} \|\mathbf{x}_i - \boldsymbol{\mu}_j\|^2, \quad (2.23)$$

where

$$\boldsymbol{\mu}_j = \frac{\sum_i w_{ij} \mathbf{x}_i}{\sum_i w_{ij}}. \quad (2.24)$$

Naturally, we want to minimize the loss function with respect to the assignment  $w_{ij}$ . However, a change in this assignment also changes  $\boldsymbol{\mu}_j$ . For this reason, it is natural to divide each update step in two parts. The first part updates the  $w_{ij}$  according to

$$w_{ij} = \begin{cases} 1, & \text{if } j = \operatorname{argmin}_l \|\mathbf{x}_i - \boldsymbol{\mu}_l\|, \\ 0, & \text{else.} \end{cases} \quad (2.25)$$

That means we attach each data point to the nearest cluster centroid. The second part is a recalculation of the centroids according to Eq. (2.24).

The algorithm is initialized by choosing at random  $k$  distinct data points as initial positions of the centroids. Then one repeats the above two-part steps until convergence, i.e., until the  $w_{ij}$  do not change anymore.

In this algorithm we use the Euclidean distance measure  $\|\cdot\|$ . It is advisable to standardize the data such that each feature has mean zero and standard deviation of one when average over all data points. Otherwise (if some features are overall numerically smaller than others), the differences in various features may be weighted very differently by the algorithm.

Furthermore, the results depend on the initialization. One should re-run the algorithm with a few different initializations to avoid running into bad local minima.

Applications of  $k$ -means are manifold: in economy they include marked segmentation, in science any classification problem such as that of phases of matter, document clustering, image compression (color reduction), etc.. In general it helps to build intuition about the data at hand.

# 3 Supervised Learning without Neural Networks

*Supervised learning* is the term for a machine learning task, where we are given a dataset consisting of input-output pairs  $\{(\mathbf{x}_1, y_1), \dots, (\mathbf{x}_m, y_m)\}$  and our task is to "learn" a function which maps input to output  $f : \mathbf{x} \mapsto y$ . Here we chose a vector-valued input  $\mathbf{x}$  and only a single real number as output  $y$ , but in principle also the output can be vector valued. The output data that we have is called the *ground truth* and sometimes also referred to as "labels" of the input. In contrast to supervised learning, all algorithms presented so far were unsupervised, because they just relied on input-data, without any ground truth or output data.

Within the scope of supervised learning, there are two main types of tasks: *Classification* and *Regression*. In a classification task, our output  $y$  is a discrete variable corresponding to a classification category. An example of such a task would be to distinguish stars with a planetary system (exoplanets) from those without given time series of images of such objects. On the other hand, in a regression problem, the output  $y$  is a continuous number or vector. For example predicting the quantity of rainfall based on meteorological data from the previous days.

In this section, we first familiarize ourselves with linear methods for achieving these tasks. Neural networks, in contrast, are a non-linear method for supervised classification and regression tasks.

## 3.1 Linear regression

Linear regression, as the name suggests, simply means to fit a linear model to a dataset. Consider a dataset consisting of input-output pairs  $\{(\mathbf{x}_1, y_1), \dots, (\mathbf{x}_m, y_m)\}$ , where the inputs are  $n$ -component vectors  $\mathbf{x}^T = (x_1, x_2, \dots, x_n)$  and the output  $y$  is a real-valued number. The linear model then takes the form

$$f(\mathbf{x}|\boldsymbol{\beta}) = \beta_0 + \sum_{j=1}^n \beta_j x_j \quad (3.1)$$

or in matrix notation

$$f(\mathbf{x}|\boldsymbol{\beta}) = \tilde{\mathbf{x}}^T \boldsymbol{\beta} \quad (3.2)$$

where  $\tilde{\mathbf{x}}^T = (1, x_1, x_2, \dots, x_n)$  and  $\boldsymbol{\beta} = (\beta_0, \dots, \beta_n)^T$  are  $(n+1)$  dimensional row vectors.

The aim then is to find parameters  $\hat{\boldsymbol{\beta}}$  such that  $f(\mathbf{x}|\hat{\boldsymbol{\beta}})$  is a good *estimator* for the output value  $y$ . In order to quantify what it means to be a "good" estimator, one need to specify a real-valued *loss function*  $L(\boldsymbol{\beta})$ , sometimes also called a *cost function*. The good set of parameters  $\hat{\boldsymbol{\beta}}$  is then the minimizer of this loss function

$$\hat{\boldsymbol{\beta}} = \underset{\boldsymbol{\beta}}{\operatorname{argmin}} L(\boldsymbol{\beta}). \quad (3.3)$$

There are many, inequivalent, choices for this loss function. For our purpose, we

choose the loss function to be *residual sum of squares* (RSS) defined as

$$\begin{aligned}\text{RSS}(\boldsymbol{\beta}) &= \sum_{i=1}^m [y_i - f(\mathbf{x}_i | \boldsymbol{\beta})]^2 \\ &= \sum_{i=1}^m \left( y_i - \beta_0 - \sum_{j=1}^n \beta_j x_{ij} \right)^2,\end{aligned}\tag{3.4}$$

where the sum runs over the  $m$  samples of the dataset. This loss function is sometimes also called the *L2-loss* and can be seen as a measure of the distance between the output values from the dataset  $y_i$  and the corresponding predictions  $f(\mathbf{x}_i | \boldsymbol{\beta})$ .

It is convenient to define the  $m$  by  $(n + 1)$  data matrix  $\widetilde{X}$ , each row of which corresponds to an input sample  $\tilde{\mathbf{x}}_i^T$ , as well as the output vector  $\mathbf{Y}^T = (y_1, \dots, y_m)$ . With this notation, Eq. (3.4) can be expressed succinctly as a matrix equation

$$\text{RSS}(\boldsymbol{\beta}) = (\mathbf{Y} - \widetilde{X}\boldsymbol{\beta})^T(\mathbf{Y} - \widetilde{X}\boldsymbol{\beta}).\tag{3.5}$$

The minimum of  $\text{RSS}(\boldsymbol{\beta})$  can be easily solved by considering the partial derivatives with respect to  $\boldsymbol{\beta}$ , i.e.,

$$\begin{aligned}\frac{\partial \text{RSS}}{\partial \boldsymbol{\beta}} &= -2\widetilde{X}^T(\mathbf{Y} - \widetilde{X}\boldsymbol{\beta}), \\ \frac{\partial^2 \text{RSS}}{\partial \boldsymbol{\beta} \partial \boldsymbol{\beta}^T} &= 2\widetilde{X}^T\widetilde{X}.\end{aligned}\tag{3.6}$$

At the minimum,  $\frac{\partial \text{RSS}}{\partial \boldsymbol{\beta}} = 0$  and  $\frac{\partial^2 \text{RSS}}{\partial \boldsymbol{\beta} \partial \boldsymbol{\beta}^T}$  is positive-definite. Assuming  $\widetilde{X}^T\widetilde{X}$  is full-rank and hence invertible, we can obtain the solution  $\hat{\boldsymbol{\beta}}$  as

$$\begin{aligned}\frac{\partial \text{RSS}}{\partial \boldsymbol{\beta}} \bigg|_{\boldsymbol{\beta}=\hat{\boldsymbol{\beta}}} &= 0, \\ \implies \widetilde{X}^T\widetilde{X}\hat{\boldsymbol{\beta}} &= \widetilde{X}^T\mathbf{Y}, \\ \implies \hat{\boldsymbol{\beta}} &= (\widetilde{X}^T\widetilde{X})^{-1}\widetilde{X}^T\mathbf{Y}.\end{aligned}\tag{3.7}$$

If  $\widetilde{X}^T\widetilde{X}$  is not full-rank, which can happen if certain data features are perfectly correlated (e.g.,  $x_1 = 2x_3$ ), the solution to  $\widetilde{X}^T\widetilde{X}\boldsymbol{\beta} = \widetilde{X}^T\mathbf{Y}$  can still be found, but it would not be unique. Note that the RSS is not the only possible choice for the loss function and a different choice would lead to a different solution.

What we have done so far is uni-variate linear regression, that is linear regression where the output  $y$  is a single real-valued number. The generalisation to the multi-variate case, where the output is a  $p$ -component vector  $\mathbf{y}^T = (y_1, \dots, y_p)$ , is straightforward. The model takes the form

$$f_k(\mathbf{x} | \boldsymbol{\beta}) = \beta_{0k} + \sum_{j=1}^n \beta_{jk} x_j.\tag{3.8}$$

where the parameters  $\beta_{jk}$  now have an additional index  $k = 1, \dots, p$ . Considering the parameters  $\boldsymbol{\beta}$  as a  $(n + 1)$  by  $p$  matrix, we can show that the solution takes the same form as before [Eq. (3.7)] with  $Y$  as a  $m$  by  $p$  output matrix.

### 3.1.1 Statistical analysis

Let us stop here and evaluate the quality of the method we have just introduced. At the same time, we will take the opportunity to introduce some statistics notions, which will be useful throughout the book.

Up to now, we have made no assumptions about the dataset we are given, we simply stated that it consisted of input-output pairs,  $\{(\mathbf{x}_1, y_1), \dots, (\mathbf{x}_m, y_m)\}$ . In order to assess the accuracy of our model in a mathematically clean way, we have to make an additional assumption. The output data  $y_1, \dots, y_m$  may arise from some measurement or observation. Then, each of these values will generically be subject to errors  $\epsilon_1, \dots, \epsilon_m$  by which the values deviate from the “true” output without errors,

$$y_i = y_i^{\text{true}} + \epsilon_i, \quad i = 1, \dots, m. \quad (3.9)$$

We assume that this error  $\epsilon$  is a Gaussian random variable with mean  $\mu = 0$  and variance  $\sigma^2$ , which we denote by  $\epsilon \sim \mathcal{N}(0, \sigma^2)$ . Assuming that a linear model in Eq. (3.1) is a suitable model for our dataset, we are interested in the following question: How does our solution  $\hat{\beta}$  as given in Eq. (3.7) compare with the true solution  $\beta^{\text{true}}$  which obeys

$$y_i = \beta_0^{\text{true}} + \sum_{j=1}^n \beta_j^{\text{true}} x_{ij} + \epsilon_i, \quad i = 1, \dots, m? \quad (3.10)$$

In order to make statistical statements about this question, we have to imagine that we can fix the inputs  $\mathbf{x}_i$  of our dataset and repeatedly draw samples for our outputs  $y_i$ . Each time we will obtain a different value for  $y_i$  following Eq. (3.10), in other words the  $\epsilon_i$  are uncorrelated random numbers. This allows us to formalise the notion of an *expectation value*  $E(\dots)$  as the average over an infinite number of draws. For each draw, we obtain a new dataset, which differs from the other ones by the values of the outputs  $y_i$ . With each of these datasets, we obtain a different solution  $\hat{\beta}$  as given by Eq. (3.7). The expectation value  $E(\hat{\beta})$  is then simply the average value we obtained across an infinite number of datasets. The deviation of this average value from the “true” value given perfect data is called the *bias* of the model,

$$\text{Bias}(\hat{\beta}) = E(\hat{\beta}) - \beta^{\text{true}}. \quad (3.11)$$

For the linear regression we study here, the bias is exactly zero, because

$$\begin{aligned} E(\hat{\beta}) &= E\left((\widetilde{X}^T \widetilde{X})^{-1} \widetilde{X}^T (\mathbf{Y}^{\text{true}} + \epsilon)\right) \\ &= \beta^{\text{true}}, \end{aligned} \quad (3.12)$$

where the second line follows because  $E(\epsilon) = \mathbf{0}$  and  $(\widetilde{X}^T \widetilde{X})^{-1} \widetilde{X}^T \mathbf{Y}^{\text{true}} = \beta^{\text{true}}$ . Equation (3.12) implies linear regression is unbiased. Note that other machine learning algorithms will in general be biased.

What about the standard error or uncertainty of our solution? This information is contained in the *covariance matrix*

$$\text{Var}(\hat{\beta}) = E\left([\hat{\beta} - E(\hat{\beta})][\hat{\beta} - E(\hat{\beta})]^T\right). \quad (3.13)$$

The covariance matrix can be computed for the case of linear regression using the solution in Eq. (3.7), the expectation value in Eq. (3.12) and the assumption in Eq. (3.10) that  $Y = Y^{\text{true}} + \epsilon$  yielding

$$\begin{aligned}\text{Var}(\hat{\beta}) &= E\left([\hat{\beta} - E(\hat{\beta})][\hat{\beta} - E(\hat{\beta})]^T\right) \\ &= E\left(\left[(\tilde{X}^T \tilde{X})^{-1} \tilde{X}^T \epsilon\right] \left[(\tilde{X}^T \tilde{X})^{-1} \tilde{X}^T \epsilon\right]^T\right) \\ &= E\left((\tilde{X}^T \tilde{X})^{-1} \tilde{X}^T \epsilon \epsilon^T \tilde{X} (\tilde{X}^T \tilde{X})^{-1}\right).\end{aligned}\quad (3.14)$$

This expression can be simplified by using the fact that our input matrices  $\tilde{X}$  are independent of the draw such that

$$\begin{aligned}\text{Var}(\hat{\beta}) &= (\tilde{X}^T \tilde{X})^{-1} \tilde{X}^T E(\epsilon \epsilon^T) \tilde{X} (\tilde{X}^T \tilde{X})^{-1} \\ &= (\tilde{X}^T \tilde{X})^{-1} \tilde{X}^T \sigma^2 I \tilde{X} (\tilde{X}^T \tilde{X})^{-1} \\ &= \sigma^2 (\tilde{X}^T \tilde{X})^{-1}.\end{aligned}\quad (3.15)$$

Here, the second line follows from the fact that different samples are uncorrelated, which implies that  $E(\epsilon \epsilon^T) = \sigma^2 I$  with  $I$  the identity matrix. The diagonal elements of  $\sigma^2 (\tilde{X}^T \tilde{X})^{-1}$  then correspond to the variance

$$\begin{aligned}\text{Var}(\hat{\beta}) &= E\left([\hat{\beta} - E(\hat{\beta})][\hat{\beta} - E(\hat{\beta})]^T\right) \\ &= \sigma^2 (\tilde{X}^T \tilde{X})^{-1}.\end{aligned}\quad (3.16)$$

of the individual parameters  $\beta_i$ . The standard error or uncertainty is then  $\sqrt{\text{Var}(\hat{\beta}_i)}$ .

There is one more missing element: we have not explained how to obtain the variances  $\sigma^2$  of the outputs  $y$ . In an actual machine learning task, we would not know anything about the true relation, as given in Eq. (3.10), governing our dataset. The only information we have access to is a single dataset. Therefore, we have to estimate the variance using the samples in our dataset, which is given by

$$\hat{\sigma}^2 = \frac{1}{m - n - 1} \sum_{i=1}^m (y_i - f(\mathbf{x}_i | \hat{\beta}))^2, \quad (3.17)$$

where  $y_i$  are the output values from our dataset and  $f(\mathbf{x}_i | \hat{\beta})$  is the corresponding prediction. Note that we normalized the above expression by  $(m - n - 1)$  instead of  $m$  to ensure that  $E(\hat{\sigma}^2) = \sigma^2$ , meaning that  $\hat{\sigma}^2$  is an unbiased estimator of  $\sigma^2$ .

Our ultimate goal is not simply to fit a model to the dataset. We want our model to generalize to inputs not within the dataset. To assess how well this is achieved, let us consider the prediction  $\tilde{\mathbf{a}}^T \hat{\beta}$  on a new random input-output pair  $(\mathbf{a}, y_0)$ . The output is again subject to an error  $y_0 = \tilde{\mathbf{a}}^T \beta^{\text{true}} + \epsilon$ . In order to compute the expected error of the prediction, we compute the expectation value of the loss function over these previously unseen data. This is also known as the *test or generalization error*. For the square-distance loss function, this is the *mean square error* (MSE)

$$\begin{aligned}\text{MSE}(\hat{\beta}) &= E\left((y_0 - \tilde{\mathbf{a}}^T \hat{\beta})^2\right) \\ &= E\left((\epsilon + \tilde{\mathbf{a}}^T \beta^{\text{true}} - \tilde{\mathbf{a}}^T \hat{\beta})^2\right) \\ &= E(\epsilon^2) + [\tilde{\mathbf{a}}^T (\beta^{\text{true}} - E(\hat{\beta}))]^2 + E\left([\tilde{\mathbf{a}}^T (\hat{\beta} - E(\hat{\beta}))]^2\right) \\ &= \sigma^2 + [\tilde{\mathbf{a}}^T \text{Bias}(\hat{\beta})]^2 + \tilde{\mathbf{a}}^T \text{Var}(\hat{\beta}) \tilde{\mathbf{a}}.\end{aligned}\quad (3.18)$$

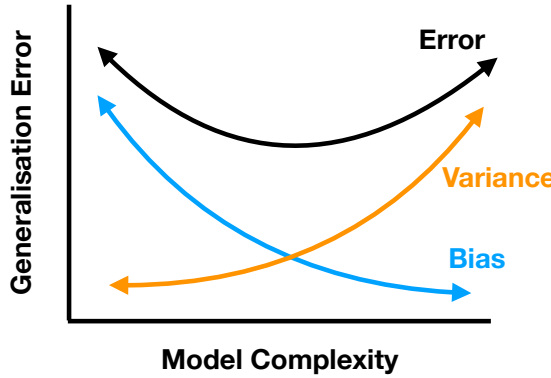


Figure 7: Schematic depiction of the bias-variance tradeoff.

There are three terms in the expression. The first term is the irreducible or intrinsic uncertainty of the dataset. The second term represents the bias and the third term is the variance of the model. For RSS linear regression, the estimate is unbiased so that

$$\text{MSE}(\hat{\boldsymbol{\beta}}) = \sigma^2 + \tilde{\mathbf{a}}^T \text{Var}(\hat{\boldsymbol{\beta}}) \tilde{\mathbf{a}}. \quad (3.19)$$

Based on the assumption that the dataset indeed derives from a linear model as given by Eq. (3.10) with a Gaussian error, it can be shown that the RSS solution, Eq. (3.7), gives the minimum error among all unbiased linear estimators, Eq. (3.1). This is known as the Gauss-Markov theorem.

This completes our error analysis of the method.

### 3.1.2 Regularization and the bias-variance tradeoff

Although the RSS solution has the minimum error among unbiased linear estimators, the expression for the generalisation error, Eq. (3.18), suggests that we can actually still reduce the error by sacrificing some bias in our estimate.

A possible way to reduce generalisation error is actually to drop some data features. From the  $n$  data features  $\{x_1, \dots, x_n\}$ , we can pick a reduced set  $\mathcal{M}$ . For example, we can choose  $\mathcal{M} = \{x_1, x_3, x_7\}$ , and define our new linear model as

$$f(\mathbf{x}|\boldsymbol{\beta}) = \beta_0 + \sum_{j \in \mathcal{M}} \beta_j x_j. \quad (3.20)$$

This is equivalent to fixing some parameters to zero, i.e.,  $\beta_k = 0$  if  $x_k \notin \mathcal{M}$ . Minimizing the RSS with this constraint results in a biased estimator but the reduction in model variance can sometimes help to reduce the overall generalisation error. For a small number of features  $n \sim 20$ , one can search exhaustively for the best subset of features that minimises the error, but beyond that the search becomes computationally unfeasible.

A common alternative is called *ridge regression*. In this method, we consider the same linear model given in Eq. (3.1) but with a modified loss function

$$L_{\text{ridge}}(\boldsymbol{\beta}) = \sum_{i=1}^m [y_i - f(\mathbf{x}_i|\boldsymbol{\beta})]^2 + \lambda \sum_{j=0}^n \beta_j^2, \quad (3.21)$$

where  $\lambda > 0$  is a positive parameter. This is almost the same as the RSS apart from the term proportional to  $\lambda$  [c.f. Eq. (3.4)]. The effect of this new term is to

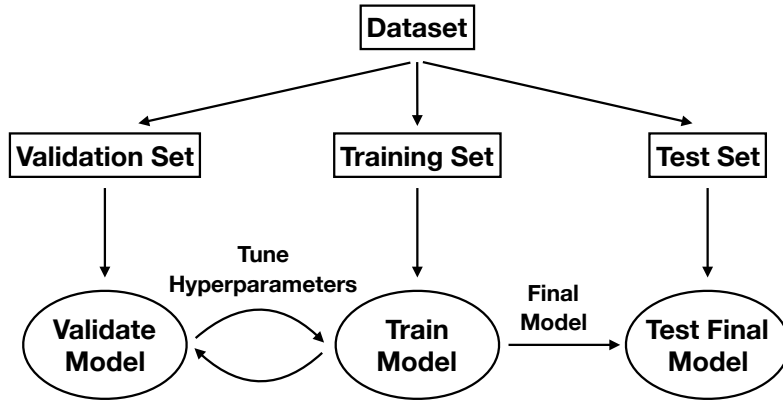


Figure 8: Machine Learning Workflow.

penalize large parameters  $\beta_j$  and bias the model towards smaller absolute values. The parameter  $\lambda$  is an example of a *hyper-parameter*, which is kept fixed during the training. On fixing  $\lambda$  and minimising the loss function, we obtain the solution

$$\hat{\beta}_{\text{ridge}} = (\widetilde{X}^T \widetilde{X} + \lambda I)^{-1} \widetilde{X}^T \mathbf{Y}, \quad (3.22)$$

from which we can see that as  $\lambda \rightarrow \infty$ ,  $\hat{\beta}_{\text{ridge}} \rightarrow \mathbf{0}$ . By computing the bias and variance,

$$\begin{aligned} \text{Bias}(\hat{\beta}_{\text{ridge}}) &= -\lambda(\widetilde{X}^T \widetilde{X} + \lambda I)^{-1} \beta^{\text{true}} \\ \text{Var}(\hat{\beta}_{\text{ridge}}) &= \sigma^2(\widetilde{X}^T \widetilde{X} + \lambda I)^{-1} \widetilde{X}^T \widetilde{X} (\widetilde{X}^T \widetilde{X} + \lambda I)^{-1}, \end{aligned} \quad (3.23)$$

it is also obvious that increasing  $\lambda$  increases the bias, while reducing the variance. This is the tradeoff between bias and variance. By appropriately choosing  $\lambda$  it is possible that generalisation error can be reduced. We will introduce in the next section a common strategy how to find the optimal value for  $\lambda$ .

The techniques presented here to reduce the generalization error, namely dropping of features and biasing the model to small parameters, are part of a large class of methods known as *regularization*. Comparing the two methods, we can see a similarity. Both methods actually reduce the complexity of our model. In the former, some parameters are set to zero, while in the latter, there is a constraint which effectively reduces the magnitude of all parameters. A less complex model has a smaller variance but larger bias. By balancing these competing effects, generalisation can be improved, as illustrated schematically in Fig. 7.

In the next chapter, we will see that these techniques are useful beyond applications to linear methods. We illustrate the different concepts in the following example.

### 3.1.3 Example

We illustrate the concepts of linear regression using a medical dataset. In the process, we will also familiarize ourselves with the standard machine learning workflow [see Fig. 8]. For this example, we are given 10 data features, namely age, sex, body mass index, average blood pressure, and six blood serum measurements from 442 diabetes

patients, and our task is train a model  $f(\mathbf{x}|\boldsymbol{\beta})$  [Eq. (3.1)] to predict a quantitative measure of the disease progression after one year.

Recall that the final aim of a machine-learning task is not to obtain the smallest possible value for the loss function such as the RSS, but to minimise the generalisation error on unseen data [c.f. Eq. (3.18)]. The standard approach relies on a division of the dataset into three subsets: training set, validation set and test set. The standard workflow is summarised in Box 1.

**Box 1: ML Workflow**

1. Divide the dataset into training set  $\mathcal{T}$ , validation set  $\mathcal{V}$  and test set  $\mathcal{S}$ . A common ratio for the split is 70 : 15 : 15.
2. Pick the hyperparameters, e.g.,  $\lambda$  in Eq. (3.21).
3. Train the model with only the training set, in other words minimize the loss function on the training set. [This corresponds to Eq. (3.7) or (3.22) for the linear regression, where  $\widetilde{X}$  only contains the training set.]
4. Evaluate the MSE (or any other chosen metric) on the validation set, [c.f. Eq. (3.18)]

$$\text{MSE}_{\text{validation}}(\hat{\boldsymbol{\beta}}) = \frac{1}{|\mathcal{V}|} \sum_{j \in \mathcal{V}} (y_j - f(\mathbf{x}_j | \hat{\boldsymbol{\beta}}))^2. \quad (3.24)$$

This is known as the *validation error*.

5. Pick a different value for the hyperparameters and repeat steps 3 and 4, until validation error is minimized.
6. Evaluate the final model on the test set

$$\text{MSE}_{\text{test}}(\hat{\boldsymbol{\beta}}) = \frac{1}{|\mathcal{S}|} \sum_{j \in \mathcal{S}} (y_j - f(\mathbf{x}_j | \hat{\boldsymbol{\beta}}))^2. \quad (3.25)$$

It is important to note that the test set  $\mathcal{S}$  was not involved in optimizing either parameters  $\boldsymbol{\beta}$  or the hyperparameters such as  $\lambda$ .

Applying this procedure to the diabetes dataset<sup>3</sup>, we obtain the results in Fig. 9. We compare RSS linear regression with the ridge regression, and indeed we see that by appropriately choosing the regularisation hyperparameter  $\lambda$ , the generalisation error can be minimized.

As side remark regarding the ridge regression, we can see on the left of Fig. 10, that as  $\lambda$  increases, the magnitude of the parameters, Eq. (3.22),  $\hat{\boldsymbol{\beta}}_{\text{ridge}}$  decreases. Consider on the other hand, a different form of regularisation, which goes by the name *lasso regression*, where the loss function is given by

$$L_{\text{lasso}}(\boldsymbol{\beta}) = \sum_{i=1}^m [y_i - f(\mathbf{x}_i | \boldsymbol{\beta})]^2 + \alpha \sum_{j=0}^n |\beta_j|. \quad (3.26)$$

Despite the similarities, lasso regression has a very different behaviour as depicted on the right of Fig. 10. Notice that as  $\alpha$  increases some parameters actually vanish

<sup>3</sup>Source: <https://www4.stat.ncsu.edu/~boos/var.select/diabetes.html>

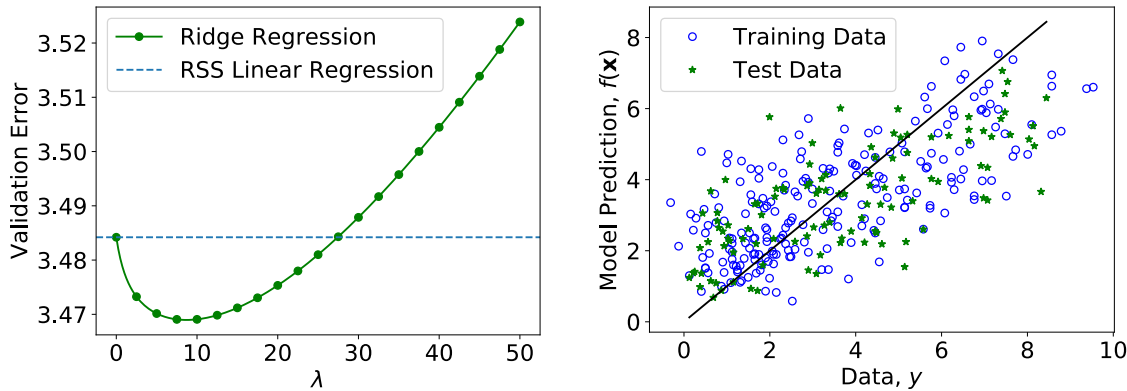


Figure 9: **Ridge Regression on Diabetes patients dataset.** Left: Validation error versus  $\lambda$ . Right: Test data versus the prediction from the trained model. If the prediction were free of any error, all the points would fall on the blue line.

and can be ignored completely. This actually corresponds to dropping certain data features completely and can be useful if we are interested in selecting the most important features in a dataset.

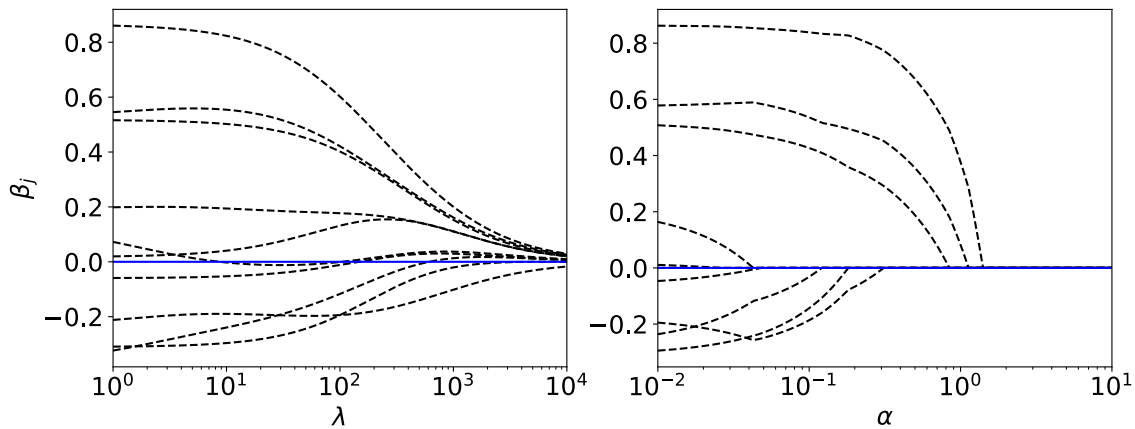


Figure 10: **Evolution of the model parameters.** Increasing the hyperparameter  $\lambda$  or  $\alpha$  leads to a reduction of the absolute value of the model parameters, here shown for the ridge (left) and Lasso (right) regression for the Diabetes dataset.

## 3.2 Linear classifiers and their extensions

### 3.2.1 Binary classification and support vector machines

In a classification problem, the aim is to categorize the inputs into one of a finite set of classes. Formulated as a supervised learning task, the dataset again consists of input-output pairs, i.e.  $\{(\mathbf{x}_1, y_1), \dots, (\mathbf{x}_m, y_m)\}$  with  $\mathbf{x} \in \mathbb{R}^n$ . However, unlike regression problems, the output  $y$  is a discrete integer number representing one of the classes. In a binary classification problem, in other words a problem with only two classes, it is natural to choose  $y \in \{-1, 1\}$ .

We have introduced linear regression in the previous section as a method for supervised learning when the output is a real number. Here, we will see how we

can use the same model for a binary classification task. If we look at the regression problem, we first note that geometrically

$$f(\mathbf{x}|\boldsymbol{\beta}) = \beta_0 + \sum_{j=1}^n \beta_j x_j = 0 \quad (3.27)$$

defines a hyperplane perpendicular to the vector with elements  $\beta_{j \geq 1}$ . If we fix the length  $\sum_{j=1}^n \beta_j^2 = 1$ , then  $f(\mathbf{x}|\boldsymbol{\beta})$  measures the (signed) distance of  $\mathbf{x}$  to the hyperplane with a sign depending on which side of the plane the point  $\mathbf{x}_i$  lies. To use this model as a classifier, we thus define

$$F(\mathbf{x}|\boldsymbol{\beta}) = \text{sign } f(\mathbf{x}|\boldsymbol{\beta}), \quad (3.28)$$

which yields  $\{+1, -1\}$ . If the two classes are (completely) linearly separable, then the goal of the classification is to find a hyperplane that separates the two classes in feature space. Specifically, we look for parameters  $\boldsymbol{\beta}$ , such that

$$y_i \tilde{\mathbf{x}}_i^T \boldsymbol{\beta} > M, \quad \forall i, \quad (3.29)$$

where  $M$  is called the *margin*. The optimal solution  $\hat{\boldsymbol{\beta}}$  then maximizes this margin. Note that instead of fixing the norm of  $\beta_{j \geq 1}$  and maximizing  $M$ , it is customary to minimize  $\sum_{j=1}^n \beta_j^2$  setting  $M = 1$  in Eq. (3.29).

In most cases, the two classes are not completely separable. In order to still find a good classifier, we allow some of the points  $\mathbf{x}_i$  to lie within the margin or even on the wrong side of the hyperplane. For this purpose, we rewrite the optimization constraint Eq. (3.29) to

$$y_i \tilde{\mathbf{x}}_i^T \boldsymbol{\beta} > (1 - \xi_i), \text{ with } \xi_i \geq 0, \quad \forall i. \quad (3.30)$$

We can now define the optimization problem as finding

$$\min_{\boldsymbol{\beta}, \{\xi_i\}} \frac{1}{2} \sum_{j=1}^n \beta_j^2 + C \sum_i \xi_i \quad (3.31)$$

subject to the constraint Eq. (3.30). Note that the second term with hyperparameter  $C$  acts like a regularizer, in particular a lasso regularizer. As we have seen in the example of the previous section, such a regularizer tries to set as many  $\xi_i$  to zero as possible.

We can solve this constrained minimization problem by introducing Lagrange multipliers  $\alpha_i$  and  $\mu_i$  and solving

$$\min_{\boldsymbol{\beta}, \{\xi_i\}} \frac{1}{2} \sum_{j=1}^n \beta_j^2 + C \sum_i \xi_i - \sum_i \alpha_i [y_i \tilde{\mathbf{x}}_i^T \boldsymbol{\beta} - (1 - \xi_i)] - \sum_i \mu_i \xi_i, \quad (3.32)$$

which yields the conditions

$$\beta_j = \sum_i \alpha_i y_i x_{ij}, \quad (3.33)$$

$$0 = \sum_i \alpha_i y_i \quad (3.34)$$

$$\alpha_i = C - \mu_i, \quad \forall i. \quad (3.35)$$

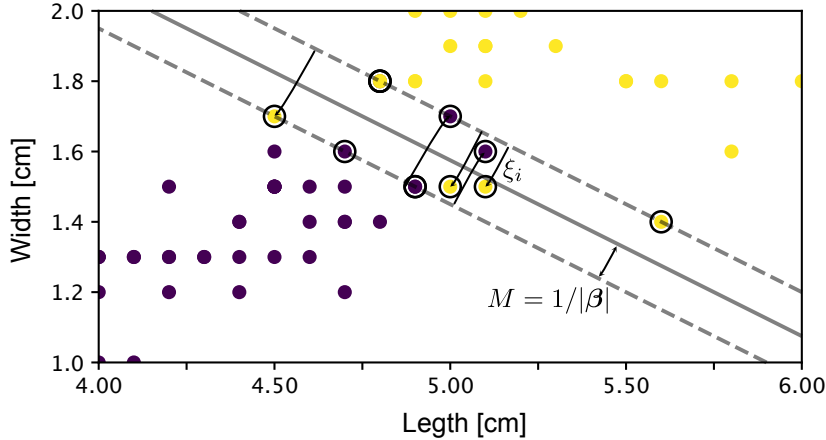


Figure 11: **Binary classification.** Hyperplane separating the two classes and margin  $M$  of the linear binary classifier. The support vectors are denoted by a circle around them.

It is numerically simpler to solve the dual problem

$$\min_{\{\alpha_i\}} \frac{1}{2} \sum_{i,i'} \alpha_i \alpha_{i'} y_i y_{i'} \mathbf{x}_i^T \mathbf{x}_{i'} - \sum_i \alpha_i \quad (3.36)$$

subject to  $\sum_i \alpha_i y_i = 0$  and  $0 \leq \alpha_i \leq C$ <sup>4</sup>. Using Eq. (3.33), we can reexpress  $\beta_j$  to find

$$f(\mathbf{x}|\{\alpha_i\}) = \sum_i \alpha_i y_i \mathbf{x}^T \mathbf{x}_i + \beta_0, \quad (3.40)$$

where the sum only runs over the points  $\mathbf{x}_i$ , which lie within the margin, as all other points have  $\alpha_i \equiv 0$  [see Eq. (3.37)]. These points are thus called the *support vectors* and are denoted in Fig. 11 with a circle around them. Finally, note that we can use Eq. (3.37) again to find  $\beta_0$ .

### The Kernel trick and support vector machines

We have seen in our discussion of PCA that most data is not separable linearly. However, we have also seen how the kernel trick can help us in such situations. In particular, we have seen how a non-linear function  $\Phi(\mathbf{x})$ , which we first apply to the data  $\mathbf{x}$ , can help us separate data that is not linearly separable. Importantly, we never actually use the non-linear function  $\Phi(\mathbf{x})$ , but only the kernel. Looking at the dual optimization problem Eq. (3.36) and the resulting classifier Eq. (3.40), we see that, as in the case of Kernel PCA, only the kernel  $K(\mathbf{x}, \mathbf{y}) = \Phi(\mathbf{x})^T \Phi(\mathbf{y})$  enters, simplifying the problem. This non-linear extension of the binary classifier is called a *support vector machine*.

<sup>4</sup>Note that the constraints for the minimization are not equalities, but actually inequalities. A solution thus has to fulfil the additional Karush-Kuhn-Tucker constraints

$$\alpha_i [y_i \tilde{\mathbf{x}}_i^T \beta - (1 - \xi_i)] = 0, \quad (3.37)$$

$$\mu_i \xi_i = 0, \quad (3.38)$$

$$y_i \tilde{\mathbf{x}}_i^T \beta - (1 - \xi_i) > 0. \quad (3.39)$$

### 3.2.2 More than two classes: logistic regression

In the following, we are interested in the case of  $p$  classes with  $p > 2$ . After the previous discussion, it seems natural for the output to take the integer values  $y = 1, \dots, p$ . However, it turns out to be helpful to use a different, so-called *one-hot encoding*. In this encoding, the output  $y$  is instead represented by the  $p$ -dimensional unit vector in  $y$  direction  $\mathbf{e}^{(y)}$ ,

$$y \longrightarrow \mathbf{e}^{(y)} = \begin{bmatrix} e_1^{(y)} \\ \vdots \\ e_y^{(y)} \\ \vdots \\ e_p^{(y)} \end{bmatrix} = \begin{bmatrix} 0 \\ \vdots \\ 1 \\ \vdots \\ 0 \end{bmatrix}, \quad (3.41)$$

where  $e_l^{(y)} = 1$  if  $l = y$  and zero for all other  $l = 1, \dots, p$ . A main advantage of this encoding is that we are not forced to choose a potentially biasing ordering of the classes as we would when arranging them along the ray of integers.

A linear approach to this problem then again mirrors the case for linear regression. We fit a multi-variate linear model, Eq. (3.8), to the one-hot encoded dataset  $\{(\mathbf{x}_1, \mathbf{e}^{(y_1)}), \dots, (\mathbf{x}_m, \mathbf{e}^{(y_m)})\}$ . By minimising the RSS, Eq. (3.4), we obtain the solution

$$\hat{\beta} = (\tilde{X}^T \tilde{X})^{-1} \tilde{X}^T Y, \quad (3.42)$$

where  $Y$  is the  $m$  by  $p$  output matrix. The prediction given an input  $\mathbf{x}$  is then a  $p$ -dimensional vector  $\mathbf{f}(\mathbf{x}|\hat{\beta}) = \tilde{\mathbf{x}}^T \hat{\beta}$ . On a generic input  $\mathbf{x}$ , it is obvious that the components of this prediction vector would be real valued, rather than being one of the one-hot basis vectors. To obtain a class prediction  $F(\mathbf{x}|\hat{\beta}) = 1, \dots, p$ , we simply take the index of the largest component of that vector, i.e.,

$$F(\mathbf{x}|\hat{\beta}) = \text{argmax}_k f_k(\mathbf{x}|\hat{\beta}). \quad (3.43)$$

The *argmax* function is a non-linear function and is a first example of what is referred to as *activation function*.

For numerical minimization, it is better to use a smooth activation function. Such an activation function is given by the *softmax* function

$$F_k(\mathbf{x}|\hat{\beta}) = \frac{e^{-f_k(\mathbf{x}|\hat{\beta})}}{\sum_{k'=1}^p e^{-f_{k'}(\mathbf{x}|\hat{\beta})}}. \quad (3.44)$$

Importantly, the output of the softmax function is a probability  $P(y = k|\mathbf{x})$ , since  $\sum_k F_k(\mathbf{x}|\hat{\beta}) = 1$ . This extended linear model is referred to as *logistic regression*<sup>5</sup>.

The current linear approach based on classification of one-hot encoded data generally works poorly when there are more than two classes. We will see in the next chapter that relatively straightforward non-linear extensions of this approach can lead to much better results.

---

<sup>5</sup>Note that the softmax function for two classes is the logistic function.

## 4 Supervised Learning with Neural Networks

In the previous chapter, we covered the basics of machine learning using conventional methods such as linear regression and principle component analysis. In the present chapter, we move towards a more complex class of machine learning models: *neural networks*. Neural networks have been central to the recent vast success of machine learning in many practical applications.

The idea for the design of a neural network model is an analogy to how biological organisms process information. Biological brains contain neurons, electrically activated nerve cells, connected by synapses that facilitate information transfer between neurons. The machine learning equivalent of this structure, the so-called artificial neural networks or neural networks in short, is a mathematical function developed with the same principles in mind. It is composed from elementary functions, the *neurons*, which are organized in *layers* that are connected to each other. To simplify the notation, a graphical representation of the neurons and network is used, see Fig. 12. The connections in the graphical representation means that the output from one set of neurons (forming one layer) serves as the input for the next set of neurons (the next layer). This defines a sense of direction in which information is handed over from layer to layer, and thus the architecture is referred to as a feed-forward neural network.

In general, an artificial neural network is simply an example of a variational non-linear function that maps some (potentially high-dimensional) input data to a desired output. Neural networks are remarkably powerful and it has been proven that under some mild structure assumptions they can approximate any smooth function arbitrarily well as the number of neurons tends to infinity. A drawback is that neural networks typically depend on a large amount of parameters. In the following, we will learn how to construct these neural networks and find optimal values for the variational parameters.

In this chapter, we are going to discuss one option for optimizing neural networks: the so-called *supervised learning*. A machine learning process is called supervised whenever we use training data comprising input-output pairs, in other words input with known correct answer (the label), to teach the network-required task.

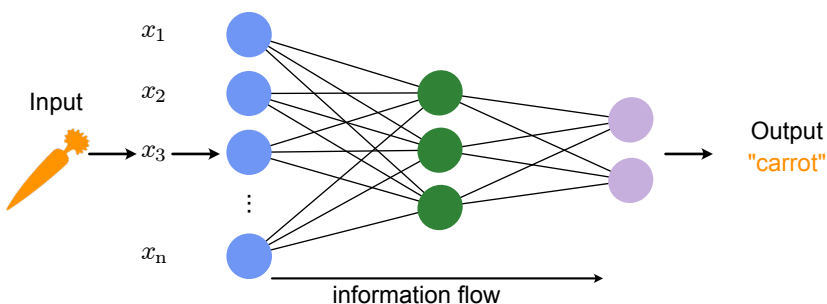


Figure 12: **Neural Network.** Graphical representation and basic architecture.

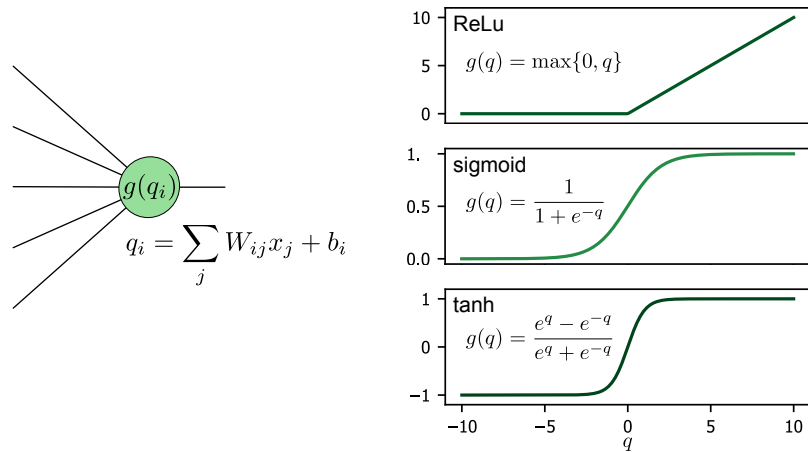


Figure 13: **The artificial neuron.** Left: schematic of a single neuron and its functional form. Right: examples of the commonly used activation functions: ReLU, sigmoid function and hyperbolic tangent.

## 4.1 Computational neurons

The basic building block of a neural network is the neuron. Let us consider a single neuron which we assume to be connected to  $k$  neurons in the preceding layer, see Fig. 13 left side. The neuron corresponds to a function  $f : \mathbb{R}^k \rightarrow \mathbb{R}$  which is a composition of a linear function  $q : \mathbb{R}^k \rightarrow \mathbb{R}$  and a non-linear (so-called *activation function*)  $g : \mathbb{R} \rightarrow \mathbb{R}$ . Specifically,

$$f(z_1, \dots, z_k) = g(q(z_1, \dots, z_k)) \quad (4.1)$$

where  $z_1, z_2, \dots, z_k$  are the outputs of the neurons from the preceding layer to which the neuron is connected.

The linear function is parametrized as

$$q(z_1, \dots, z_k) = \sum_{j=1}^k w_j z_j + b. \quad (4.2)$$

Here, the real numbers  $w_1, w_2, \dots, w_k$  are called *weights* and can be thought of as the “strength” of each respective connection between neurons in the preceding layer and this neuron. The real parameter  $b$  is known as the *bias* and is simply a constant offset <sup>6</sup>. The weights and biases are the variational parameters we will need to optimize when we train the network.

The activation function  $g$  is crucial for the neural network to be able to approximate any smooth function, since so far we merely performed a linear transformation. For this reason,  $g$  has to be nonlinear. In analogy to biological neurons,  $g$  represents the property of the neuron that it “spikes”, i.e., it produces a noticeable output only when the input potential grows beyond a certain threshold value. The most common choices for activation functions, shown in Fig. 13, include:

- *ReLU*: ReLU stands for rectified linear unit and is zero for all numbers smaller than zero, while a linear function for all positive numbers.

<sup>6</sup>Note that this bias is unrelated to the bias we learned about in regression.

- *Sigmoid*: The sigmoid function, usually taken as the logistic function, is a smoothed version of the step function.
- *Hyperbolic tangent*: The hyperbolic tangent function has a similar behaviour as sigmoid but has both positive and negative values.
- *Softmax*: The softmax function is a common activation function for the last layer in a classification problem (see below).

The choice of activation function is part of the neural network architecture and is therefore not changed during training (in contrast to the variational parameters weights and bias, which are adjusted during training). Typically, the same activation function is used for all neurons in a layer, while the activation function may vary from layer to layer. Determining what a good activation function is for a given layer of a neural network is typically a heuristic rather than systematic task.

Note that the softmax provides a special case of an activation function as it explicitly depends on the output of the  $q$  functions in the other neurons of the same layer. Let us label by  $l = 1, \dots, n$  the  $n$  neurons in a given layer and by  $q_l$  the output of their respective linear transformation. Then, the *softmax* is defined as

$$g_l(q_1, \dots, q_n) = \frac{e^{-q_l}}{\sum_{l'=1}^n e^{-q_{l'}}} \quad (4.3)$$

for the output of neuron  $l$ . A useful property of softmax is that

$$\sum_l g_l(q_1, \dots, q_n) = 1, \quad (4.4)$$

so that the layer output can be interpreted as a probability distribution. The softmax function is thus a continuous generalization of the argmax function introduced in the previous chapter.

## 4.2 A simple network structure

Now that we understand how a single neuron works, we can connect many of them together and create an artificial neural network. The general structure of a simple (feed-forward) neural network is shown in Fig. 14. The first and last layers are the input and output layers (blue and violet, respectively, in Fig. 14) and are called *visible layers* as they are directly accessed. All the other layers in between them are neither accessible for input nor providing any direct output, and thus are called *hidden layers* (green layer in Fig. 14).

Assuming we can feed the input to the network as a vector, we denote the input data with  $\mathbf{x}$ . The network then transforms this input into the output  $\mathbf{F}(\mathbf{x})$ , which in general is also a vector. As a simple and concrete example, we write the complete functional form of a neural network with one hidden layer as shown in Fig. 14,

$$\mathbf{F}(\mathbf{x}) = \mathbf{g}^{[2]} \left( W^{[2]} \mathbf{g}^{[1]} \left( W^{[1]} \mathbf{x} + \mathbf{b}^{[1]} \right) + \mathbf{b}^{[2]} \right). \quad (4.5)$$

Here,  $W^{[n]}$  and  $\mathbf{b}^{[n]}$  are the weight matrix and bias vectors of the  $n$ -th layer. Specifically,  $W^{[1]}$  is the  $k \times l$  weight matrix of the hidden layer with  $k$  and  $l$  the number of neurons in the input and hidden layer, respectively.  $W_{ij}^{[1]}$  is the  $j$ -the entry of

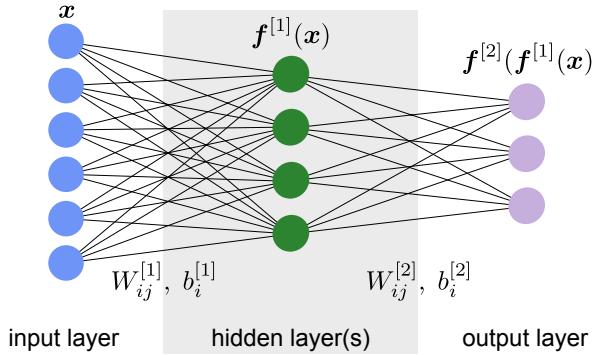


Figure 14: **Simple neural network.** Architecture and variational parameters.

the weight vector of the  $i$ -th neuron in the hidden layer, while  $b_i^{[1]}$  is the bias of this neuron. The  $W_{ij}^{[2]}$  and  $b_i^{[2]}$  are the respective quantities for the output layer. This network is called *fully connected* or *dense*, because each neuron in a given layer takes as input the output from all the neurons in the previous layer, in other words all weights are allowed to be non-zero.

Note that for the evaluation of such a network, we first calculate all the neurons' values of the first hidden layer, which feed into the neurons of the second hidden layer and so on until we reach the output layer. This procedure, which is possible only for feed-forward neural networks, is obviously much more efficient than evaluating the nested function of each output neuron independently.

### 4.3 Training

Adjusting all the weights and biases to achieve the task given using data samples  $\mathcal{D} = \{(\mathbf{x}_1, \mathbf{y}_1), \dots, (\mathbf{x}_m, \mathbf{y}_m)\}$  constitutes the *training* of the network. In other words, the training is the process that makes the network an approximation to the mathematical function  $\mathbf{F}(\mathbf{x}) = \mathbf{y}$  that we want it to represent. Since each neuron has its own bias and weights, a potentially huge number of variational parameters, and we will need to adjust all of them.

We have already seen in the previous chapter how one in principle trains a variational function. For the purpose of learning, we introduce a *loss function*  $L(W, B)$ , which characterizes how well the network is doing at predicting the correct output for each input. The loss function now depends, through the neural network, on all the weights and biases that we collectively denote by the vectors  $W$  and  $B$ .

The choice of loss function may strongly impact the efficiency of the training and is based on heuristics (as was the case with the choice of activation functions). In the previous chapter, we already encountered one loss function, the mean square error

$$L(\theta) = \frac{1}{2m} \sum_{i=1}^m \|\mathbf{F}(\mathbf{x}_i) - \mathbf{y}_i\|_2^2. \quad (4.6)$$

Here,  $\|\mathbf{a}\|_2 = \sqrt{\sum_i a_i^2}$  is the *L2 norm* and thus, this loss function is also referred to as *L2 loss*. An advantage of the L2 loss is that it is a smooth function of the variational parameters. Another natural loss function is the *mean absolute error*,

which is given by

$$L(\theta) = \frac{1}{2m} \sum_{i=1}^m \|\mathbf{F}(\mathbf{x}_i) - \mathbf{y}_i\|_1, \quad (4.7)$$

where  $\|\mathbf{a}\|_1 = \sum_i |a_i|$  denotes the *L1* norm. This loss function is thus also called the *L1 loss*. Note that the *L2* norm, given the squares, puts more weight on outliers than the *L1* loss. The two loss functions introduced so far are the most common loss functions for networks providing a continuous output. For discrete classification problems, a great choice is the *cross-entropy* between true label,  $\mathbf{y}_i$  and the network output,  $\mathbf{F}(\mathbf{x}_i)$  defined as

$$L_{\text{ent}}(\theta) = - \sum_{i=1}^m [\mathbf{y}_i \cdot \ln(\mathbf{F}(\mathbf{x}_i)) + (1 - \mathbf{y}_i) \cdot \ln(1 - \mathbf{F}(\mathbf{x}_i))], \quad (4.8)$$

where the logarithm is taken element-wise. This loss function is also called *negative log likelihood*. It is here written for outputs that lie between 0 and 1, as is the case when the activation function of the last layer of the network is sigmoid  $\sigma(z) = 1/(1 + e^{-z})$ . (The cross-entropy is preferably combined with sigmoid activation in the last layer.)

Of these loss functions the cross entropy is probably the least intuitive one. We want to understand what it means and gain some intuition about it. The different cost functions actually differ by the speed of the learning process. The learning rate is largely determined by the partial derivatives of the cost function  $\partial L / \partial \theta$ . Slow learning appears when these derivatives become small. Let us consider the toy example of a single neuron with sigmoid activation  $F(x) = \sigma(wx + b)$  and a single input-output pair  $\{x, y\} = \{1, 0\}$ . Then the quadratic cost function has derivatives

$$\frac{\partial L}{\partial w} = \frac{\partial L}{\partial b} = \sigma(w + b)\sigma'(w + b). \quad (4.9)$$

We observe that this derivative gets very small for  $\sigma(w + b) \rightarrow 1$ , because  $\sigma'$  gets very small in that limit. Therefore, a slowdown of learning appears. This slowdown is also observed in more complex neural networks with L2 loss, we considered the simple case here only to be able to say something analytically.

Given this observation, we want to see whether the cross entropy can improve the situation. We again compute the derivative of the cost function with respect to the weights for a single term in the sum and a network that is composed of a single sigmoid and a general input-output pair  $\{x, y\}$

$$\begin{aligned} \frac{\partial L_{\text{ent}}}{\partial w} &= - \left( \frac{y}{\sigma(wx + b)} - \frac{1 - y}{1 - \sigma(wx + b)} \right) \sigma'(wx + b)x \\ &= \frac{\sigma'(wx + b)x}{\sigma(wx + b)[1 - \sigma(wx + b)]} [\sigma(wx + b) - y] \\ &= x[\sigma(wx + b) - y], \end{aligned} \quad (4.10)$$

where in the last step we used that  $\sigma'(z) = \sigma(z)[1 - \sigma(z)]$ . This is a much better result than what we got for the L2 loss. The learning rate is here directly proportional to the error between data point and prediction  $[\sigma(wx + b) - y]$ . The mathematical reason for this change is that  $\sigma'(z)$  cancels out due to this specific form of the cross entropy. A similar expression holds true for the derivative with respect to  $b$ ,

$$\frac{\partial L_{\text{ent}}}{\partial b} = [\sigma(wx + b) - y]. \quad (4.11)$$

In fact, if we insisted that we want the very intuitive form of Eqs. (4.10) and (4.11) for the gradients, we can derive the cost function for the sigmoid activation function to be the cross-entropy. This follows simply because

$$\frac{\partial L}{\partial b} = \frac{\partial L}{\partial F} F' \quad (4.12)$$

and  $F' = F(1 - F)$  for the sigmoid activation, which, in comparison to Eq. (4.11), yields

$$\frac{\partial L}{\partial F} = \frac{F - y}{F(1 - F)}, \quad (4.13)$$

which, when integrated with respect to  $F$ , gives exactly the cross-entropy (up to a constant). We can thus, starting from Eqs. (4.10) and (4.11), think of the choice of cost functions as a backward engineering. Following this logic, we can think of other pairs of final layer activations and cost functions that may work well together.

What happens if we change the activation function in the last layer from sigmoid to softmax? For the loss function, we consider just the first term in the cross entropy for the shortness of presentation (for softmax, this form is appropriate, as compared to a sigmoid activation)

$$L(\theta) = - \sum_{i=1}^m \mathbf{y}_i \cdot \ln(\mathbf{F}(\mathbf{x}_i)), \quad (4.14)$$

where again the logarithm is taken element-wise. For concreteness, let us look at one-hot encoded classification problem. Then, all  $\mathbf{y}_i$  labels are vectors with exactly one entry “1”. Let that entry have index  $n_i$  in the vector. The loss function then reads

$$L(\theta) = - \sum_{i=1}^m \ln(F_{n_i}(\mathbf{x}_i)). \quad (4.15)$$

Due to the properties of the softmax,  $F_{n_i}(\mathbf{x}_i)$  is always  $\leq 1$ , so that loss function is minimized, if it approaches 1, the value of the label. For the gradients, we obtain

$$\begin{aligned} \frac{\partial L}{\partial b_j} &= - \sum_{i=1}^m \frac{1}{F_{n_i}(\mathbf{x}_i)} \frac{\partial F_{n_i}(\mathbf{x}_i)}{\partial b_j} \\ &= - \sum_{i=1}^m \frac{1}{F_{n_i}(\mathbf{x}_i)} [F_{n_i}(\mathbf{x}_i) \delta_{n_i, j} - F_{n_i}(\mathbf{x}_i)^2] \\ &= \sum_{i=1}^m [F_{n_i}(\mathbf{x}_i) - y_{n_i}]. \end{aligned} \quad (4.16)$$

We observe that again, the gradient has a similar favorable structure to the previous case, in that it is linearly dependent on the error that the network makes. (The same can be found for the derivatives with respect to the weights.)

Once we have defined a loss function, we also already understand how to train the network: we need to minimize  $L(\theta)$  with respect to  $W$  and  $B$ . However,  $L$  is typically a high-dimensional function and may have many nearly degenerate minima. Unlike in the previous chapter, finding the loss function’s absolute minimum exactly is typically intractable analytically and may come at prohibitive costs computationally. The practical goal is therefore rather to find a “good” instead than the absolute

minimum through training. Having found such “good” values for  $W, B$ , the network can then be applied on previously unseen data.

It remains to be explained how to minimize the loss function. Here, we employ an iterative method called *gradient descent*. Intuitively, the method corresponds to “walking down the hill” in our many parameter landscape until we reach a (local) minimum. For this purpose, we use the (discrete) derivative of the cost function to update all the weights and biases incrementally and search for the minimum of the function via tiny steps on the many-dimensional surface. More specifically, we can update all weights and biases in each step as

$$\theta_\alpha \rightarrow \theta_\alpha - \eta \frac{\partial L(\theta)}{\partial \theta_\alpha}. \quad (4.17)$$

The variable  $\eta$ , also referred to as *learning rate*, specifies the size of step we use to walk the landscape—if it is too small in the beginning, we might get stuck in a local minimum early on, while for too large  $\eta$  we might never find a minimum. The learning rate is a hyperparameter of the training algorithm. Note that gradient descent is just a discrete many-variable version of the analytical search for extrema which we know from calculus: An extremum is characterized by vanishing derivatives in all directions, which results in convergence in the gradient descent algorithm outlined above.

While the process of optimizing the many variables of the loss function is mathematically straightforward to understand, it presents a significant numerical challenge: For each variational parameter, for instance a weight in the  $k$ -th layer  $W_{ij}^{[k]}$ , the partial derivative  $\partial L / \partial W_{ij}^{[k]}$  has to be computed. And this has to be done each time the network is evaluated for a new dataset during training. Naively, one could assume that the whole network has to be evaluated each time. Luckily there is an algorithm that allows for an efficient and parallel computation of all derivatives—it is known as *backpropagation*. The algorithm derives directly from the chain rule of differentiation for nested functions and is based on two observations:

- (1) The loss function is a function of the neural network  $F(\mathbf{x})$ , that is  $L \equiv L(F)$ .
- (2) To determine the derivatives in layer  $k$  only the derivatives of the following layer, given as Jacobi matrix

$$D\mathbf{f}^{[l]}(\mathbf{z}^{[l-1]}) = \partial \mathbf{f}^{[l]} / \partial \mathbf{z}^{[l-1]}, \quad (4.18)$$

with  $l > k$  and  $\mathbf{z}^{[l-1]}$  the output of the previous layer, as well as

$$\frac{\partial \mathbf{z}^{[k]}}{\partial \theta_\alpha^{[k]}} = \frac{\partial \mathbf{g}^{[k]}}{\partial q_i^{[k]}} \frac{\partial q_i^{[k]}}{\partial \theta_\alpha} = \begin{cases} \frac{\partial \mathbf{g}^{[k]}}{\partial q_i^{[k]}} z_j^{[k-1]} & \theta_\alpha = W_{ij} \\ \frac{\partial \mathbf{g}^{[k]}}{\partial q_i^{[k]}} & \theta_\alpha = b_i \end{cases} \quad (4.19)$$

are required. The derivatives  $\mathbf{z}^{[l]}$  are the same for all parameters.

The calculation of the Jacobi matrix thus has to be performed only once for every update. In contrast to the evaluation of the network itself, which is propagating

forward, (output of layer  $n$  is input to layer  $n + 1$ ), we find that a change in the Output propagates backwards through the network. Hence the name<sup>7</sup>.

The full algorithm looks then as follows:

### Algorithm 2: Backpropagation

**Input:** Loss function  $L$  that in turn depends on the neural network, which is parametrized by weights and biases, summarized as  $\theta = \{W, b\}$ .

**Output:** Partial derivatives  $\partial L / \partial \theta_{\alpha}^{[n]}$  with respect to all parameters  $\theta^{[n]}$  of all layers  $k = 1 \dots n$ .

Calculate the derivatives with respect to the parameters of the output layer:  $\partial L / \partial W_{ij}^{[n]} = (\nabla L)^T \frac{\partial g^{[n]}}{\partial q_i^{[n]}} z_j^{[n-1]}$ ,  $\partial L / \partial b_i^{[n]} = (\nabla L)^T \frac{\partial g^{[n]}}{\partial q_i^{[n]}}$

**for**  $k = n \dots 1$  **do**

    Calculate the Jacobi matrices for layer  $k$ :  $Dg^{[k]} = (\partial g^{[k]} / \partial q^{[k]})$  and  $Df^{[k]} = (\partial f^{[k]} / \partial z^{[k-1]})$ ;

    Multiply all following Jacobi matrices to obtain the derivatives of layer  $k$ :  $\partial L / \partial \theta_{\alpha}^{[k]} = (\nabla L)^T Df^{[n]} \dots Df^{[k+1]} Dg^{[k]} (\partial q^{[k]} / \partial \theta_{\alpha}^{[k]})$ ;

**end**

A remaining question is when to actually perform updates to the network parameters. One possibility would be to perform the above procedure for each training data individually. Another extreme is to use all the training data available and perform the update with an averaged derivative. Not surprisingly, the answer lies somewhere in the middle: Often, we do not present training data to the network one item at the time, but the full training data is divided into so-called *batches*, a group of training data that is fed into the network together. Chances are the weights and biases can be adjusted better if the network is presented with more information in each training step. However, the price to pay for larger batches is a higher computational cost. Therefore, the batch size can greatly impact the efficiency of training. The random partitioning of the training data into batches is kept for a certain number of iterations, before a new partitioning is chosen. The consecutive iterations carried out with a chosen set of batches constitute a training *epoch*.

## 4.4 Simple example: MNIST

As we discussed in the introduction, the recognition of hand-written digits 0, 1, … 9 is the “Drosophila” of machine learning with neural networks. There is a dataset with tens of thousands of examples of hand-written digits, the so-called MNIST data set. Each data sample in the MNIST dataset, a  $28 \times 28$  grayscale image, comes with a *label*, which holds the information which digit is stored in the image. The difficulty of learning to recognize the digits is that handwriting styles are incredibly

<sup>7</sup>Backpropagation is actually a special case of a set of techniques known as *automatic differentiation* (AD). AD makes use of the fact that any computer program can be composed of elementary operations (addition, subtraction, multiplication, division) and elementary functions ( $\sin, \exp, \dots$ ). By repeated application of the chain rule, derivatives of arbitrary order can be computed automatically.

personal and different people will write the digit “4” slightly differently. It would be very challenging to hardcode all the criteria to recognize “4” and not confuse it with, say, a “9”.

We can use a simple neural network as introduced earlier in the chapter to tackle this complex task. We will use a network as shown in Fig. 14 and given in Eq. (4.5) to do just that. The input is the image of the handwritten digit, transformed into a  $k = 28^2$  long vector, the hidden layer contains  $l$  neurons and the output layer has  $p = 10$  neurons, each corresponding to one digit in the one-hot encoding. The output is then a probability distribution over these 10 neurons that will determine which digit the network identifies.

As an exercise, we build a neural network according to these guidelines and train it. How exactly one writes the code depends on the library of choice, but the generic structure will be the following:

### Example 1: MNIST

1. *Import the data:* The MNIST database is available for download at <http://yann.lecun.com/exdb/mnist/>
2. *Define the model:*
  - *Input layer:*  $28^2 = 784$  neurons (the greyscale value of each pixel of the image, normalized to a value in  $[0, 1]$ , is one component of the input vector).
  - *Fully connected hidden layer:* Here one can experiment, starting from as few as 10 neurons. The use of a sigmoid activation function is recommended, but others can in principle be used.
  - *Output layer:* Use 10 neurons, one for each digit. The proper activation function for this classification task is, as discussed, a softmax function.
3. *Choose the loss function:* Since we are dealing with a classification task, we use the cross-entropy, Eq. (4.8).
4. *Train and evaluate the model:* Follow the standard machine-learning workflow to train<sup>a</sup> and evaluate the model. However, unlike in the regression example of the previous chapter, where we evaluated the model using the mean square error, here we are rather interested in the accuracy of our prediction.

<sup>a</sup>Most ML packages have some type of ‘train’ function built in, so no need to worry about implementing back-propagation by hand. All that is needed here is to call the ‘train’ function

With the training completed, we want to understand how well the final model performs in recognizing handwritten digits. For that, we introduce the *accuracy* defined by

$$\text{accuracy} = \frac{\text{correct predictions}}{\text{total predictions}}. \quad (4.20)$$

If we use 30 hidden neurons, set the learning rate to  $\eta = 0.5$  (a mini-batch size of 10 and train for 30 epochs), we obtain an accuracy of 95.49 %. With a quadratic

cost we obtain only slightly worse results of 95.42%. For 100 hidden neurons, we obtain 96.82%. That is a considerable improvement over a quadratic cost, where we obtain 96.59%. (Meaning that now about 1 in 14 wrongly classified pictures will now be correctly classified.) Still, these numbers are not even close to state of the art neural network performances. The reason is that we have used the simplest possible all-to-all connected architecture with only one hidden layer. Below, we will introduce more advanced neural network features and show how to increase the performance.

Before doing so, we briefly introduce other important measures used to characterize the performance of specifically **binary-classification** models in statistics are: *precision*, *specificity* and *recall*. In the language of true (false) positives (negatives) the precision is defined as

$$\text{precision} = \frac{\text{true positives}}{\text{true positives} + \text{false positives}}. \quad (4.21)$$

Recall (also referred to as sensitivity) is defined as

$$\text{recall} = \frac{\text{true positives}}{\text{true positives} + \text{false negatives}}. \quad (4.22)$$

While recall can be interpreted as true positive rate as it represents the ratio between actual positives and outcomes identified as positive, the specificity is an analogous measures for negatives

$$\text{specificity} = \frac{\text{true negatives}}{\text{true negatives} + \text{false positives}}. \quad (4.23)$$

Note, however, that these measures can be misleading, in particular when dealing with very unbalanced data sets.

## 4.5 Regularization

In the previous sections, we have illustrated an artificial neural network that is constructed analogous to neuronal networks in the brain. A model is only given a rough structure a priori, within which they have a huge number of parameters to adjust by learning from the training set. While we already understand that this is an extraordinarily powerful process, this method of learning comes with its own set of challenges. The most prominent of them is the generalization of the rules learned from training data to unseen data.

We have already encountered in the previous chapter how the naive optimization of a linear model reduces the generalization. However, we have also seen how the generalization error can be improved using regularization. Training neural network comes with the same issue and the same solution: we are always showing the algorithm we built the training that is limited in one way or another and we need to make sure that the neural network does not learn particularities of that given training set, but actually extracts a general knowledge.

The step zero to avoid over-fitting is to create sufficiently representative and diverse training set. Once this is taken care of, we can take several steps for the regularization of the network. The simplest, but at the same time most powerful

option is introducing *dropout layers*. This regularization is very similar to dropping features that we discussed for linear regression. However, the dropout layer ignores a randomly selected subset of neuron outputs in the network only during training. Which neurons are dropped is chosen at random for each training step. This regularization procedure is illustrated in Fig. 15. By randomly discarding a certain fraction of neurons we ensure that the network does not get fixed at small particular features of the training set and is better equipped to recognize the more general features. Another way of looking at it is that this procedure corresponds to training a large number of neural networks with different neuron connections in parallel. The fraction of neurons that are ignored in a dropout layer is a hyperparameter that is fixed a priori. Maybe it is counter-intuitive but the best performance is often achieved when this number is sizable, between 20% and 50%. It shows the remarkable resilience of the network against fluctuations.

As for the linear models, regularization can also be achieved by adding regularization terms  $R$  to the  $L$ ,  $L \rightarrow L + R$ . Again, the two most common regularization terms are *L1*- or *Lasso*-regularisation, where

$$R_{L1} = \frac{\lambda}{2} \sum_j |W_j|, \quad (4.24)$$

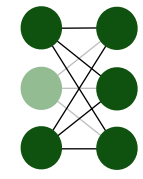


Figure 15:  
**Dropout layer**

and the sum runs over all weights  $W_j$  of the network, as well as the *L2*-regularization, or ridge regression, which we already discussed for linear regression with

$$R_{L2} = \frac{\lambda}{2} \sum_j W_j^2, \quad (4.25)$$

where the sum runs again over all weights  $W_j$  of the network. As for the linear models, *L2* regularization shrinks all parameters symmetrically, whereas *L1*-regularization usually causes a subset of parameters to vanish. For this reason, the method is also called *weight decay*. Either way, both *L1* and *L2* regularizations restrict the expressiveness of the neural network, thus encouraging it to learn generalizable features rather than overfitting specific features of the data set.

The weights are commonly initialized with small values and increase during training. This naturally limits the capacity of the network, because for very small weights it effectively acts as a linear model (when one approximates the activation function by a linear function). Only once the weights become bigger, the network explores its nonlinearity.

Another regularization technique consists in artificially enlarging the data set. Data is often costly, but we have extra knowledge about what further data might look like and feed this information in the machine learning workflow. For instance, going back to the MNIST example, we may shift or tilt the existing images or apply small transformations to them. By doing that, researchers were able to improve MNIST performance by almost 1 percent<sup>8</sup>. In particular if we know symmetries of the problem from which the data originates (such as time translation invariance, invariance under spatial translations or rotations), effective generation of augmented datasets is possible. Another option is the addition of various forms of noise to data

<sup>8</sup>See Simard et al., <http://dx.doi.org/10.1109/ICDAR.2003.1227801>

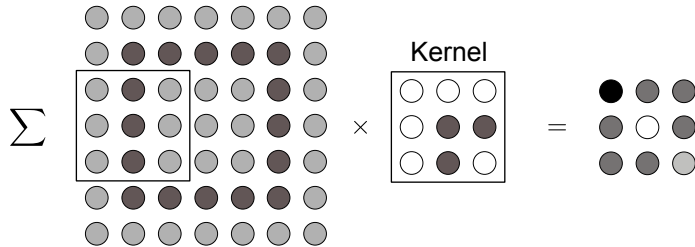


Figure 16: **Convolutional layer in 2D.** Here with filter size  $k = 3$  and stride  $s = 2$ . The filter is first applied to the  $3 \times 3$  sub-image in the top left of the input, which yields the first pixel in the feature map. The filter then moves  $s$  neurons to the right, which yields the next pixel and so on. After moving all the way to the right, the filter moves  $s$  pixels down and starts from the left again until reaching the bottom right.

in order to prevent overfitting to the existing noise or in general resilience of the neural network to noise. Finally, for classification problems in particular, data may not be distributed between categories equally. To avoid a bias, it is the desirable to enhance the data in the underrepresented categories.

## 4.6 Convolutional neural networks

The fully-connected simple single-layer architecture for a neural network is in principle universally applicable. However, this architecture is often inefficient and hard to train. In this section, we introduce more advanced neural-network layers and examples of the types of problems for which they are suitable.

### 4.6.1 Convolutional layers

The achieved accuracy in the MNIST example above was not as high as one may have hoped, being much worse than the performance of a human. A main reason was that, using a dense network structure, we discarded all local information contained in the pictures. In other words, connecting every input neuron with every neuron in the next layer, the information whether two neurons are close to each other is lost. This information is, however, not only crucial for pictures, but quite often for input data with an underlying geometric structure or natural notion of ‘distance’ in its correlations. To use this local information, so-called *convolutional layers* were introduced. The neural networks that contain such layers are called *convolutional neural networks* (CNNs).

The key idea behind convolutional layers is to identify certain (local) patterns in the data. In the example of the MNIST images, such patterns could be straight and curved lines, or corners. A pattern is then encoded in a *kernel* or *filter* in the form of weights, which are again part of the training. The convolutional layer then compares these patterns with a local patch of the input data. Mathematically, identifying the features in the data corresponds to a convolution  $(f * x)(t) = \sum_{\tau} f(\tau)x(t - \tau)$  of the kernel  $f$  with the original data  $x$ .

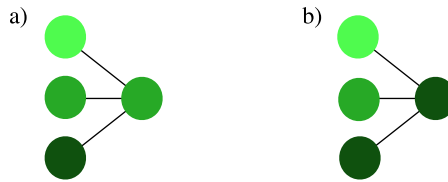


Figure 17: **Pooling layer** (a) an average pooling and (b) a max pooling layer (both  $n = 3$ ).

For two-dimensional data, such as shown in the example in Fig. 16, we write the discrete convolution explicitly as

$$q_{i,j} = \sum_{m=1}^k \sum_{n=1}^k f_{n,m} x_{si-m, sj-n} + b_0, \quad (4.26)$$

where  $f_{n,m}$  are the weights of the kernel, which has linear size  $k$ , and  $b_0$  is a bias. Finally,  $s$  is called *stride* and refers to the number of pixels the filter moves per application. The output,  $q$ , is called *feature map*. Note that the dimension of the feature map is  $n_q \times n_q$  with  $n_q = \lfloor (n_{in} - k)/s + 1 \rfloor$  when the input image is of dimensions  $n_{in} \times n_{in}$ : application of a convolutional layer thus reduces the image size, an effect not always intended. To avoid this reduction, the original data can be *padded*, for example by adding zeros around the border of the data to ensure the feature map has the same dimension as the input data.

For typical convolutional networks, one applies a number of filters for each layer in parallel, where each filter is trained to recognize different features. For instance, one filter could start to be sensitive to contours in an image, while another filter recognizes the brightness of a region. Further, while filters in the first layers may be sensitive to local patterns, the ones in the later layers recognize larger structures. This distribution of functionalities between filters happens automatically, it is not preconceived when building the neural network.

## 4.6.2 Pooling

Another very useful layer, in particular in combination with convolutional layers, is the *pooling layer*. Each neuron in the pooling layer takes input from  $n$  (neighboring) neurons in the previous layer—in the case of a convolutional network for each feature map individually—and only retains the most significant information. Thus, the pooling layer helps to reduce the spatial dimension of the data. What is considered significant depends on the particular circumstances: Picking the neuron with the maximum input among the  $n$ , called *max pooling*, detects whether a given feature is present in the window. Furthermore, max pooling is useful to avoid *dead neurons*, in other words neurons that are stuck with a value near 0 irrespective of the input and such a small gradient for its weights and biases that this is unlikely to change with further training. This is a scenario that can often happen especially when using the ReLU activation function. *Average pooling*, in other words taking the average value of the  $n$  inputs is a straight forward compression. Note that unlike other layers, the pooling layer has just a small set of  $n$  connections with no adjustable weights. The functionality of the pooling layer is shown in Fig. 17 (a) and (b).

Figure 18: Comparison of DNA and random sequences.

An extreme case of pooling is global pooling, where the full input is converted to a single output. Using a max pooling, this would then immediately tell us, whether a given feature is present in the data.

#### 4.6.3 Example: DNA sequencing

With lowering costs and expanding applications, DNA sequencing has become a widespread tool in biological research. Especially the introduction of high-throughput sequencing methods and the related increase of data has required the introduction of data science methods into biology. Sequenced data is extremely complex and thus a great playground for machine learning applications. Here, we consider a simple classification as an example. The primary structure of DNA consists of a linear sequence of basic building blocks called nucleotides. The key component of nucleotides are nitrogen bases: Adenine (A), Guanine (G), Cytosine (C), and Thymine (T). The order of the bases in the linear chains defines the DNA sequence. Which sequences are meaningful is determined by a set of complex specific rules. In other words, there are series of letters A, G, C, and T that correspond to DNA and while many other sequences do not resemble DNA. Trying to distinguish between strings of nitrogen bases that correspond to human DNA and those that do not is a simple example of a classification task that is at the same time not so easy for an untrained human eye.

In Fig. 18, we show a comparison of five strings of human DNA and five strings of 36 randomly generated letters A, G, C, and T. Without deeper knowledge it is hard to distinguish the two classes and even harder to find the set of empirical rules that quantify their distinction. We can let a neural network have a go and see if it performs any better than us studying these sequences by visual analysis.

We have all ingredients to build a binary classifier that will be able to distinguish between DNA and non-DNA sequences. First, we download a freely available database of the human genome from <https://genome.ucsc.edu><sup>9</sup>. Here, we downloaded a database of encoding genomes that contains 100000 sequences of human DNA (each is 36 letters long). Additionally, we generate 100000 random sequences of letters A, G, C, T. The learning task we are facing now is very similar to the MNIST classification, though in the present case, we only have two classes. Note, however, that we generated random sequences of bases and labeled them as random, even though we might have accidentally created sequences that do correspond to human DNA. This limits the quality of our data set and thus naturally also the final performance of the network.

The model we choose here has a standard architecture and can serve as a guiding

<sup>9</sup><http://hgdownload.cse.ucsc.edu/goldenpath/hg19/encodeDCC/wgEncodeUwRepliSeq/wgEncodeUwRepliSeqBg02esG1bAlnRep1.bam>

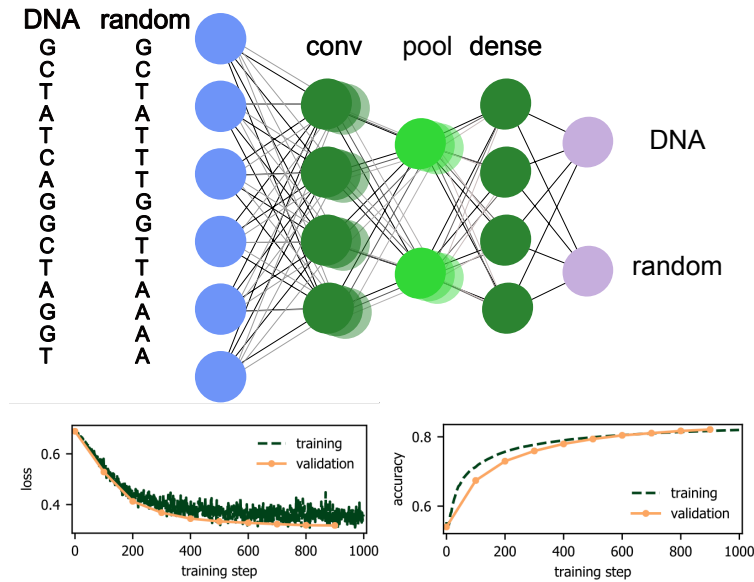


Figure 19: **Neural network classification of DNA sequences.** The two lower panels show loss function and accuracy on the training (evaluation) data in green (orange) as a function of the training step respectively.

example for supervised learning with neural networks that will be useful in many other scenarios. In particular, we implement the following architecture:

### Example 2: DNA classification

1. *Import the data* from <http://genome.uscs.edu>
2. *Define the model:*
  - *Input layer:* The input layer has dimension  $36 \times 4$  (36 entries per DNA sequence, 4 to encode each of 4 different bases A, G, C, T)  
*Example:*  $[[1,0,0,0], [0,0,1,0], [0,0,1,0], [0,0,0,1]] = \text{ACCT}$
  - *Convolutional layer:* Kernel size  $k = 4$ , stride  $s = 1$  and number of filters  $N = 64$ .
  - *Pooling layer:* max pooling over  $n = 2$  neurons, which reduces the output of the previous layer by a factor of 2.
  - *Dense layer:* 256 neurons with a ReLU activation function.
  - *Output layer:* 2 neurons (DNA and non-DNA output) with softmax activation function.
3. *Loss function:* Cross-entropy between DNA and non-DNA.

A schematic of the network structure as well as the evolution of the loss and the accuracy measured over the training and validation sets with the number of training steps are shown in Fig. 19. Comparing the accuracies of the training and validation sets is a standard way to avoid overfitting: On the examples from the training set we can simply check the accuracy during training. When training and validation

accuracy reach the same number, this indicates that we are not overfitting on the training set since the validation set is never used to adjust the weights and biases. A decreasing validation accuracy despite an increasing training accuracy, on the other hand, is a clear sign of overfitting.

We see that this simple convolutional network is able to achieve around 80% accuracy. By downloading a larger training set, ensuring that only truly random sequences are labeled as such, and by optimizing the hyper-parameters of the network, it is likely that an even higher accuracy can be achieved. We also encourage you to test other architectures: one can try to add more layers (both convolutional and dense), adjust the size of the convolution kernel or stride, add dropout layers, and finally, test whether it is possible to reach higher accuracies without over-fitting on the training set.

#### 4.6.4 Example: advanced MNIST

We can now revisit the MNIST example and approach the classification with the more advanced neural network structures of the previous section. In particular, we use the following architecture

##### Example 3: Advanced MNIST

1. *Input layer*:  $28^2 = 784$  neurons.
2. *Convolutional layer 1*: Kernel size  $k = 5$ , stride  $s = 1$  and number of filters  $N = 32$  with a ReLU activation function.
3. *Pooling layer*: max pooling over  $n = 2 \times 2$  neurons.
4. *Convolutional layer 2*: Kernel size  $k = 5$ , stride  $s = 1$  and number of filters  $N = 64$  with a ReLU activation function.
5. *Pooling layer*: max pooling over  $n = 2 \times 2$  neurons.
6. *Dropout*: dropout layer for regularization with a 50% dropout probability.
7. *Dense layer*: 1000 neurons with a ReLU activation function.
8. *Output layer*: 10 neurons with softmax activation function.

For the loss function, we again use cross-entropy between the output and the labels. Notice here the repeated structure of convolutional layers and pooling layers. This is a very common structure for deep convolutional networks. With this model, we achieve an accuracy on the MNIST test set of 98.8%, a massive improvement over the simple dense network.

## 4.7 Recurrent neural networks

We have seen in the previous section how the convolutional neural network allows to retain local information through the use of filters. While this context-sensitivity

of the CNN is applicable in many situations, where geometric information is important, there are situations we have more than neighborhood relations, namely sequential order. An element is before or after an other, not simply next to it. A common situation, where the order of the input is important, is with time-series data. Examples are measurements of a distant star collected over years or the events recorded in a detector after a collision in a particle collider. The classification task in these examples could be the determination whether the star has an exoplanet, or whether a Higgs boson was observed, respectively. Another example without any temporal structure in the data is the prediction of a protein's functions from its primary amino-acid sequence.

A property that the above examples have in common is that the length of the input data is not necessarily always fixed for all samples. This emphasizes again another weakness of both the dense network and the CNN: The networks only work with fixed-size input and there is no good procedure to decrease or increase the input size. While we can in principle always cut our input to a desired size, of course, this finite window is not guaranteed to contain the relevant information.

In this final section on supervised learning, we introduce one more neural network architecture that solves both problems discussed above: *recurrent neural networks* (RNNs). The key idea behind a recurrent neural network is that input is passed to the network one element after another—unlike for other neural networks, where an input ‘vector’ is given the network all at once—and to recognize context, the network keeps an internal state, or memory, that is fed back to the network together with the next input. Recurrent neural networks were developed in the context of *natural language processing* (NLP), the field of processing, translating and transforming spoken or written language input, where clearly, both context and order are crucial pieces of information. However, over the last couple of years, RNNs have found applications in many fields in the sciences.

The special structure of a RNN is depicted in Fig. 20. At step  $t$ , the input  $\mathbf{x}_t$  and the (hidden) internal state of the last step  $\mathbf{h}_{t-1}$  are fed to the network to calculate  $\mathbf{h}_t$ . The new hidden memory of the RNN is finally connected to the output layer  $\mathbf{y}_t$ . As shown in Fig. 20, this is equivalent to having many copies of the input-output architecture, where the hidden layers of the copies are connected to each other. The RNN cell itself can have a very simple structure with a single activation function.

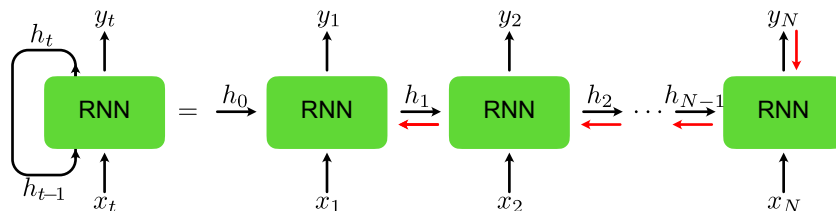


Figure 20: **Recurrent neural network architecture.** The input  $x_t$  is fed into the recurrent cell together with the (hidden) memory  $h_{t-1}$  of the previous step to produce the new memory  $h_t$  and the output  $y_t$ . One can understand the recurrent structure via the “unwrapped” depiction of the structure on the right hand side of the figure. The red arrows indicate how gradients are propagated back in time for updating the network parameters.

Concretely, in each step of a simple RNN we update the hidden state as

$$\mathbf{h}_t = \tanh(W_{hh}\mathbf{h}_{t-1} + W_{xh}\mathbf{x}_{t-1} + \mathbf{b}_h), \quad (4.27)$$

where we used for the nonlinearity the hyperbolic tangent, a common choice, which is applied element-wise. Further, if the input data  $\mathbf{x}_t$  has dimension  $n$  and the hidden state  $\mathbf{h}_t$  dimension  $m$ , the weight matrices  $W_{hh}$  and  $W_{xh}$  have dimensions  $m \times m$  and  $m \times n$ , respectively. Finally, the output at step  $t$  can be calculated using the hidden state  $\mathbf{h}_t$ ,

$$\mathbf{y}_t = W_{ho}\mathbf{h}_t. \quad (4.28)$$

A schematic of this implementation is depicted in Fig. 21(a). Note that in this simplest implementation, the output is only a linear operation on the hidden state. A straight forward extension—necessary in the case of a classification problem—is to add a non-linear element to the output as well, i.e.,

$$\mathbf{y}_t = \mathbf{g}(W_{ho}\mathbf{h}_t + \mathbf{b}_y) \quad (4.29)$$

with  $\mathbf{g}(\mathbf{q})$  some activation function, such as a softmax. Note that while in principle an output can be calculated at every step, this is only done after the last input element in a classification task.

An interesting property of RNNs is that the weight matrices and biases, the parameters we learn during training, are the same for each input element. This property is called *parameter sharing* and is in stark contrast to dense networks. In the latter architecture, each input element is connected through its own weight matrix. While it might seem that this property could be detrimental in terms of representability of the network, it can greatly help extracting sequential information: Similar to a filter in a CNN, the network does not need to learn the exact location of some specific sequence that carries the important information, it only learns to recognize this sequence somewhere in the data. Note that the way each input element is processed differently is instead implemented through the hidden memory.

Parameter sharing is, however, also the root of a major problem when training a simple RNN. To see this, remember that during training, we update the network parameters using gradient descent. As in the previous sections, we can use backpropagation to achieve this optimization. Even though the unwrapped representation of the RNN in Fig. 20 suggests a single hidden layer, the gradients for the backpropagation have to also propagate back through time. This is depicted in Fig. 20 with the red arrows<sup>10</sup>. Looking at the backpropagation algorithm in Sec. 4.3, we see that to use data points from  $N$  steps back, we need to multiply  $N - 1$  Jacobi matrices  $D\mathbf{f}^{[t']}$  with  $t - N < t' \leq t$ . Using Eq. (4.28), we can write each Jacobi matrix as a product of the derivative of the activation function,  $\partial_q \tanh(q)$ , with the weight matrix. If either of these factors<sup>11</sup> is much smaller (much larger) than 1, the gradients decrease (grow) exponentially. This is known as the problem of *vanishing gradients* (*exploding gradients*) and makes learning long-term dependencies with simple RNNs practically impossible.

Note that the problem of exploding gradients can be mitigated by clipping the gradients, in other words scaling them to a fixed size. Furthermore, we can use the

<sup>10</sup>In the context of RNNs, backpropagation is thus referred to as *backpropagation through time* (BPTT).

<sup>11</sup>For the weight matrix this means the singular values.

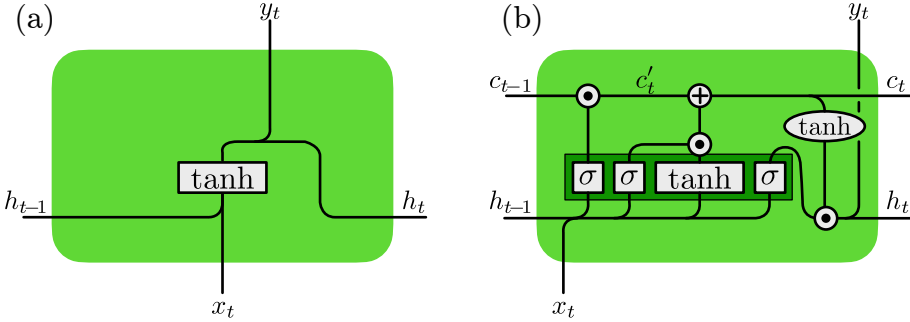


Figure 21: **Comparison of (a) a simple RNN and (b) a LSTM.** The boxes denote neural networks with the respective activation function, while the circles denote element-wise operations. The dark green box indicates that the four individual neural networks can be implemented as one larger one.

ReLU activation function instead of a hyperbolic tangent, as the derivative of the ReLU for  $q > 0$  is always 1. However, the problem of the shared weight matrices can not so easily be resolved. In order to learn long-time dependencies, we have to introduce a different architecture. In the following, we will discuss the long short-term memory (LSTM) network. This architecture and its variants are used in most applications of RNNs nowadays.

#### 4.7.1 Long short-term memory

The key idea behind the LSTM is to introduce another state to the RNN, the so-called *cell state*, which is passed from cell to cell, similar to the hidden state. However, unlike the hidden state, no matrix multiplication takes place, but information is added or removed to the cell state through *gates*. The LSTM then commonly comprises four gates which correspond to three steps: the forget step, the input and update step, and finally the output step. We will in the following go through all of these steps individually.

##### Forget step

In this step, specific information of the cell state is forgotten. Specifically, we update the cell state as

$$c'_t = \sigma(W_{hf}h_{t-1} + W_{xf}x_t + b_f) \odot c_{t-1}. \quad (4.30)$$

where  $\sigma$  is the sigmoid function (applied element-wise) and  $\odot$  denotes element-wise multiplication. Note that this step multiplies each element of the gate state with a number  $\in (0, 1)$ , in other words elements multiplied with a number close to 0 forget their previous memory.

##### Input and update step

In the next step, we decide what and how much to add to the cell state. For this purpose, we first decide what to add to the state. We first define what we would like to add to the cell,

$$g_t = \tanh(W_{hu}h_{t-1} + W_{xu}x_t + b_u), \quad (4.31)$$

which due to the hyperbolic tangent,  $-1 < g_t^\alpha < 1$  for each element. However, we do not necessarily update each element of the cell state, but rather we introduce

another gate, which determines whether to actually write to the cell,

$$\mathbf{i}_t = \sigma(W_{hi}\mathbf{h}_{t-1} + W_{xi}\mathbf{x}_t + \mathbf{b}_i), \quad (4.32)$$

again with  $0 < i_t^\alpha < 1$ . Finally, we update the cell state

$$\mathbf{c}_t = \mathbf{c}'_t + \mathbf{i}_t \odot \mathbf{g}_t. \quad (4.33)$$

### Output step

In the final step, we decide how much of the information stored in the cell state should be written to the new hidden state,

$$\mathbf{h}_t = \sigma(W_{ho}\mathbf{h}_{t-1} + W_{xo}\mathbf{x}_t + \mathbf{b}_o) \odot \tanh(\mathbf{c}_t). \quad (4.34)$$

The full structure of the LSTM with the four gates and the element-wise operations is schematically shown in Fig. 21(b). Note that we can concatenate the input  $\mathbf{x}_t$  and hidden memory  $\mathbf{h}_{t-1}$  into a vector of size  $n + m$  and write one large weight matrix  $W$  of size  $4m \times (m + n)$ .

So far, we have only used the RNN in a supervised setting for classification purposes, where the input is a sequence and the output a single class at the end of the full sequence. A network that performs such a task is thus called a many-to-one RNN. We will see in the next section, that unlike the other network architectures encountered in this section, RNNs can straight-forwardly be used for unsupervised learning, usually as one-to-many RNNs.

# 5 Unsupervised Learning

In Sec. 4, we discussed supervised learning tasks, for which datasets consist of input-output pairs, or data-label pairs. More often than not, however, we have data without labels and would like to extract information from such a dataset. Clustering problems fall in this category, for instance: We suspect that the data can be divided into different types, but we do not know which features distinguish these types.

Mathematically, we can think of the data  $\mathbf{x}$  as samples that were drawn from a probability distribution  $P(\mathbf{x})$ . The unsupervised learning task is to implicitly represent this distribution with a model, for example represented by a neural network. The model can then be used to study properties of the distribution or to generate new ‘artificial’ data. The models we encounter in this chapter are thus also referred to as *generative models*. In general, unsupervised learning is conceptually more challenging than supervised learning. At the same time, unsupervised algorithms are highly desirable, since unlabelled data is much more abundant than labelled data. Moreover, we can in principle use a generative model for a classification task by learning the joint probability distribution of the data-label pair.

In this chapter, we will introduce three types of neural networks that are specific to unsupervised learning tasks: *Restricted Boltzmann machines*, *autoencoders*, and *generative adversarial networks*. Furthermore, we will discuss how the RNN introduced in the previous chapter can also be used for an unsupervised task.

## 5.1 Restricted Boltzmann machine

*Restricted Boltzmann Machines* (RBM) are a class of generative stochastic neural networks. More specifically, given some (binary) input data  $\mathbf{x} \in \{0, 1\}^{n_v}$ , an RBM can be trained to approximate the probability distribution of this input. Moreover, once the neural network is trained to approximate the distribution of the input, we can sample from the network, in other words we generate new instances from the learned probability distribution.

The RBM consists of two layers (see Fig. 22) of *binary units*. Each binary unit is a variable which can take the values 0 or 1. We call the first (input) layer visible and the second layer hidden. The visible layer with input variables  $\{v_1, v_2, \dots, v_{n_v}\}$ , which we collect in the vector  $\mathbf{v}$ , is connected to the hidden layer with variables  $\{h_1, h_2, \dots, h_{n_h}\}$ , which we collect in the vector  $\mathbf{h}$ . The role of the hidden layer is to mediate correlations between the units of the visible layer. In contrast to the neural networks we have seen in the previous chapter, the hidden layer is not followed by an output layer. Instead, the RBM represents a probability distribution  $P_{\text{rbm}}(\mathbf{v})$ , which depends on variational parameters represented by the weights and biases of a neural network. The RBM, as illustrated by the graph in Fig. 22, is a special case of a network structure known as a Boltzmann machine with the restriction that a unit in the visible layer is only connected to hidden units and vice versa, hence the name *restricted* Boltzmann machine.

The structure of the RBM is motivated from statistical physics: To each choice of the binary vectors  $\mathbf{v}$  and  $\mathbf{h}$ , we assign a value we call the energy

$$E(\mathbf{v}, \mathbf{h}) = - \sum_i a_i v_i - \sum_j b_j h_j - \sum_{ij} v_i W_{ij} h_j, \quad (5.1)$$

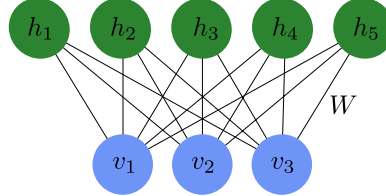


Figure 22: **Restricted Boltzmann machine.** Each of the three visible units and five hidden units represents a variable that can take the values  $\pm 1$  and the connections between them represent the entries  $W_{ij}$  of the weight matrix that enters the energy function (5.1).

where the vectors  $\mathbf{a}$ ,  $\mathbf{b}$ , and the matrix  $W$  are the variational parameters of the model. Given the energy, the probability distribution over the configurations  $(\mathbf{v}, \mathbf{h})$  is defined as

$$P_{\text{rbm}}(\mathbf{v}, \mathbf{h}) = \frac{1}{Z} e^{-E(\mathbf{v}, \mathbf{h})}, \quad (5.2)$$

where

$$Z = \sum_{\mathbf{v}, \mathbf{h}} e^{-E(\mathbf{v}, \mathbf{h})} \quad (5.3)$$

is a normalisation factor called the partition function. The sum in Eq. (5.3) runs over all binary vectors  $\mathbf{v}$  and  $\mathbf{h}$ , i.e., vectors with entries 0 or 1. The probability that the model assigns to a visible vector  $\mathbf{v}$  is then the marginal over the joint probability distribution Eq. (5.2),

$$P_{\text{rbm}}(\mathbf{v}) = \sum_{\mathbf{h}} P_{\text{rbm}}(\mathbf{v}, \mathbf{h}) = \frac{1}{Z} \sum_{\mathbf{h}} e^{-E(\mathbf{v}, \mathbf{h})}. \quad (5.4)$$

As a result of the restriction, the visible units, with the hidden units fixed, are mutually independent: given a choice of the hidden units  $\mathbf{h}$ , we have an **independent** probability distribution for **each** visible unit given by

$$P_{\text{rbm}}(v_i = 1 | \mathbf{h}) = \sigma(a_i + \sum_j W_{ij} h_j), \quad i = 1, \dots, n_v, \quad (5.5)$$

where  $\sigma(x) = 1/(1 + e^{-x})$  is the sigmoid function. Similarly, with the visible units fixed, the individual hidden units are also mutually independent with the probability distribution

$$P_{\text{rbm}}(h_j = 1 | \mathbf{v}) = \sigma(b_j + \sum_i v_i W_{ij}) \quad j = 1, \dots, n_h. \quad (5.6)$$

The visible (hidden) units can thus be interpreted as artificial neurons connected to the hidden (visible) units with sigmoid activation function and bias  $\mathbf{a}$  ( $\mathbf{b}$ ). A direct consequence of this mutual independence is that sampling a vector  $\mathbf{v}$  or  $\mathbf{h}$  reduces to sampling every component individually. Notice that this simplification comes about due to the restriction that visible (hidden) units do not directly interact amongst themselves, i.e. there are no terms proportional to  $v_i v_j$  or  $h_i h_j$  in Eq. (5.1). In the following, we explain how one can train an RBM and discuss possible applications of RBMs.

### 5.1.1 Training an RBM

Consider a set of binary input data  $\mathbf{x}_k$ ,  $k = 1, \dots, M$ , drawn from a probability distribution  $P_{\text{data}}(\mathbf{x})$ . The aim of the training is to tune the parameters  $\{\mathbf{a}, \mathbf{b}, W\}$  in an RBM such that after training  $P_{\text{rbm}}(\mathbf{x}) \approx P_{\text{data}}(\mathbf{x})$ . The standard approach to solve this problem is the maximum likelihood principle, in other words we want to find the parameters  $\{\mathbf{a}, \mathbf{b}, W\}$  which maximize the probability that our model produces the data  $\mathbf{x}_k$ .

Maximizing the likelihood  $\mathcal{L}(\mathbf{a}, \mathbf{b}, W) = \prod P_{\text{rbm}}(\mathbf{x}_k)$  is equivalent to training the RBM using a loss function we have encountered before, the negative log-likelihood

$$L(\mathbf{a}, \mathbf{b}, W) = - \sum_{k=1}^M \log P_{\text{rbm}}(\mathbf{x}_k). \quad (5.7)$$

For the gradient descent, we need derivatives of the loss function of the form

$$\frac{\partial L(\mathbf{a}, \mathbf{b}, W)}{\partial W_{ij}} = - \sum_{k=1}^M \frac{\partial \log P_{\text{rbm}}(\mathbf{x}_k)}{\partial W_{ij}}. \quad (5.8)$$

This derivative consists of two terms,

$$\frac{\partial \log P_{\text{rbm}}(\mathbf{x})}{\partial W_{ij}} = x_i P_{\text{rbm}}(h_j = 1 | \mathbf{x}) - \sum_{\mathbf{v}} v_i P_{\text{rbm}}(h_j = 1 | \mathbf{v}) P_{\text{rbm}}(\mathbf{v}) \quad (5.9)$$

and similarly simple forms are found for the derivatives with respect to the components of  $\mathbf{a}$  and  $\mathbf{b}$ . We can then iteratively update the parameters just as we have done in Chapter 4,

$$W_{ij} \rightarrow W_{ij} - \eta \frac{\partial L(\mathbf{a}, \mathbf{b}, W)}{\partial W_{ij}} \quad (5.10)$$

with a sufficiently small learning rate  $\eta$ . As we have seen in the previous chapter in the context of backpropagation, we can reduce the computational cost by replacing the summation over the whole data set in Eq. (5.8) with a summation over a small randomly chosen batch of samples. This reduction in the computational cost comes at the expense of noise, but at the same time it can help to improve generalization.

However, there is one more problem: The second summation in Eq. (5.9), which contains  $2^{n_v}$  terms, cannot be efficiently evaluated exactly. Instead, we have to approximate the sum by sampling the visible layer  $\mathbf{v}$  from the marginal probability distribution  $P_{\text{rbm}}(\mathbf{v})$ . This sampling can be done using *Gibbs sampling* as follows:

#### Algorithm 3: Gibbs sampling

```

Input: Any visible vector  $\mathbf{v}(0)$ 
Output: Visible vector  $\mathbf{v}(r)$ 
for  $n = 1 \dots r$  do
  | sample  $\mathbf{h}(n)$  from  $P_{\text{rbm}}(\mathbf{h} | \mathbf{v} = \mathbf{v}(n-1))$ ;
  | sample  $\mathbf{v}(n)$  from  $P_{\text{rbm}}(\mathbf{v} | \mathbf{h} = \mathbf{h}(n))$ ;
end

```

With sufficiently many steps  $r$ , the vector  $\mathbf{v}(r)$  is an unbiased sample drawn from  $P_{\text{rbm}}(\mathbf{v})$ . By repeating the procedure, we can obtain multiple samples to estimate the summation. Note that this is still rather computationally expensive, requiring multiple evaluations on the model.

The key innovation which allows the training of an RBM to be computationally feasible was proposed by Geoffrey Hinton (2002). Instead of obtaining multiple samples, we simply perform the Gibbs sampling with  $r$  steps and estimate the summation with a single sample, in other words we replace the second summation in Eq. (5.9) with

$$\sum_{\mathbf{v}} v_i P_{\text{rbm}}(h_j = 1 | \mathbf{v}) P_{\text{rbm}}(\mathbf{v}) \rightarrow v'_i P_{\text{rbm}}(h_j = 1 | \mathbf{v}'), \quad (5.11)$$

where  $\mathbf{v}' = \mathbf{v}(r)$  is simply the sample obtained from  $r$ -step Gibbs sampling. With this modification, the gradient, Eq. (5.9), can be approximated as

$$\frac{\partial \log P_{\text{rbm}}(\mathbf{x})}{\partial W_{ij}} \approx x_i P_{\text{rbm}}(h_j = 1 | \mathbf{x}) - v'_i P_{\text{rbm}}(h_j = 1 | \mathbf{v}'). \quad (5.12)$$

This method is known as *contrastive divergence*. Although the quantity computed is only a biased estimator of the gradient, this approach is found to work well in practice. The complete algorithm for training a RBM with  $r$ -step contrastive divergence can be summarised as follows:

#### Algorithm 4: Contrastive divergence

```

Input: Dataset  $\mathcal{D} = \{\mathbf{x}_1, \mathbf{x}_2, \dots, \mathbf{x}_M\}$  drawn from a distribution  $P(x)$ 
initialize the RBM weights  $\{\mathbf{a}, \mathbf{b}, \mathbf{W}\}$ ;
Initialize  $\Delta W_{ij} = \Delta a_i = \Delta b_j = 0$ ;
while not converged do
    select a random batch  $S$  of samples from the dataset  $\mathcal{D}$  ;
    forall  $\mathbf{x} \in S$  do
        Obtain  $\mathbf{v}'$  by  $r$ -step Gibbs sampling starting from  $\mathbf{x}$ 
         $\Delta W_{ij} \leftarrow \Delta W_{ij} - x_i P_{\text{rbm}}(h_j = 1 | \mathbf{x}) + v'_i P_{\text{rbm}}(h_j = 1 | \mathbf{v}')$ 
    end
     $W_{ij} \leftarrow W_{ij} - \eta \Delta W_{ij}$ 
    (and similarly for  $\mathbf{a}$  and  $\mathbf{b}$ )
end

```

Having trained the RBM to represent the underlying data distribution  $P(\mathbf{x})$ , there are a few ways one can use the trained model:

1. **Pretraining** We can use  $\mathbf{W}$  and  $\mathbf{b}$  as the initial weights and biases for a deep network (c.f. Chapter 4), which is then fine-tuned with gradient descent and backpropagation.
2. **Generative Modelling** As a generative model, a trained RBM can be used to generate new samples via Gibbs sampling (Alg. 3). Some potential uses of the generative aspect of the RBM include *recommender systems* and *image reconstruction*. In the following subsection, we provide an example, where an RBM is used to reconstruct a noisy signal.

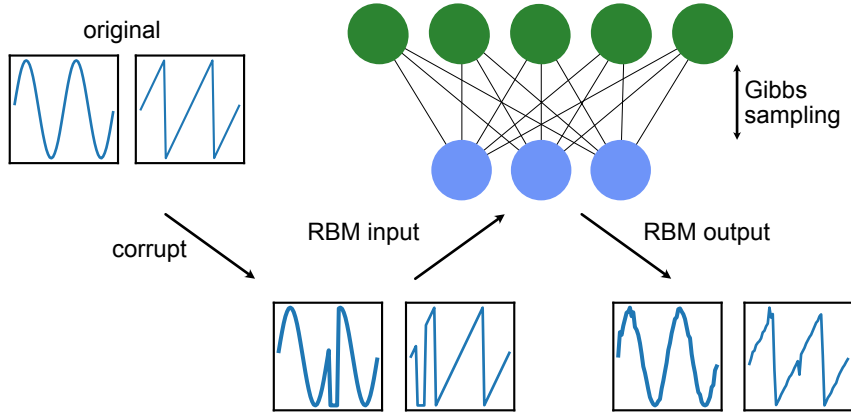


Figure 23: **Signal reconstruction.** Using an RBM to repair a corrupted signal, here a sine and a sawtooth waveform.

### 5.1.2 Example: signal or image reconstruction/denoising

A major drawback of the simple RBMs for their application is the fact that they only take binary data as input. As an example, we thus look at simple periodic waveforms with 60 sample points. In particular, we use sawtooth, sine, and square waveforms. In order to have quasi-continuous data, we use eight bits for each point, such that our signal can take values from 0 to 255. Finally, we generate samples to train with a small variation in the maximum value, the periodicity, as well as the center point of each waveform.

After training the RBM using the contrastive divergence algorithm, we now have a model which represents the data distribution of the binarized waveforms. Consider now a signal which has been corrupted, meaning some parts of the waveform have not been received, in other words they are set to 0. By feeding this corrupted data into the RBM and performing a few iterations of Gibbs sampling (Alg. 3), we can obtain a reconstruction of the signal, where the missing part has been repaired, as can be seen at the bottom of Fig. 23.

Note that the same procedure can be used to reconstruct or denoise images. Due to the limitation to binary data, however, the picture has to either be binarized, or the input size to the RBM becomes fairly large for high-resolution pictures. It is thus not surprising that while RBMs have been popular in the mid-2000s, they have largely been superseded by more modern architectures such as *generative adversarial networks* which we shall explore later in the chapter. However, they still serve a pedagogical purpose and could also provide inspiration for future innovations, in particular in science. A recent example is the idea of using an RBM to represent a quantum mechanical state.

## 5.2 Training an RNN without supervision

In Sec. 4, the RNN was introduced as a classification model. Instead of classifying sequences of data, such as time series, the RNN can also be trained to generate

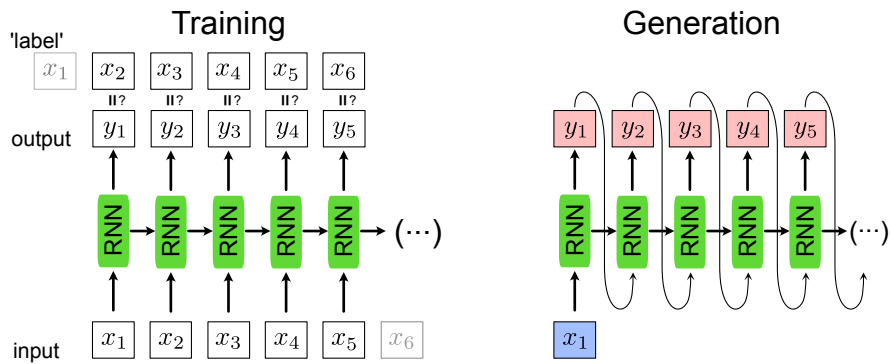


Figure 24: **RNN used as a generator.** For training, left, the input data shifted by one,  $x_{t+1}$ , are used as the label. For the generation of new sequences, right, we input a single data point  $x_1$  and the RNN uses the recurrent steps to generate a new sequence.

valid sequences itself. Given the RNN introduced in Sec. 4.7, the implementation of such a generator is straight-forward and does not require a new architecture. The main difference is that the output  $y_t$  of the network given the data point  $x_t$  is a guess of the subsequent data point  $x_{t+1}$  instead of the class to which the whole sequence belongs to. This means in particular that the input and output size are now the same. For training this network, we can once again use the cross-entropy or (negative) log-likelihood as a loss function,

$$L_{\text{ent}} = - \sum_{t=1}^{m-1} \mathbf{x}_{t+1} \cdot \ln(\mathbf{y}_t), \quad (5.13)$$

where  $\mathbf{x}_{t+1}$  is now the ‘label’ for the input  $\mathbf{x}_t$  and  $\mathbf{y}_t$  is the output of the network and  $t$  runs over the input sequence with length  $m$ . This training is schematically shown in Fig. 24.

For generating a new sequence, it is enough to have one single input point  $\mathbf{x}_1$  to start the sequence. Note that since we now can start with a single data point  $\mathbf{x}_1$  and generate a whole sequence of data points  $\{\mathbf{y}_t\}$ , this mode of using an RNN is referred to as *one-to-many*. This sequence generation is shown in Fig. 24, left.

### 5.2.1 Example: generating molecules with an RNN

To illustrate the concept of sequence generation using recurrent neural networks, we use an RNN to generate new molecules. The first question we need to address is how to encode a chemical structure into input data—of sequential form no less—that a machine learning model can read. A common representation of molecular graphs used in chemistry is the *simplified molecular-input line-entry system*, or SMILES. Figure 25 shows examples of such SMILES strings for the caffeine, ethanol, and aspirin molecules. We can use the dataset *Molecular Sets*<sup>12</sup>, which contains  $\sim 1.9\text{M}$  molecules written in the SMILES format.

Using the SMILES dataset, we create a dictionary to translate each character that appears in the dataset into an integer. We further use one-hot-encoding to

<sup>12</sup><https://github.com/molecularsets/moses>

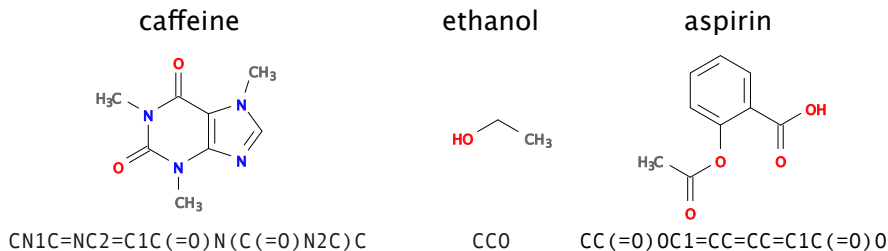


Figure 25: **SMILES.** Examples of molecules and their representation in SMILES.

feed each character separately to the RNN. This creates a map from characters in SMILES strings onto an array of numbers. Finally, in order to account for the variable size of the molecules and hence, the variable length of the strings, we can introduce a ‘stop’ character such that the network learns and later generates sequences of arbitrary length.

We are now ready to use the SMILES strings for training our network as described above, where the input is a one-hot-encoded vector and the output is again a vector of the same size. Note, however, that similar to a classification task, the output vector is a probability distribution over the characters the network believes could come next. Unlike a classification task, where we consider the largest output the best guess of the network, here we sample in each step from the probability distribution  $\mathbf{y}_t$  to again have a one-hot-encoded vector for the input of the next step.

### 5.3 Autoencoders

Autoencoders are neuron-based generative models, initially introduced for dimensionality reduction. The original purpose, thus, is similar to that of PCA or t-SNE that we already encountered in Sec. 2, namely the reduction of the number of features that describe our input data. Unlike for PCA, where we have a clear recipe how to reduce the number of features, an autoencoder learns the best way of achieving the dimensionality reduction. An obvious question, however, is how to measure the quality of the compression, which is essential for the definition of a loss function and thus, training. In the case of t-SNE, we introduced two probability distributions based on the distance of samples in the original and feature space, respectively, and minimized their difference, for example using the Kullback-Leibler divergence.

The solution the autoencoder uses is to have a neural network do first, the dimensionality reduction, or encoding to the *latent space*,  $\mathbf{x} \mapsto \mathbf{e}(\mathbf{x}) = \mathbf{z}$ , and then, the decoding back to the original dimension,  $\mathbf{z} \mapsto \mathbf{d}(\mathbf{z})$ , see Fig. 26. This architecture allows us to directly compare the original input  $\mathbf{x}$  with the reconstructed output  $\mathbf{d}(\mathbf{e}(\mathbf{x}))$ , such that the autoencoder trains itself unsupervised by minimizing the difference. A good example of a loss function that achieves successful training and that we have encountered already several times is the cross entropy,

$$L_{\text{ae}} = - \sum_i \mathbf{x}_i \cdot \ln[\mathbf{d}(\mathbf{e}(\mathbf{x}_i))]. \quad (5.14)$$

In other words, we compare point-wise the difference between the input to the encoder with the decoder’s output.

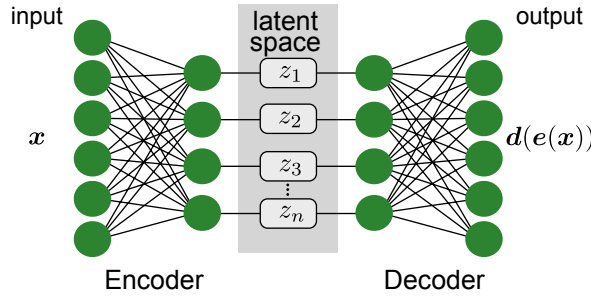


Figure 26: **General autoencoder architecture.** A neural network is used to contract a compressed representation of the input in the latent space. A second neural network is used to reconstruct the original input.

Intuitively, the latent space with its lower dimension presents a bottleneck for the information propagation from input to output. The goal of training is to find and keep the most relevant information for the reconstruction to be optimal. The latent space then corresponds to the reduced space in PCA and t-SNE. Note that much like in t-SNE but unlike in PCA, the new features are in general not independent.

### 5.3.1 Variational autoencoders

A major problem of the approach introduced in the previous section is its tendency to overfitting. As an extreme example, a sufficiently complicated encoder-decoder pair could learn to map all data in the training set onto a single variable and back to the data. Such a network would indeed accomplish completely lossless compression and decompression. However, the network would not have extracted any useful information from the dataset and thus, would completely fail to compress and decompress previously unseen data. Moreover, as in the case of the dimensionality-reduction schemes discussed in Sec. 2, we would like to analyze the latent space images and extract new information about the data. Finally, we might also want to use the decoder part of the autoencoder as a generator for new data. For these reasons, it is essential that we combat overfitting as we have done in the previous chapters by regularization.

The question then becomes how one can effectively regularize the autoencoder. First, we need to analyze what properties we would like the latent space to fulfil. We can identify two main properties:

1. If two input data points are close (according to some measure), their images in the latent space should also be close. We call this property *continuity*.
2. Any point in the latent space should be mapped through the decoder onto a meaningful data point, a property we call *completeness*.

While there are principle ways to achieve regularization along similar paths as discussed in the previous section on supervised learning, we will discuss here a solution that is particularly useful as a generative model: the *variational autoencoder* (VAE).

The idea behind VAEs is for the encoder to output not just an exact point  $z$  in the latent space, but a (factorized) Normal distribution of points,  $\mathcal{N}(\mu, \sigma)$ . In particular, the output of the encoder comprises two vectors, the first representing the means,  $\mu$ , and the second the standard deviations,  $\sigma$ . The input for the decoder

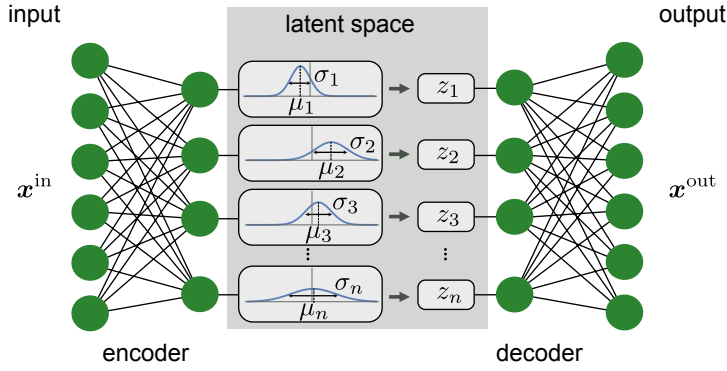


Figure 27: **Architecture of variational autoencoder.** Instead of outputting a point  $z$  in the latent space, the encoder provides a distribution  $N(\boldsymbol{\mu}, \boldsymbol{\sigma})$ , parametrized by the means  $\boldsymbol{\mu}$  and the standard deviations  $\boldsymbol{\sigma}$ . The input  $\boldsymbol{z}$  for the decoder is then drawn from  $N(\boldsymbol{\mu}, \boldsymbol{\sigma})$ .

is then sampled from this distribution,  $\boldsymbol{z} \sim \mathcal{N}(\boldsymbol{\mu}, \boldsymbol{\sigma})$ , and the original input is reconstructed and compared to the original input for training. In addition to the standard loss function comparing input and output of the VAE, we further add a regularization term to the loss function such that the distributions from the encoder are close to a standard normal distribution  $\mathcal{N}(\mathbf{0}, \mathbf{1})$ . Using the Kullback-Leibler divergence, Eq.(2.20), to measure the deviation from the standard normal distribution, the full loss function then reads

$$\begin{aligned} L_{\text{vae}} &= - \sum_i \mathbf{x}_i^{\text{in}} \ln \mathbf{x}_i^{\text{out}} + \text{KL}(\mathcal{N}(\boldsymbol{\mu}_i, \boldsymbol{\sigma}_i) \parallel \mathcal{N}(\mathbf{0}, \mathbf{1})) \\ &= - \sum_i \mathbf{x}_i^{\text{in}} \ln \mathbf{x}_i^{\text{out}} + \frac{1}{2} \sum_k [\sigma_{i,k}^2 + \mu_{i,k}^2 - 1 - 2 \ln \sigma_{i,k}]. \end{aligned} \quad (5.15)$$

In this expression, the first term quantifies the reconstruction loss with  $\mathbf{x}_i^{\text{in}}$  the input to and  $\mathbf{x}_i^{\text{out}}$  the reconstructed data from the VAE. The second term is the regularization on the latent space for each input data point, which for two (diagonal) Normal distributions can be simplified, see second line of Eq. (5.15). This procedure regularizes the training through the introduction of noise, similar to the dropout layer in Section 4. However, the regularization here not only generically increases generalization, but also enforces the desired structure in the latent space.

The structure of a VAE is shown in Fig. 27. By enforcing the mean and variance structure of the encoder output, the latent space fulfills the requirements outlined above. This type of structure can then serve as a generative model for many different data types: anything from human faces to complicated molecular structures. Hence, the variational autoencoder goes beyond extracting information from a dataset, but can be used for the scientific discovery. Note, finally, that the general structure of the variational autoencoder can be applied beyond the simple example above. As an example, a different distribution function can be enforced in the latent space other than the standard Normal distribution, or a different neural network can be used as encoder and decoder, such as a RNN.

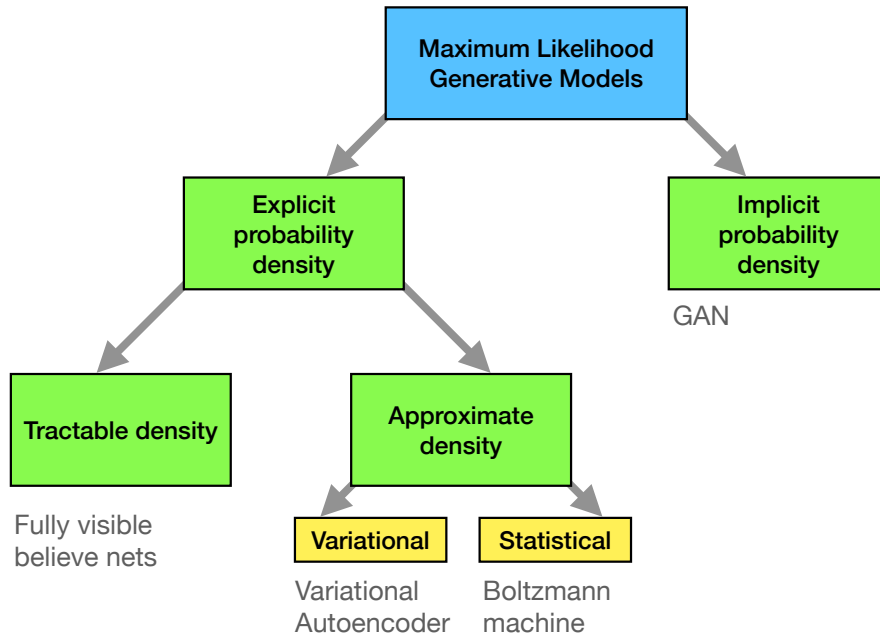


Figure 28: Maximum likelihood approaches to generative modeling.

## 5.4 Generative adversarial networks

In this section, we will be concerned with a type of generative neural network, the generative adversarial network (GAN), which gained a very high popularity in recent years. Before getting into the details about this method, we give a quick systematic overview over types of generative methods, to place GANs in proper relation to them.<sup>13</sup>.

### 5.4.1 Types of generative models

We restrict ourselves to methods that are based on the *maximum likelihood principle*. The role of the model is to provide an estimate  $p_{\text{model}}(\mathbf{x}; \boldsymbol{\theta})$  of a probability distribution parametrized by parameters  $\boldsymbol{\theta}$ . The likelihood is the probability that the model assigns to the training data

$$\prod_{i=1}^m p_{\text{model}}(\mathbf{x}_i; \boldsymbol{\theta}), \quad (5.16)$$

where  $m$  is again the number of samples in the data  $\{\mathbf{x}_i\}$ . The goal is to choose the parameters  $\boldsymbol{\theta}$  such as to maximize the likelihood. Thanks to the equality

$$\begin{aligned} \boldsymbol{\theta}^* &= \operatorname{argmax}_{\boldsymbol{\theta}} \prod_{i=1}^m p_{\text{model}}(\mathbf{x}_i; \boldsymbol{\theta}) \\ &= \operatorname{argmax}_{\boldsymbol{\theta}} \sum_{i=1}^m \log p_{\text{model}}(\mathbf{x}_i; \boldsymbol{\theta}) \end{aligned} \quad (5.17)$$

we can just as well work with the sum of logarithms, which is easier to handle. As we explained previously (see section on t-SNE), the maximization is equivalent to

<sup>13</sup>following “NIPS 2016 Tutorial: Generative Adversarial Networks” Ian Goodfellow, arXiv:1701.001160

the minimization of the cross-entropy between two probability distributions: the ‘true’ distribution  $p_{\text{data}}(\mathbf{x})$  from which the data has been drawn and  $p_{\text{model}}(\mathbf{x}; \boldsymbol{\theta})$ . While we do not have access to  $p_{\text{data}}(\mathbf{x})$  in principle, we estimate it empirically as a distribution peaked at the  $m$  data points we have.

Methods can now be distinguished by the way  $p_{\text{model}}$  is defined and evaluated (see Fig. 28). We differentiate between models that define  $p_{\text{data}}(\mathbf{x})$  *explicitly* through some functional form. They have the general advantage that maximization of the likelihood is rather straight-forward, since we have direct access to this function. The downside is that the functional forms are generically limiting the ability of the model to fit the data distribution or become computationally intractable.

Among those explicit density models, we can further distinguish between those that represent a computationally tractable density and those that do not. An example for tractable explicit density models are *fully visible belief networks* (FVBs) that decompose the probability distribution over an  $n$ -dimensional vector  $\mathbf{x}$  into a product of conditional probabilities

$$p_{\text{model}}(\mathbf{x}) = \prod_{j=1}^n p_{\text{model}}(x_j | x_1, \dots, x_{j-1}). \quad (5.18)$$

We can already see that, once we use the model to draw new samples, this is done one entry of the vector  $\mathbf{x}$  at a time (first  $x_1$  is drawn, then, knowing it,  $x_2$  is drawn etc.). This is computationally costly and not parallelizable but is useful for tasks that are anyway sequential (like generation of human speech, where the so-called WaveNet employs FVBs).

Models that encode an explicit density, but require approximations to maximize the likelihood that can either be variational in nature or use stochastic methods. We have seen examples for either. Variational methods define a lower bound to the log likelihood which can be maximized

$$\mathcal{L}(\mathbf{x}; \boldsymbol{\theta}) \leq \log p_{\text{model}}(\mathbf{x}; \boldsymbol{\theta}). \quad (5.19)$$

The algorithm produces a maximum value of the log-likelihood that is at least as high as the value for  $\mathcal{L}$  obtained (when summed over all data points). Variational autoencoders belong to this category. Their most obvious shortcoming is that  $\mathcal{L}(\mathbf{x}; \boldsymbol{\theta})$  may represent a very bad lower bound to the log-likelihood (and is in general not guaranteed to converge to it for infinite model size), so that the distribution represented by the model is very different from  $p_{\text{data}}$ . Stochastic methods, in contrast, often rely on a Markov chain process: The model is defined by a probability  $q(\mathbf{x}' | \mathbf{x})$  from which the current sample  $\mathbf{x}'$  is drawn, which depends on the previously drawn sample  $\mathbf{x}$  (but not any others). RBMs are an example for this. They have the advantage that there is some rigorously proven convergence to  $p_{\text{model}}$  with large enough size of the RBM, but the convergence may be slow. Like with FVBs, the drawing process is sequential and thus not easily parallelizable.

All these classes of models allow for explicit representations of the probability density function approximations. In contrast, for GANs and related models, there is only an indirect access to said probability density: The model allows us to sample from it. Naturally, this makes optimization potentially harder, but circumvents many of the other previously mentioned problems. In particular

- GANs can generate samples in parallel

- there are few restrictions on the form of the generator function (as compared to Boltzmann machines, for instance, which have a restricted form to make Markov chain sampling work)
- no Markov chains are needed
- no variational bound is needed and some GAN model families are known to be asymptotically consistent (meaning that for a large enough model they are approximations to any probability distribution).

GANs have been immensely successful in several application scenarios. Their superiority against other methods is, however, often assessed subjectively. Most of performance comparison have been in the field of image generation, and largely on the ImageNet database. Some of the standard tasks evaluated in this context are:

- generate an image from a sentence or phrase that describes its content (“a blue flower”)
- generate realistic images from sketches
- generate abstract maps from satellite photos
- generate a high-resolution (“super-resolution”) image from a lower resolution one
- predict a next frame in a video.

As far as more science-related applications are concerned, GANs have been used to

- predict the impact of climate change on individual houses
- generate new molecules that have been later synthesized.

In the light of these examples, it is of fundamental importance to understand that GANs enable (and excel at) problems with multi-modal outputs. That means the problems are such that a single input corresponds to many different ‘correct’ or ‘likely’ outputs. (In contrast to a mathematical function, which would always produce the same output.) This is important to keep in mind in particular in scientific applications, where we often search for *the one answer*. Only if that is not the case, GANs can actually play out their strengths.

Let us consider image super-resolution as an illustrative example: Conventional (deterministic) methods of increasing image resolution would necessarily lead to some blurring or artifacts, because the information that can be encoded in the finer pixel grid simply is not existent in the input data. A GAN, in contrast, will provide a possibility how a realistic image could have looked if it had been taken with higher resolution. This way they add information that may differ from the true scene of the image that was taken – a process that is obviously not yielding a unique answer since many versions of the information added may correspond to a realistic image.



Figure 29: Architecture of a GAN.

### 5.4.2 The working principle of GANs

The optimization of all neural network models we discussed so far was formulated as minimization of a cost function. For GANs, while such a formulation is also possible, a much more illuminating perspective is viewing the GAN as a *game* between two players, the *generator* ( $G$ ) and the *discriminator* ( $D$ ), see Fig. 29. The role of  $G$  is to generate from some random input  $z$  drawn from a simple distribution samples that could be mistaken from being drawn from  $p_{\text{data}}$ . The task of  $D$  is to classify its input as generated by  $G$  or coming from the data. Training should improve the performance of both  $D$  and  $G$  at their respective tasks simultaneously. After training is completed,  $G$  can be used to draw samples that closely resembles those drawn from  $p_{\text{data}}$ . In summary

$$\begin{aligned} D_{\theta_D} : \mathbf{x} &\mapsto \text{binary true/false,} \\ G_{\theta_G} : \mathbf{z} &\mapsto \mathbf{x}, \end{aligned} \tag{5.20}$$

where we have also indicated the two sets of parameters on which the two functions depend:  $\theta_D$  and  $\theta_G$ , respectively. The game is then defined by two cost functions. The discriminator wants to minimize  $J_D(\theta_D, \theta_G)$  by only changing  $\theta_D$ , while the generator  $J_G(\theta_D, \theta_G)$  by only changing  $\theta_G$ . So, each players cost depends on both their and the other players parameters, the latter of which cannot be controlled by the player. The solution to this game optimization problem is a (local) minimum, i.e., a point in  $(\theta_D, \theta_G)$ -space where  $J_D(\theta_D, \theta_G)$  has a local minimum with respect to  $\theta_D$  and  $J_G(\theta_D, \theta_G)$  has a local minimum with respect to  $\theta_G$ . In game theory such a solution is called a Nash equilibrium. Let us now specify possible choices for the cost functions as well as for  $D$  and  $G$ .

The most important requirement of  $G$  is that it is differentiable. It thus can (in contrast to VAEs) not have discrete variables on the output layer. A typical representation is a deep (possibly convolutional) neural network. A popular Deep Conventional architecture is called DCGAN. Then  $\theta_G$  are the networks weights and biases. The input  $z$  is drawn from some simple prior distribution, e.g., the uniform distribution or a normal distribution. (The specific choice of this distribution is secondary, as long as we use the same during training and when we use the generator by itself.) It is important that  $z$  has at least as high a dimension as  $x$  if the full multi-dimensional  $p_{\text{model}}$  is to be approximated. Otherwise the model will perform some sort of dimensional reduction. Several tweaks have also been used, such as feeding some components of  $z$  into a hidden instead of the input layer and adding noise to hidden layers.

The training proceeds in steps. At each step, a minibatch of  $x$  is drawn from the data set and a minibatch of  $z$  is sampled from the prior distribution. Using this,

gradient descent-type updates are performed: One update of  $\boldsymbol{\theta}_D$  using the gradient of  $J_D(\boldsymbol{\theta}_D, \boldsymbol{\theta}_G)$  and one of  $\boldsymbol{\theta}_G$  using the gradient of  $J_G(\boldsymbol{\theta}_D, \boldsymbol{\theta}_G)$ .

### 5.4.3 The cost functions

For  $D$ , the cost function of choice is the cross-entropy as with standard binary classifiers that have sigmoid output. Given that the labels are ‘1’ for data and ‘0’ for  $\mathbf{z}$  samples, it is simply

$$J_D(\boldsymbol{\theta}_D, \boldsymbol{\theta}_G) = -\frac{1}{2N_1} \sum_i \log D(\mathbf{x}_i) - \frac{1}{2N_2} \sum_j \log(1 - D(G(\mathbf{z}_j))), \quad (5.21)$$

where the sums over  $i$  and  $j$  run over the respective minibatches, which contain  $N_1$  and  $N_2$  points.

For  $G$  more variations of the cost functions have been explored. Maybe the most intuitive one is

$$J_G(\boldsymbol{\theta}_D, \boldsymbol{\theta}_G) = -J_D(\boldsymbol{\theta}_D, \boldsymbol{\theta}_G), \quad (5.22)$$

which corresponds to the so-called *zero-sum* or *minmax* game. Its solution is formally given by

$$\boldsymbol{\theta}_G^* = \arg \min_{\boldsymbol{\theta}_G} \max_{\boldsymbol{\theta}_D} [-J_D(\boldsymbol{\theta}_D, \boldsymbol{\theta}_G)]. \quad (5.23)$$

This form of the cost is convenient for theoretical analysis, because there is only a single target function, which helps drawing parallels to conventional optimization. However, other cost functions have been proven superior in practice. The reason is that minimization can get trapped very far from an equilibrium: When the discriminator manages to learn rejecting generator samples with high confidence, the gradient of the generator will be very small, making its optimization very hard.

Instead, we can use the cross-entropy also for the generator cost function (but this time from the generator’s perspective)

$$J_G(\boldsymbol{\theta}_D, \boldsymbol{\theta}_G) = -\frac{1}{2N_2} \sum_j \log D(G(\mathbf{z}_j)). \quad (5.24)$$

Now the generator maximizes the probability of the discriminator being mistaken. This way, each player still has a strong gradient when the player is losing the game. We observe that this version of  $J_G(\boldsymbol{\theta}_D, \boldsymbol{\theta}_G)$  has no direct dependence of the training data. Of course, such a dependence is implicit via  $D$ , which has learned from the training data. This indirect dependence also acts like a regularizer, preventing overfitting:  $G$  has no possibility to directly ‘fit’ its output to training data.

### 5.4.4 Remarks

In closing this section, we comment on a few properties of GANs, which also mark frontiers for improvements. One global problem is that GANs are typically difficult to train: they require large training sets and are highly susceptible to hyperparameter fluctuations. It is currently an active topic of research to compensate for this with the structural modification and novel loss function formulations.

**Mode collapse** — this may describe one of the most obvious problems of GANs: it refers to a situation where  $G$  does not explore the full space to which  $\mathbf{x}$  belongs, but rather maps several inputs  $\mathbf{z}$  to the same output. Mode collapse can be more or less severe. For instance a  $G$  trained on generating images may always resort to certain fragments or patterns of images. A formal reason for mode collapse is when the simultaneous gradient descent gravitates towards a solution

$$\boldsymbol{\theta}_G^* = \arg \max_{\boldsymbol{\theta}_D} \min_{\boldsymbol{\theta}_G} [-J_D(\boldsymbol{\theta}_D, \boldsymbol{\theta}_G)], \quad (5.25)$$

instead of the order in Eq. (5.23). (A priori it is not clear which of the two solutions is closer to the algorithm's doing.) Note that the interchange of min and max in general corresponds to a different solution: It is now sufficient for  $G$  to always produce one (and the same) output that is classified as data by  $D$  with very high probability. Due to the mode collapse problem, GANs are not good at exploring ergodically the full space of possible outputs. They rather produce few very good possible outputs.

One strategy to fight mode collapse is called *minibatch features*. Instead of letting  $D$  rate one sample at a time, a minibatch of real and generated samples is considered at once. It then detects whether the generated samples are unusually close to each other.

**Arithmetics with GANs** — it has been demonstrated that GANs can do linear arithmetics with inputs to add or remove abstract features from the output. This has been demonstrated using a DCGAN trained on images of faces. The gender and the feature ‘wearing glasses’ can be added or subtracted and thus changed at will. Of course such a result is only empirical, there is no formal mathematical theory why it works.

**Using GANs with labelled data** — it has been shown that, if (partially) labeled data is available, using the labels when training  $D$  may improve the performance of  $G$ . In this constellation,  $G$  has still the same task as before and does not interact with the labels. If data with  $n$  classes exist, then  $D$  will be constructed as a classifier for  $(n + 1)$  classes, where the extra class corresponds to ‘fake’ data that  $D$  attributes to coming from  $G$ . If a data point has a label, then this label is used as a reference in the cost function. If a datapoint has no label, then the first  $n$  outputs of  $D$  are summed up.

**One-sided label smoothing** — this technique is useful not only for the  $D$  in GANs but also other binary classification problems with neural networks. Often we observe that classifiers give proper results, but show a too confident probability. This overshooting confidence can be counteracted by one-sided label smoothing. The idea is to simply replace the target value for the real examples with a value slightly less than 1, e.g., 0.9. This smoothes the distribution of the discriminator. Why do we only perform this off-set one-sided and not also give a small nonzero value  $\beta$  to the fake samples target values? If we were to do this, the optimal function for  $D$  is

$$D^*(\mathbf{x}) = \frac{p_{\text{data}}(\mathbf{x}) + \beta p_{\text{model}}(\mathbf{x})}{p_{\text{data}}(\mathbf{x}) + p_{\text{model}}(\mathbf{x})}. \quad (5.26)$$

Consider now a range of  $\mathbf{x}$  for which  $p_{\text{data}}(\mathbf{x})$  is small but  $p_{\text{model}}(\mathbf{x})$  is large (a “spurious mode”).  $D^*(\mathbf{x})$  will have a peak near this spurious mode. This means  $D$  reinforces incorrect behavior of  $G$ . This will encourage  $G$  to reproduce samples that it already makes (irrespective of whether they are anything like real data).

# 6 Interpretability of Neural Networks

In particular for applications in science, we not only want to obtain a neural network that excels at performing a given task, but we also seek an understanding how the problem was solved. Ideally, we want to know underlying principles, deduce causal relations, identify abstracted notions. This is the topic of interpretability.

## 6.1 Dreaming and the problem of extrapolation

Exploring the weights and intermediate activations of a neural network in order to understand what the network has learnt, very quickly becomes unfeasible or uninformative for large network architectures. In this case, we can try a different approach, where we focus on the inputs to the neural network, rather than the intermediate activations.

More precisely, let us consider a neural network classifier  $\mathbf{f}$ , depending on the weights  $W$ , which maps an input  $\mathbf{x}$  to a probability distribution over  $n$  classes  $\mathbf{f}(\mathbf{x}|W) \in \mathbb{R}^n$ , i.e.,

$$F_i(\mathbf{x}|\theta) \geq 0 \quad \text{and} \quad \sum_i F_i(\mathbf{x}|\theta) = 1. \quad (6.1)$$

We want to minimise the distance between the output of the network  $\mathbf{f}(\mathbf{x})$  and a chosen target output  $\mathbf{y}_{\text{target}}$ , which can be done by minimizing the loss function

$$L = |\mathbf{F}(\mathbf{x}) - \mathbf{y}_{\text{target}}|^2. \quad (6.2)$$

However, unlike in supervised learning where the loss minimization was done with respect to the weights  $W$  of the network, here we are interested in minimizing with respect to the input  $\mathbf{x}$  while keeping the weights  $W$  fixed. This can be achieved using gradient descent, i.e.

$$\mathbf{x} \rightarrow \mathbf{x} - \eta \frac{\partial L}{\partial \mathbf{x}}, \quad (6.3)$$

where  $\eta$  is the learning rate. With a sufficient number of iterations, our initial input  $\mathbf{x}^0$  will be transformed into the final input  $\mathbf{x}^*$  such that

$$\mathbf{f}(\mathbf{x}^*) \approx \mathbf{y}_{\text{target}}. \quad (6.4)$$

By choosing the target output to correspond to a particular class, e.g.,  $\mathbf{y}_{\text{target}} = (1, 0, 0, \dots)$ , we are then essentially finding examples of inputs which the network would classify as belonging to the chosen class. This procedure is called *dreaming*.

Let us apply this technique to a binary classification example. We consider a dataset <sup>14</sup> consisting of images of healthy and unhealthy plant leaves. Some samples from the dataset are shown in the top row of Fig. 30. After training a deep convolutional network to classify the leaves (reaching a test accuracy of around 95%), we start with a random image as our initial input  $\mathbf{x}^0$  and perform gradient descent on the input, as described above, to arrive at the final image  $\mathbf{x}^*$  which our network confidently classifies.

---

<sup>14</sup>Source: <https://data.mendeley.com/datasets/tywbtsjrjv/1>

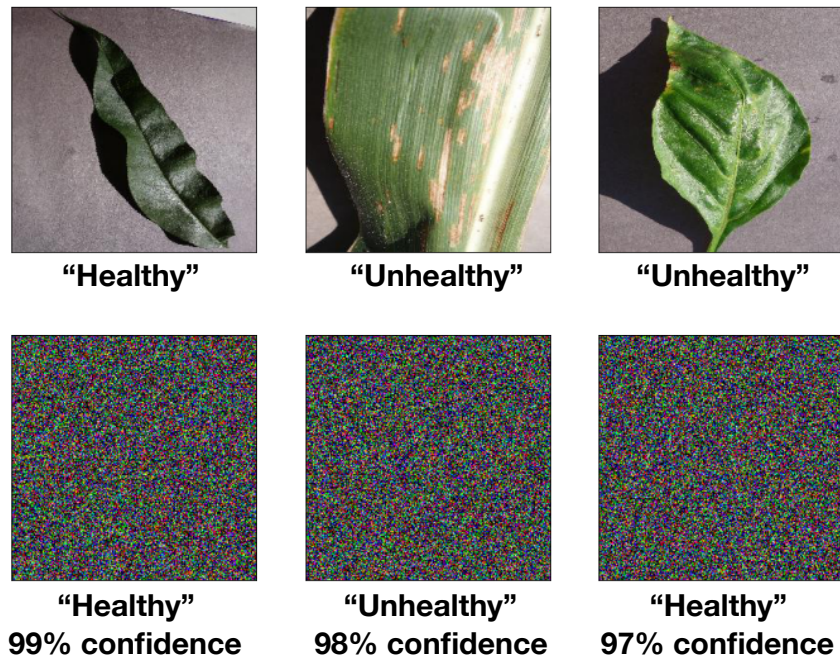


Figure 30: **Plant leaves.** Top: Some samples from the plants dataset. Bottom: Samples generated by using the "dreaming" procedure starting from random noise.

In bottom row of Fig. 30, we show three examples produced using the ‘dreaming’ technique. On first sight, it might be astonishing that the final image actually does not even remotely resemble a leaf. How could it be that the network has such a high accuracy of around 95%, yet we have here a confidently classified image which is essentially just noise. Although this seem surprising, a closer inspection reveals the problem: The noisy image  $\mathbf{x}^*$  looks nothing like the samples in the dataset with which we trained our network. By feeding this image into our network, we are asking it to make an extrapolation, which as can be seen leads to an uncontrolled behavior. This is a key issue which plagues most data driven machine learning approaches. With few exceptions, it is very difficult to train a model capable of performing reliable extrapolations. Since scientific research is often in the business of making extrapolations, this is an extremely important point of caution to keep in mind.

While it might seem obvious that any model should only be predictive for data that ‘resembles’ those in the training set, the precise meaning of ‘resembles’ is actually more subtle than one imagines. For example, if one trains a ML model using a dataset of images captured using a Canon camera but subsequently decide to use the model to make predictions on images taken with a Nikon camera, we could actually be in for a surprise. Even though the images may ‘resemble’ each other to our naked eye, the different cameras can have a different noise profile which might not be perceptible to the human eye. We shall see in the next section that even such minute image distortions can already be sufficient to completely confuse our model.

## 6.2 Adversarial attacks

As we have seen, it is possible to modify the input  $\mathbf{x}$  so that the corresponding model approximates a chosen target output. This concept can also be applied to

generate *adversarial examples*, i.e. images which have been intentionally modified to cause a model to misclassify it. In addition, we usually want the modification to be minimal or almost imperceptible to the human eye.

One common method for generating adversarial examples is known as the *fast gradient sign method*. Starting from an input  $\mathbf{x}^0$  which our model correctly classifies, we choose a target output  $\mathbf{y}^*$  which corresponds to a wrong classification, and follow the procedure described in the previous section with a slight modification. Instead of updating the input according to Eq. (6.3) we use the following update rule:

$$\mathbf{x} \rightarrow \mathbf{x} - \eta \operatorname{sign} \left( \frac{\partial L}{\partial \mathbf{x}} \right), \quad (6.5)$$

where  $L$  is given by Eq. (6.2). The  $\operatorname{sign}(\dots) \in \{-1, 1\}$  both serves to enhance the signal and also acts as constraint to limit the size of the modification. By choosing  $\eta = \frac{\epsilon}{T}$  and performing only  $T$  iterations, we can then guarantee that each component of the final input  $\mathbf{x}^*$  satisfies

$$|x_i^* - x_i^0| \leq \epsilon, \quad (6.6)$$

which is important since we want our final image  $\mathbf{x}^*$  to be only minimally modified. We summarize this algorithm as follows:

#### Algorithm 5: Fast Gradient Sign Method

**Input:** A classification model  $\mathbf{f}$ , a loss function  $L$ , an initial image  $\mathbf{x}^0$ , a target label  $\mathbf{y}_{\text{target}}$ , perturbation size  $\epsilon$  and number of iterations  $T$

**Output:** Adversarial example  $\mathbf{x}^*$  with  $|x_i^* - x_i^0| \leq \epsilon$

```

 $\eta = \epsilon/T$  ;
for  $i=1 \dots T$  do
   $\mathbf{x} = \mathbf{x} - \eta \operatorname{sign} \left( \frac{\partial L}{\partial \mathbf{x}} \right)$  ;
end

```

This process of generating adversarial examples is called an *adversarial attack*, which we can classify under two broad categories: *white box* and *black box* attacks. In a white box attack, the attacker has full access to the network  $\mathbf{f}$  and is thus able to compute or estimate the gradients with respect to the input. On the other hand, in a black box attack, the adversarial examples are generated without using the target network  $\mathbf{f}$ . In this case, a possible strategy for the attacker is to train his own model  $\mathbf{g}$ , find an adversarial example for his model and use it against his target  $\mathbf{f}$  without actually having access to it. Although it might seem surprising, this strategy has been found to work albeit with a lower success rate as compared to white box methods. We shall illustrate these concepts in the example below.

### 6.2.1 Example

We shall use the same plant leaves classification example as above. The target model  $\mathbf{f}$  which we want to 'attack' is a *pretrained* model using Google's well known *Incep-*

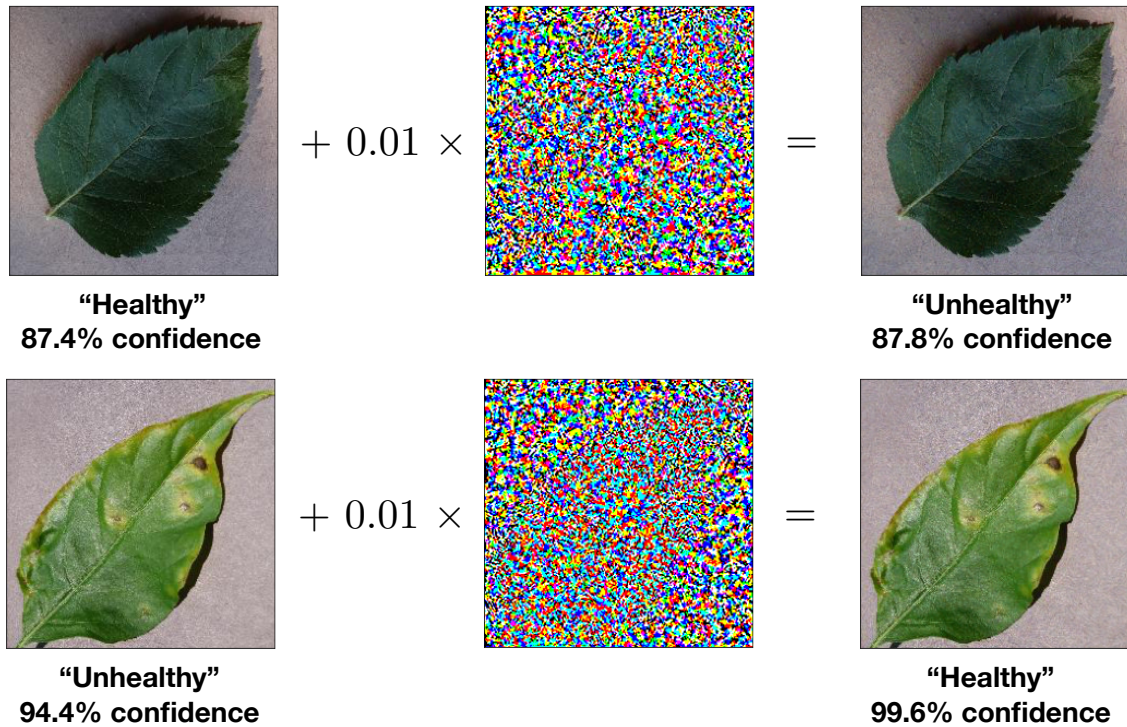


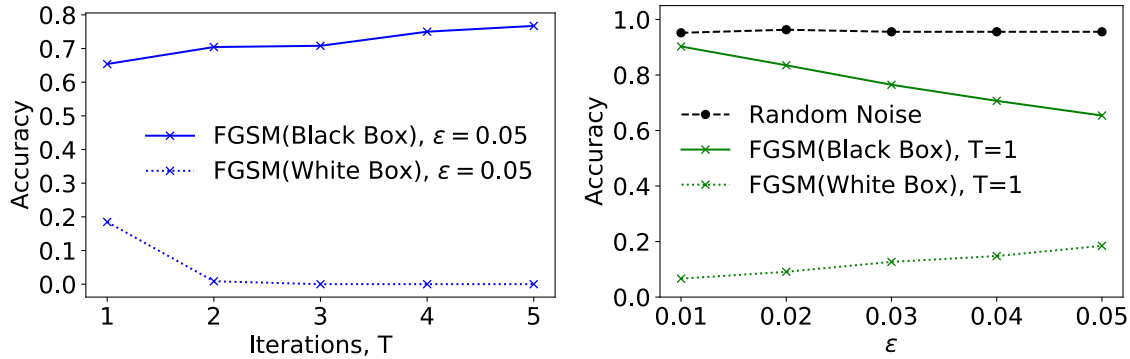
Figure 31: **Adversarial examples.** Generated using the fast gradient sign method with  $T = 1$  iteration and  $\epsilon = 0.01$ . The target model is Google’s *InceptionV3* deep convolutional network with a test accuracy of  $\sim 95\%$  on the binary ("Healthy" vs "Unhealthy") plants dataset.

*InceptionV3* deep convolutional neural network containing over 20 million parameters<sup>15</sup>. The model achieved a test accuracy of  $\sim 95\%$ . Assuming we have access to the gradients of the model  $\mathbf{f}$ , we can then consider a white box attack. Starting from an image in the dataset which the target model correctly classifies and applying the fast gradient sign method (Alg. 5) with  $\epsilon = 0.01$  and  $T = 1$ , we obtain an adversarial image which differs from the original image by almost imperceptible amount of noise as depicted on the left of Fig. 31. Any human would still correctly identify the image but yet the network, which has around 95% accuracy has completely failed.

If, however, the gradients and outputs of the target model  $\mathbf{f}$  are hidden, the above white box attack strategy becomes unfeasible. In this case, we can adopt the following ‘black box attack’ strategy. We train a secondary model  $\mathbf{g}$ , and then applying the FGSM algorithm to  $\mathbf{g}$  to generate adversarial examples for  $\mathbf{g}$ . Note that it is not necessary for  $\mathbf{g}$  to have the same network architecture as the target model  $\mathbf{f}$ . In fact, it is possible that we do not even know the architecture of our target model.

Let us consider another pretrained network based on *MobileNet* containing about 2 million parameters. After retraining the top classification layer of this model to a test accuracy of  $\sim 95\%$ , we apply the FGSM algorithm to generate some adversarial examples. If we now test these examples on our target model  $\mathbf{f}$ , we notice

<sup>15</sup>This is an example of *transfer learning*. The base model, *InceptionV3*, has been trained on a different classification dataset, *ImageNet*, with over 1000 classes. To apply this network to our binary classification problem, we simply replace the top layer with a simple duo-output dense softmax layer. We keep the weights of the base model fixed and only train the top layer.

Figure 32: **Black Box Adversarial Attack.**

a significant drop in the accuracy as shown on the graph on the right of Fig. 32. The fact that the drop in accuracy is greater for the black box generated adversarial images as compared to images with random noise (of the same scale) added to it, shows that adversarial images have some degree of transferability between models. As a side note, on the left of Fig. 32 we observe that black box attacks are more effective when only  $T = 1$  iteration of the FGSM algorithm is used, contrary to the situation for the white box attack. This is because, with more iterations, the method has a tendency towards overfitting the secondary model, resulting in adversarial images which are less transferable.

These forms of attacks highlight a serious vulnerability of such data driven machine learning techniques. Defending against such attack is an active area of research but it is largely a cat and mouse game between the attacker and defender.

### 6.3 Interpreting autoencoders

Previously we have learned about a broad scope of application of generative models. We have seen that autoencoders can serve as powerful generative models in the scientific context by extracting the compressed representation of the input and using it to generate new instances of the problem. It turns out that in the simple enough problems one can find a meaningful interpretation of the latent representation that may be novel enough to help us get new insight into the problem we are analyzing.

In 2020, the group of Renato Renner considered a machine learning perspective on one of the most historically important problems in physics: Copernicus heliocentric system of the solar orbits. Via series of careful and precise measurements of positions of objects in the night sky, Copernicus conjectured that Sun is the center of the solar system and other planets are orbiting around it. Let us now ask the following question: is it possible to build a neural network that receives the same observation angles Copernicus did and deduces the same conclusion from them?

Renner group inputted into the autoencoder the angles of Mars and Sun as observed from Earth ( $\alpha_{ES}$  and  $\alpha_{EM}$  in Fig. 33) in certain times and asked the autoencoder to predict the angles at other times. When analyzing the trained model they realized that the two latent neurons included in their model are storing information in the **heliocentric coordinates!** In particular, one observes that the information stored in the latent space is a linear combination of angles between Sun and Mars,  $\gamma_{SM}$  and Sun and Earth  $\gamma_{SE}$ . In other words, just like Copernicus, the

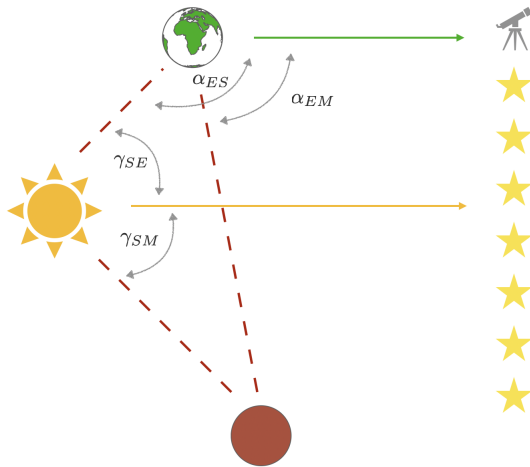


Figure 33: **The Copernicus problem.** Relation between angles in heliocentric and geocentric coordinate system.

autoencoder has learned, that the most efficient way to store the information given is to transform it into the heliocentric coordinate system.

While this fascinating example is a great way to show the generative models can be interpreted in some important cases, in general the question of interpretability is still very much open and subject to ongoing research. In the instances discussed earlier in this book, like generation of molecules, where the input is compressed through several layers of transformations requiring a complex dictionary and the dimension of the latent space is high, interpreting latent space becomes increasingly challenging.

## 7 Reinforcement Learning

In the previous sections, we have introduced data-based learning, where we are given a dataset  $\{\mathbf{x}_i\}$  for training. Depending on whether we are given labels  $y_i$  with each data point, we have further divided our learning task as either being supervised or unsupervised, respectively. The aim of machine learning is then to classify unseen data (supervised), or extract useful information from the data and generate new data resembling the data in the given dataset (unsupervised). However, the concept of learning as commonly understood certainly encompasses other forms of learning that are not falling into these data-driven categories.

An example for a form of learning not obviously covered by supervised or unsupervised learning is learning how to walk: in particular, a child that learns how to walk does not first collect data on all possible ways of successfully walking to extract rules on how to walk best. Rather, the child performs an action, sees what happens, and then adjusts their actions accordingly. This kind of learning thus happens best ‘on-the-fly’, in other words while performing the attempted task. *Reinforcement learning* formalizes this different kind of learning and introduces suitable (computational) methods.

As we will explain in the following, the framework of reinforcement learning considers an *agent*, that interacts with an *environment* through actions, which, on the one hand, changes the *state* of the agent and on the other hand, leads to a *reward*. Whereas we tried to minimize a loss function in the previous sections, the main goal of reinforcement learning is to maximize this reward by learning an appropriate *policy*. One way of reformulating this task is to find a *value function*, which associates to each state (or state-action pair) a value, or expected total reward. Note that, importantly, to perform our learning task we do not require knowledge, a *model*, of the environment. All that is needed is feedback to our actions in the form of a reward signal and a new state. We stress again that we study in the following methods that learn at each time step. One could also devise methods, where an agent tries a policy many times and judges only the final outcome.

The framework of reinforcement learning is very powerful and versatile. Examples include:

- We can train a robot to perform a task, such as using an arm to collect samples. The state of the agent is the position of the robot arm, the actions move the arm, and the agent receives a reward for each sample collected.
- We can use reinforcement learning to optimize experiments, such as chemical reactions. In this case, the state contains the experimental conditions, such as temperature, solvent composition, or pH and the actions are all possible ways of changing these state variables. The reward is a function of the yield, the purity, or the cost. Note that reinforcement learning can be used at several levels of this process: While one agent might be trained to target the experimental conditions directly, another agent could be trained to reach the target temperature by adjusting the current running through a heating element.
- We can train an agent to play a game, with the state being the current state of the game and a reward is received once for winning. The most famous example for such an agent is Google’s AlphaGo, which outperforms humans in the

game of Go. A possible way of applying reinforcement learning in the sciences is to phrase a problem as a game. An example, where such rephrasing was successfully applied, is error correction for (topological) quantum computers.

- In the following, we will use a toy example to illustrate the concepts introduced: We want to train an agent to help us with the plants in our lab: in particular, the state of the agent is the water level. The agent can turn on and off a growth lamp and it can send us a message if we need to show up to water the plants. Obviously, we would like to optimize the growth of the plants and not have them die.

As a full discussion of reinforcement learning goes well beyond the scope of this lecture, we will focus in the following on the main ideas and terminology with no claim of completeness.

## 7.1 Exploration versus exploitation

We begin our discussion with a simple example that demonstrates some important aspects of reinforcement learning. In particular, we discuss a situation, where the reward does not depend on a state, but only on the action taken. The agent is a doctor, who has to choose from  $n$  actions, the treatments, for a given disease, with the reward depending on the recovery of the patient. The doctor ‘learns on the job’ and tries to find the best treatment. The *value* of a treatment  $a \in \mathcal{A}$  is denoted by  $q_*(a) = E(r)$ , the expectation value of our reward.

Unfortunately, there is an uncertainty in the outcome of each treatment, such that it is not enough to perform each treatment just once to know the best one. Rather, only by performing a treatment many times we find a good estimate  $Q_t(a) \approx q_*(a)$ . Here,  $Q_t(a)$  is our estimate of the value of  $a$  after  $t$  (time-) steps. Obviously, we should not perform a bad treatment many times, only to have a better estimate for its failure. We could instead try each action once and then continue for the rest of the time with the action that performed best. This strategy is called a *greedy* method and *exploits* our knowledge of the system. Again, this strategy bears risks, as the uncertainty in the outcome of the treatment means that we might use a suboptimal treatment. It is thus crucial to *explore* other actions. This dilemma is called the ‘conflict between exploration and exploitation’. A common strategy is to use the best known action  $a_* = \text{argmax}_a Q_t(a)$  most of the time, but with probability  $\epsilon$  choose randomly one of the other actions. This strategy of choosing the next action is called  $\epsilon$ -*greedy*.

## 7.2 Finite Markov decision process

After this introductory example, we introduce the idealized form of reinforcement learning with a Markov decision process (MDP). At each time step  $t$ , the agent starts from a state  $S_t \in \mathcal{S}$ , performs an action  $A_t \in \mathcal{A}$ , which, through interaction with the environment, leads to a reward  $R_{t+1} \in \mathcal{R}$  and moves the agent to a new state  $S_{t+1}$ . This agent-environment interaction is schematically shown in Fig. 34. Note that we assume the space of all actions, states, and rewards to be finite, such that we talk about a *finite* MDP.

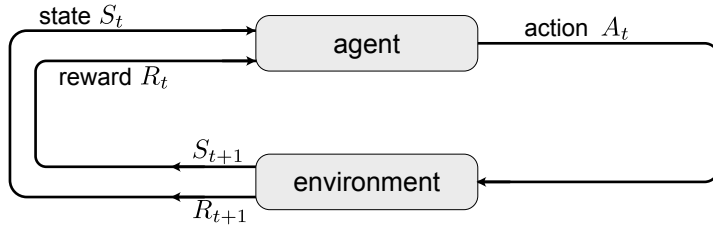


Figure 34: **Markov decision process.** Schematic of the agent-environment interaction.

For our toy example, the sensor we have only shows whether the water level is high (h) or low (l), so that the state space of our agent is  $\mathcal{S} = \{h, l\}$ . In both cases, our agent can choose to turn the growth lamps on or off, or in the case of low water, he can choose to send us a message so we can go and water the plants. The available actions are thus  $\mathcal{A} = \{\text{on, off, text}\}$ . When the growth lamps are on, the plants grow faster, which leads to a bigger reward,  $r_{\text{on}} > r_{\text{off}} > 0$ . Furthermore, there is a penalty for texting us, but an even bigger penalty for letting the plants die,  $0 > r_{\text{text}} > r_{\text{fail}}$ .

A model of the environment provides the probability of ending in state  $s'$  with reward  $r$ , starting from a state  $s$  and choosing the action  $a$ ,  $p(s', r|s, a)$ . In this case, the dynamics of the Markov decision process is completely characterized. Note that the process is a Markov process, since the next state and reward only depend on the current state and chosen action.

In our toy example, being in state ‘high’ and having the growth lamp on will provide a reward of  $r_{\text{on}}$  and keep the agent in ‘high’ with probability  $p(h, r_{\text{on}}|h, \text{on}) = \alpha$ , while with  $1 - \alpha$  the agent will end up with a low water level. However, if the agent turns the lamps off, the reward is  $r_{\text{off}}$  and the probability of staying in state ‘high’ is  $\alpha' > \alpha$ . For the case of a low water level, the probability of staying in low despite the lamps on is  $p(l, r_{\text{on}}|l, \text{on}) = \beta$ , which means that with probability  $1 - \beta$ , our plants run out of water. In this case, we will need to get new plants and we will water them, of course, such that  $p(h, r_{\text{fail}}|l, \text{on}) = 1 - \beta$ . As with high water levels, turning the lamps off reduces our rewards, but increases our chance of not losing the plants,  $\beta' > \beta$ . Finally, if the agent should choose to send us a text, we will refill the water, such that  $p(h, r_{\text{text}}|l, \text{text}) = 1$ . The whole Markov process is summarized in the *transition graph* in Fig. 35.

From the probability for the next reward and state, we can also calculate the expected reward starting from state  $s$  and choosing action  $a$ , namely

$$r(s, a) = \sum_{r \in \mathcal{R}} r \sum_{s' \in \mathcal{S}} p(s', r|s, a). \quad (7.1)$$

Obviously, the value of an action now depends on the state the agent is in, such that we write  $q_*(s, a)$ . Alternatively, we can also assign to each state a value  $v_*(s)$ , which quantizes the optimal reward from this state.

Finally, we can define what we want to accomplish by learning: knowing our current state  $s$ , we want to know what action to choose such that our future total reward is maximized. Importantly, we want to accomplish this without any prior knowledge of how to optimize rewards directly. This poses yet another question: what is the total reward? We usually distinguish tasks with a well-defined end point

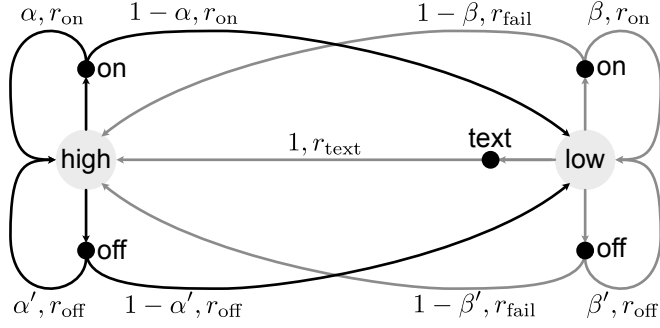


Figure 35: **Transition graph of the MDP for the plant-watering agent.** The states ‘high’ and ‘low’ are denoted with large circles, the actions with small black circles, and the arrows correspond to the probabilities and rewards.

$t = T$ , so-called *episodic tasks*, from *continuous tasks* that go on for ever. The total reward for the former is simply the total *return*

$$G_t = R_{t+1} + R_{t+2} + R_{t+3} + \cdots + R_T. \quad (7.2)$$

As such a sum is not guaranteed to converge for a continuous task, the total reward is the *discounted return*

$$G_t = R_{t+1} + \gamma R_{t+2} + \gamma^2 R_{t+3} + \cdots = \sum_{k=0}^{\infty} \gamma^k R_{t+k+1}, \quad (7.3)$$

with  $0 \leq \gamma < 1$  the discount rate. Equation (7.3) is more general and can be used for an episodic task by setting  $\gamma = 1$  and  $R_t = 0$  for  $t > T$ . Note that for rewards which are bound, this sum is guaranteed to converge to a finite value.

### 7.3 Policies and value functions

A policy  $\pi(a|s)$  is the probability of choosing the action  $a$  when in state  $s$ . We can thus formulate our learning task as finding the policy that maximizes our reward and reinforcement learning as adapting an agent’s policy as a result of its experience. For a given policy, we can define the value function of a state  $s$  as the expected return from starting in that state and using the policy function  $\pi$  for choosing all our future actions. We can write this as

$$v_{\pi}(s) \equiv E_{\pi}(G_t|S_t = s). \quad (7.4)$$

Alternatively, we can define the action-value function of  $\pi$  as

$$q_{\pi}(s, a) \equiv E_{\pi}(G_t|S_t = s, A_t = a). \quad (7.5)$$

This is the expectation value for the return starting in state  $s$  and choosing action  $a$ , but using the policy  $\pi$  for all future actions. Note that one of the key ideas of reinforcement learning is to use such value functions, instead of the policy, to organize our learning process.

The value function of Eq. (7.4) satisfies a self-consistency equation,

$$v_\pi(s) = E_\pi(R_{t+1} + \gamma G_{t+1} | S_t = s) \quad (7.6)$$

$$= \sum_a \pi(a|s) \sum_{s',r} p(s',r|s,a) [r + \gamma v_\pi(s')]. \quad (7.7)$$

This equation, known as the *Bellman equation*, relates the value of state  $s$  to the expected reward and the (discounted) value of the next state after having chosen an action under the policy  $\pi(a|s)$ .

As an example, we can write the Bellman equation for the strategy of always leaving the lamps on in our toy model. Then, we find the system of linear equations

$$v_{\text{on}}(\text{h}) = p(\text{h}, r_{\text{on}}|\text{h}, \text{on}) [r_{\text{on}} + \gamma v_{\text{on}}(\text{h})] + p(\text{l}, r_{\text{on}}|\text{h}, \text{on}) [r_{\text{on}} + \gamma v_{\text{on}}(\text{l})] \\ = r_{\text{on}} + \gamma [\alpha v_{\text{on}}(\text{h}) + (1 - \alpha) v_{\text{on}}(\text{l})], \quad (7.8)$$

$$v_{\text{on}}(\text{l}) = \beta [r_{\text{on}} + \gamma v_{\text{on}}(\text{l})] + (1 - \beta) [r_{\text{fail}} + \gamma v_{\text{on}}(\text{h})], \quad (7.9)$$

from which we can solve easily for  $v_{\text{on}}(\text{h})$  and  $v_{\text{on}}(\text{l})$ .

Instead of calculating the value function for all possible policies, we can directly try and find the optimal policy  $\pi_*$ , for which  $v_{\pi_*}(s) > v_{\pi'}(s)$  for all policies  $\pi'$  and  $s \in \mathcal{S}$ . For this policy, we find the *Bellman optimality equations*

$$v_*(s) = \max_a q_{\pi_*}(s, a) \\ = \max_a E(R_{t+1} + \gamma v_*(S_{t+1}) | S_t = s, A_t = a) \quad (7.10)$$

$$= \max_a \sum_{s',r} p(s',r|s,a) [r + \gamma v_*(s')]. \quad (7.11)$$

Importantly, the Bellman optimality equations do not depend on the actual policy anymore. As such, Eq. (7.11) defines a non-linear system of equations, which for a sufficiently simple MDP can be solved explicitly. For our toy example, the two equations for the value functions are

$$v_*(\text{h}) = \max \begin{cases} r_{\text{on}} + \gamma [\alpha v_*(\text{h}) + (1 - \alpha) v_*(\text{l})] \\ r_{\text{off}} + \gamma [\alpha' v_*(\text{h}) + (1 - \alpha') v_*(\text{l})] \end{cases} \quad (7.12)$$

and

$$v_*(\text{l}) = \max \begin{cases} \beta [r_{\text{on}} + \gamma v_*(\text{l})] + (1 - \beta) [r_{\text{fail}} + \gamma v_*(\text{h})] \\ \beta' [r_{\text{off}} + \gamma v_*(\text{l})] + (1 - \beta') [r_{\text{fail}} + \gamma v_*(\text{h})] \\ r_{\text{text}} + \gamma v_*(\text{h}) \end{cases} . \quad (7.13)$$

Note that equivalent equations to Eqs. (7.10) and (7.11) hold for the state-action value function

$$q_*(s, a) = E(R_{t+1} + \gamma \max_{a'} q_*(S_{t+1}, a')) \quad (7.14)$$

$$= \sum_{s',r} p(s',r|s,a) [r + \gamma \max_{a'} q_*(s',a')]. \quad (7.15)$$

Once we know  $v_*$ , the optimal policy  $\pi_*(a|s)$  is the greedy policy that chooses the action  $a$  that maximizes the right-hand side of Eq. (7.11). If, instead, we know  $q_*(s, a)$ , then we can directly choose the action which maximizes  $q_*(s, a)$ , namely  $\pi_*(a|s) = \text{argmax}_{a'} q_*(s, a')$ , without looking one step ahead.

While Eqs (7.11) or (7.15) can be solved explicitly for a sufficiently simple system, such an approach, which corresponds to an exhaustive search, is often not feasible. In the following, we distinguish two levels of complexity: First, if the explicit solution is too hard, but we can still keep track of all possible value functions—we can choose either the state or the state-action value function—we can use a *tabular* approach. A main difficulty in this case is the evaluation of a policy, or prediction, which is needed to improve on the policy. While various methods for *policy evaluation* and *policy improvement* exist, we will discuss in the following an approach called *temporal-difference learning*. Second, in many cases the space of possible states is much too large to allow for a complete knowledge of all value functions. In this case, we additionally need to approximate the value functions. For this purpose, we can use the methods encountered in the previous chapters, such as (deep) neural networks.

## 7.4 Temporal-difference learning

If we cannot explicitly solve the Bellman optimality equations—the case most often encountered—then we need to find the optimal policy by some other means. If the state space is still small enough to keep track of all value functions, we can tabulate the value function for all the states and a given policy and thus, speak of *tabular methods*. The most straight-forward approach, referred to as *policy iteration*, proceeds in two steps: First, given a policy  $\pi(a|s)$ , the value function  $v_\pi(s)$  is evaluated. Second, after this *policy evaluation*, we can improve on the given policy  $\pi(a|s)$  using the greedy policy

$$\pi'(a|s) = \operatorname{argmax}_a \sum_{s',r} p(s',r|s,a)[r + \gamma v_\pi(s')]. \quad (7.16)$$

This second step is called *policy improvement*. The full policy iteration then proceeds iteratively

$$\pi_0 \rightarrow v_{\pi_0} \rightarrow \pi_1 \rightarrow v_{\pi_1} \rightarrow \pi_2 \rightarrow \dots \quad (7.17)$$

until convergence to  $v_*$  and hence  $\pi_*$ . Note that, indeed, the Bellman optimality equation (7.11) is the fixed-point equation for this procedure.

Policy iteration requires a full evaluation of the value function of  $\pi_k$  for every iteration  $k$ , which is usually a costly calculation. Instead of fully evaluating the value function under a fixed policy, we can also directly try and calculate the optimal value function by iteratively solving the Bellman optimality equation,

$$v^{[k+1]}(s) = \max_a \sum_{s',r} p(s',r|s,a)[r + \gamma v^{[k]}(s')]. \quad (7.18)$$

Note that once we have converged to the optimal value function, the optimal policy is given by the greedy policy corresponding to the right-hand side of Eq. (7.16). An alternative way of interpreting this iterative procedure is to perform policy improvement every time we update the value function, instead of finishing the policy evaluation each time before policy improvement. This procedure is called *value iteration* and is an example of a *generalized policy iteration*, the idea of allowing policy evaluation and policy improvement to interact while learning.

In the following, we want to use such a generalized policy iteration scheme for the (common) case, where we do not have a model for our environment. In this model-free case, we have to perform the (generalized) policy improvement using only our interactions with the environment. It is instructive to first think about how to evaluate a policy. We have seen in Eqs. (7.4) and (7.6) that the value function can also be written as an expectation value,

$$v_\pi(s) = E_\pi(G_t|S_t = s) \quad (7.19)$$

$$= E_\pi(R_{t+1} + \gamma v_\pi(S_{t+1})|S_t = s). \quad (7.20)$$

We can thus either try to directly sample the expectation value of the first line—this can be done using *Monte Carlo sampling* over possible state-action sequences—or we try to use the second line to iteratively solve for the value function. In both cases, we start from state  $S_t$  and choose an action  $A_t$  according to the policy we want to evaluate. The agent’s interaction with the environment results in the reward  $R_{t+1}$  and the new state  $S_{t+1}$ . Using the second line, Eq. (7.20), goes under the name *temporal-difference learning* and is in many cases the most efficient method. In particular, we make the following updates

$$v_\pi^{[k+1]}(S_t) = v_\pi^{[k]}(S_t) + \alpha[R_{t+1} + \gamma v_\pi^{[k]}(S_{t+1}) - v_\pi^{[k]}(S_t)]. \quad (7.21)$$

The expression in the brackets is the difference between our new estimate and the old estimate of the value function and  $\alpha < 1$  is a learning rate. As we look one step ahead for our new estimate, the method is called one-step temporal difference method.

We now want to use generalized policy iteration to find the optimal value. We already encountered a major difficulty when improving a policy using a value function based on experience in Sec. 7.1: it is difficult to maintain enough exploration over possible action-state pairs and not end up exploiting the current knowledge. However, this sampling is crucial for both Monte Carlo methods and the temporal-difference learning we discuss here. In the following, we will discuss two different methods of performing the updates, both working on the state-action value function, instead of the value function. Both have in common that we look one step ahead to update the state-action value function. A general update should then be of the form

$$q^{[k+1]}(S_t, a) = q^{[k]}(S_t, a) + \alpha[R_{t+1} + \gamma q^{[k]}(S_{t+1}, a') - q^{[k]}(S_t, a)] \quad (7.22)$$

and the question is then what action  $a$  we should take for the state-action pair and what action  $a'$  should be taken in the new state  $S_{t+1}$ .

Starting from a state  $S_0$ , we first choose an action  $A_0$  according to a policy derived from the current estimate of the state-action value function <sup>16</sup>, such as an  $\epsilon$ -greedy policy. For the first approach, we perform updates as

$$q^{[k+1]}(S_t, A_t) = q^{[k]}(S_t, A_t) + \alpha[R_{t+1} + \gamma q^{[k]}(S_{t+1}, A_{t+1}) - q^{[k]}(S_t, A_t)]. \quad (7.23)$$

As above, we are provided a reward  $R_{t+1}$  and a new state  $S_{t+1}$  through our interaction with the environment. To choose the action  $A_{t+1}$ , we again use a policy derived

---

<sup>16</sup>We assume here an episodic task. At the very beginning of training, we may initialize the state-action value function randomly.

from  $Q^{[k]}(s = S_{t+1}, a)$ . Since we are using the policy for choosing the action in the next state  $S_{t+1}$ , this approach is called *on-policy*. Further, since in this particular case, we use the quintuple  $S_t, A_t, R_{t+1}, S_{t+1}, A_{t+1}$ , this algorithm is referred to as *Sarsa*. Finally, note that for the next step, we use  $S_{t+1}, A_{t+1}$  as the state-action pair for which  $q^{[k]}(s, a)$  is updated.

Alternatively, we only keep the state  $S_t$  from the last step and first choose the action  $A_t$  for the update using the current policy. Then, we choose our action from state  $S_{t+1}$  in greedy fashion, which effectively uses  $Q^{[k]}(s = S_t, a)$  as an approximation for  $q_*(s = S_t, a)$ . This leads to

$$q^{[k+1]}(S_t, A_t) = q^{[k]}(S_t, A_t) + \alpha[R_{t+1} + \gamma \max_a q^{[k]}(S_{t+1}, a) - q^{[k]}(S_t, A_t)]. \quad (7.24)$$

and is a so-called *off-policy* approach. The algorithm, a variant of which is used in AlphaGo, is called *Q-learning*.

## 7.5 Function approximation

When the state-action space becomes very large, we face two problems: First, we can not use tabular methods anymore, since we can not store all values. Second and more important, even if we could store all the values, the probability of visiting all state-action pairs with the above algorithms becomes increasingly unlikely, in other words most states will never be visited during training. Ideally, we should thus identify states that are ‘similar’, assign them ‘similar’ value, and choose ‘similar’ actions when in these states. This grouping of similar states is exactly the kind of *generalization* we tried to achieve in the previous sections. Not surprisingly, reinforcement learning is most successful when combined with neural networks.

In particular, we can parametrize a value function  $\hat{v}_\pi(s; \theta)$  and try to find parameters  $\theta$  such that  $\hat{v}_\pi(s; \theta) \approx v_\pi(s)$ . This approximation can be done using the supervised-learning methods encountered in the previous sections, where the target, or label, is given by the new estimate. In particular, we can use the *mean squared value error* to formulate a gradient descent method for an update procedure analogous to Eq. (7.21). Starting from a state  $S$  and choosing an action  $A$  according to the policy  $\pi(a|S)$ , we update the parameters

$$\theta^{[k+1]} = \theta^{[k]} + \alpha[R + \gamma \hat{v}_\pi(S'; \theta^{[k]}) - \hat{v}_\pi(S; \theta^{[k]})] \nabla \hat{v}_\pi(S; \theta^{[k]}) \quad (7.25)$$

with  $0 < \alpha < 1$  again the learning rate. Note that, even though the new estimate also depends on  $\theta^{[k]}$ , we only take the derivative with respect to the old estimate. This method is thus referred to as *semi-gradient method*. In a similar fashion, we can reformulate the Sarsa algorithm introduced for generalized gradient iteration.

## 8 Concluding remarks

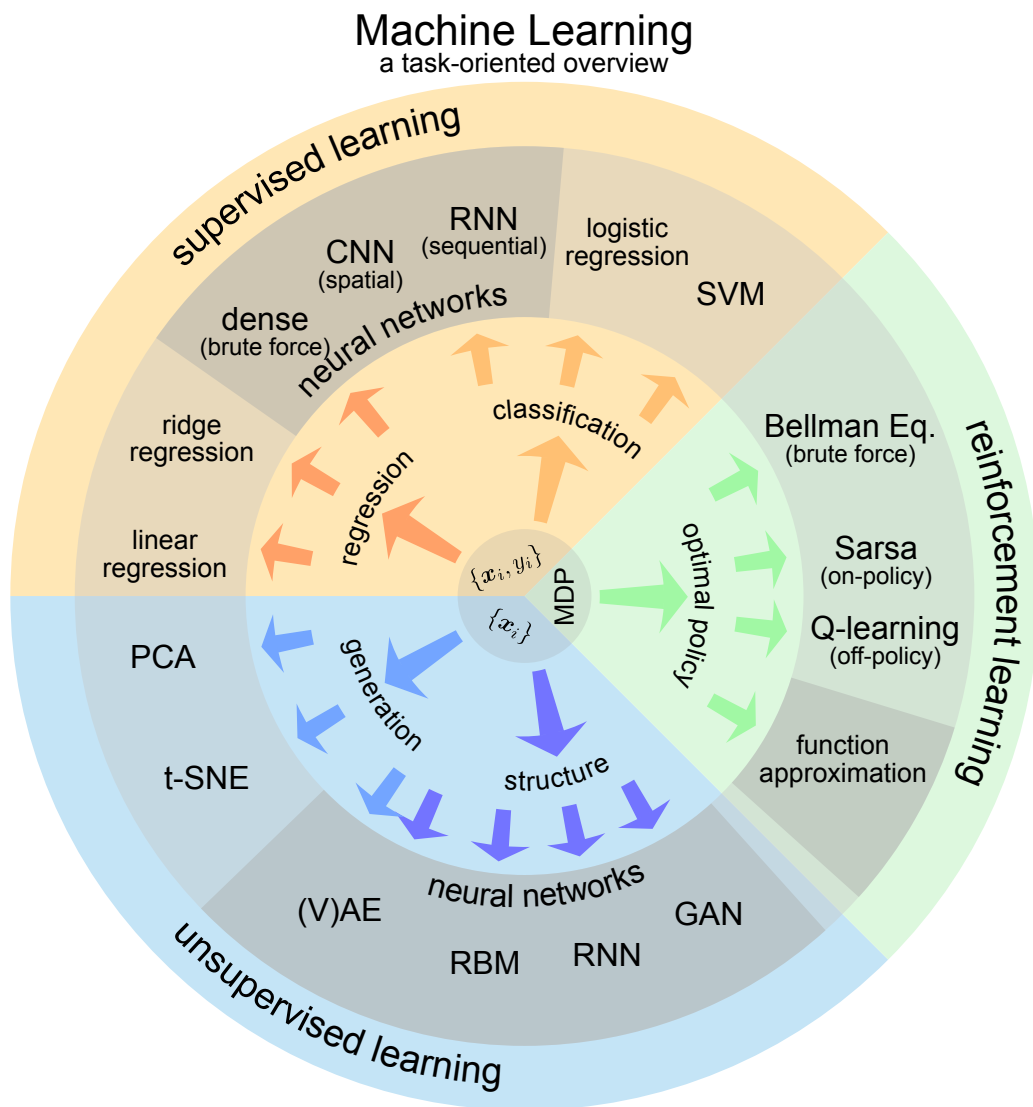
In this lecture, ‘Introduction to Machine Learning for the Sciences’, we have discussed common structures and algorithms of machine learning to analyze data or learn policies to achieve a given goal. Even though machine learning is often associated with neural networks, we have first introduced methods commonly known from statistical analysis, such as linear regression. Neural networks, which we used for most of this lecture, are much less controlled than these conventional methods. As an example, we do not try to find an absolute minimum in the optimization procedure, but one of many almost degenerate minima. This uncertainty might feel like a loss of control to a scientist, but it is crucial for the successful generalization of the trained network.

The goal of our discussions was not to provide the details needed for an actual implementation—as all standard algorithms are provided by standard libraries such as TensorFlow or PyTorch, this is indeed not necessary—but to give an overview over the most important terminology and the common algorithms. We hope that such an overview is helpful for reading the literature and deciding, whether a given method is suitable for your own problems.

To help with the use of machine learning in your own research, here a few lessons for a successful machine learner:

1. Your learning result can only be as good as your data set.
2. Understand your data, its structure and biases.
3. Try simpler algorithms first.
4. Don’t be afraid of lingo. Not everything that sounds fancy actually is.
5. Neural networks are better at interpolating than extrapolating.
6. Neural networks represent smooth functions well, not discontinuous or spiky ones.

Regarding the use of machine learning in a scientific setting, several points should be kept in mind. First, unlike in many other applications, scientific data often exhibits specific structure, correlations, or biases, which are known beforehand. It is thus important to use our prior knowledge in the construction of the neural network and the loss function. There are also many situations, where the output of the network has to satisfy conditions, such as symmetries, to be meaningful in a given context. This should ideally be included in the definition of the network. Finally, scientific analysis needs to be well defined and reproducible. Machine learning, with its intrinsic stochastic nature, does not easily satisfy these conditions. It is thus crucial to document carefully the architecture and all hyperparameters of a network and training. The results should be compared to conventional statistical methods, their robustness to variations in the structure of the network and the hyperparameters should be checked.



©MHF

Figure 36: **Machine Learning overview.** Methods covered in this lecture from the point of view of tasks.